Northern Climate ExChange

independent information, shared understanding, action on climate change

COMMUNITY ADAPTATION PROJECT

MAYO LANDSCAPE HAZARDS: GEOLOGICAL MAPPING FOR CLIMATE CHANGE ADAPTATION PLANNING

MARCH, 2011

Canada

Indian and Northern Affairs Canada | Affaires indiennes et du Nord Canada

Yukon College

Northern Climate ExChange

independent information, shared understanding, action on climate change

COMMUNITY ADAPTATION PROJECT

MAYO LANDSCAPE HAZARDS: GEOLOGICAL MAPPING FOR CLIMATE CHANGE ADAPTATION PLANNING

MARCH, 2011

Canada Indian and Northern Affairs Canada / Affaires indiennes et du Nord Canada

Yukon Energy, Mines and Resources

uOttawa

University of Alberta

Yukon Geological Survey

Yukon College

Printed in Whitehorse, Yukon, 2011 by Integraphics Ltd, 411D Strickland St.

This publication may be obtained from:

Northern Climate ExChange
c/o Yukon Research Centre, Yukon College
500 College Drive
PO Box 2799
Whitehorse, YT
Y1A 5K4

Supporting research documents that were not published with this report may also be obtained from the above address.

Recommended citation:

Northern Climate Exchange, 2011. Mayo Landscape Hazards: Geological Mapping for Climate Change Adaptation Planning. Yukon Research Centre, Yukon College, 64 p. and 2 maps.

Production by Leyla Weston, Whitehorse, Yukon.

Front cover photograph: Aerial photo of Mayo, Yukon, looking south over the Stewart River.

PREFACE

This report is part of a series of adaptation projects launched and produced by the Northern Climate ExChange, Yukon Research Centre, Yukon College. The scope of the report has been defined through a collaboration between the Northern Climate ExChange; Yukon Geological Survey, Government of Yukon; University of Alberta; University of Ottawa; and EBA Engineering Consultants Ltd. The project was funded by Indian and Northern Affairs Canada's Impact and Adaptations Program. The project began April 2010 and was completed in March 2011.

The objective of this project was to identify landscape hazards in the Village of Mayo and nearby surroundings by compiling geoscience data from various field studies and scientific reviews (surficial geology, permafrost and hydrology). This data was used to create a map of landscape hazards that delineate low, moderate and high-risk areas in the Mayo region. Potential impacts of a changing climate were incorporated in the identification of these three hazard zones.

Concurrent to the Hazards Mapping Project, the Northern Climate ExChange has begun developing an adaptation plan for the community of Mayo. The hazards project has contributed significantly to the assessment of vulnerability for the community of Mayo. In particular, the Hazards Mapping Project has increased the understanding of how landscape characteristics may change in Mayo as regional climate conditions change. This information will be utilized in the adaptation plan to provide the basis for evaluating how community infrastructure, security and well-being may be influenced and how the community might take action to respond.

This report is prepared as a guide, and not as a document upon which to base planning decisions. It is not intended for use as a basis for site selection for development, but rather as a guide in identifying areas that would require additional engineering studies, should development be desired.

The Northern Climate ExChange would like to continue doing Hazard Mapping Assessments for adaptation planning in other Yukon communities. We welcome any input or suggestions that you may have to improve future projects. Please contact me at (867) 668-8862, or by email at lkinnear@yukoncollege.yk.ca.

Lacia Kinnear

NCE Coordinator, Yukon Research Centre

Lead Authors on the Report

Kristen Kennedy	Yukon Geological Survey, Government of Yukon
Lacia Kinnear	Northern Climate ExChange, Yukon Research Centre, Yukon College
Fabrice Calmels	University of Alberta
Philip Bonaventure	University of Ottawa
Antoni Lewkowicz	University of Ottawa
Bronwyn Benkert	Northern Climate ExChange, Yukon Research Centre, Yukon College
Ryan Hennessey	Northern Climate ExChange, Yukon Research Centre, Yukon College

Contributors

Richard Trimbel	EBA Engineering Consultants Ltd.
Nancy Fresco	Scenarios Network for Alaska Planning, University of Alaska Fairbanks

Technical Advisors

Jeff Bond	Yukon Geological Survey, Government of Yukon
Sarah Laxton	Yukon Geological Survey, Government of Yukon

Technical Editing and Layout Leyla Weston, private consultant, Whitehorse, Yukon

Acknowledgements

The project team would like to thank all the participants in this project for their enthusiasm and commitment. We would like to express our appreciation to the Yukon Geological Survey, Yukon Research Centre, University of Alberta, University of Ottawa, Government of Yukon, and all those noted above for their support.

Chris Burn and Rick Janowicz are acknowledged for providing insight into the project. We are especially grateful to Leyla Weston who provided the technical editing and layout.

We would especially like to thank the Village of Mayo and the First Nation of Na-Cho Nyäk Dun for supporting this project and welcoming us on their lands and within the Traditional Territory of the Na-Cho Nyäk Dun.

This project would not have been possible without the various summer field assistants whose commitment was unfailing. We would also like to acknowledge our Local Adaptation Coordinator, Susan Stuart of Mayo for the commitment that she has given throughout this project.

Funding for this project was provided by Indian and Northern Affairs Canada and the Government of Canada. Administrative support has been provided through Yukon College and the Yukon Research Centre.

TABLE OF CONTENTS

INTRODUCTION AND PROJECT DESCRIPTION

As outlined in the 2005 Arctic Climate Impact Assessment (Huntington and Weller, 2005), climate change is identified as a significant challenge for northern communities, where the impacts of a warming climate are already having a considerable effect. Many people living in small, isolated communities in northern Yukon are concerned about climate-related risks in their local area. Because adverse impacts are a reality, we must implement measures to reduce or moderate the negative effects of climate change. This is known as climate change adaptation. The first step in adaptation planning is the identification and characterization of vulnerabilities. Only then can we identify adaptation needs, which will result in the development of new policies and programs, as well as provide opportunities to reduce the negative impacts of current and future climate change.

There are two important terms to define when discussing climate change adaptation:

- *vulnerability* - refers to the susceptibility to harm in a system in response to a stimulus or stimuli; and
- *adaptive capacity* - reflects a community's potential or ability to address, plan for, or adapt to risk.

Vulnerability, at a local level, is conditioned by social, economic, cultural, political and biophysical conditions and processes operating at multiple temporal and spatial scales and in turn affects community exposure and adaptive capacity. To understand vulnerabilities within the landscape, we must assess the environmental conditions that may be affected by climate change and may therefore pose hazards to safe and sustainable development. Factors to be considered include permafrost and ground ice, surface water drainage, groundwater dynamics, surficial geology and slope stability. These factors combine to create landscape hazards that can pose risks to infrastructure, and may be exacerbated in a changing climate. Insights related to these hazards can be used to direct investigations that will support future adaptation and town planning processes.

The objective of this project is to identify landscape hazards in the Village of Mayo and nearby surroundings (Figure 1) by gathering and mapping geoscience data (surficial geology, permafrost conditions and hydrology). This data is used to create a map of landscape hazards based on geotechnical properties that suggest low, moderate and high-risk areas in the Mayo region. Potential impacts of a changing climate are incorporated in the identification of these three hazard zones.

This report is prepared as a guide and not as a document upon which to base planning decisions. It should not be used for site selection for development, but rather treated as a guide in identifying areas that would require additional engineering studies, should development be desired.

This project is a partnership between the Northern Climate ExChange, Yukon Research Centre, Yukon College; Yukon Geological Survey; EBA Engineering; University of Alberta; and University of Ottawa.

APPROACH AND METHODS

The goal of hazards mapping in the Mayo region is to identify landforms, sediments and landscape processes that may pose a threat to ongoing and future development under current and changing climate conditions. Surficial mapping studies were undertaken in order

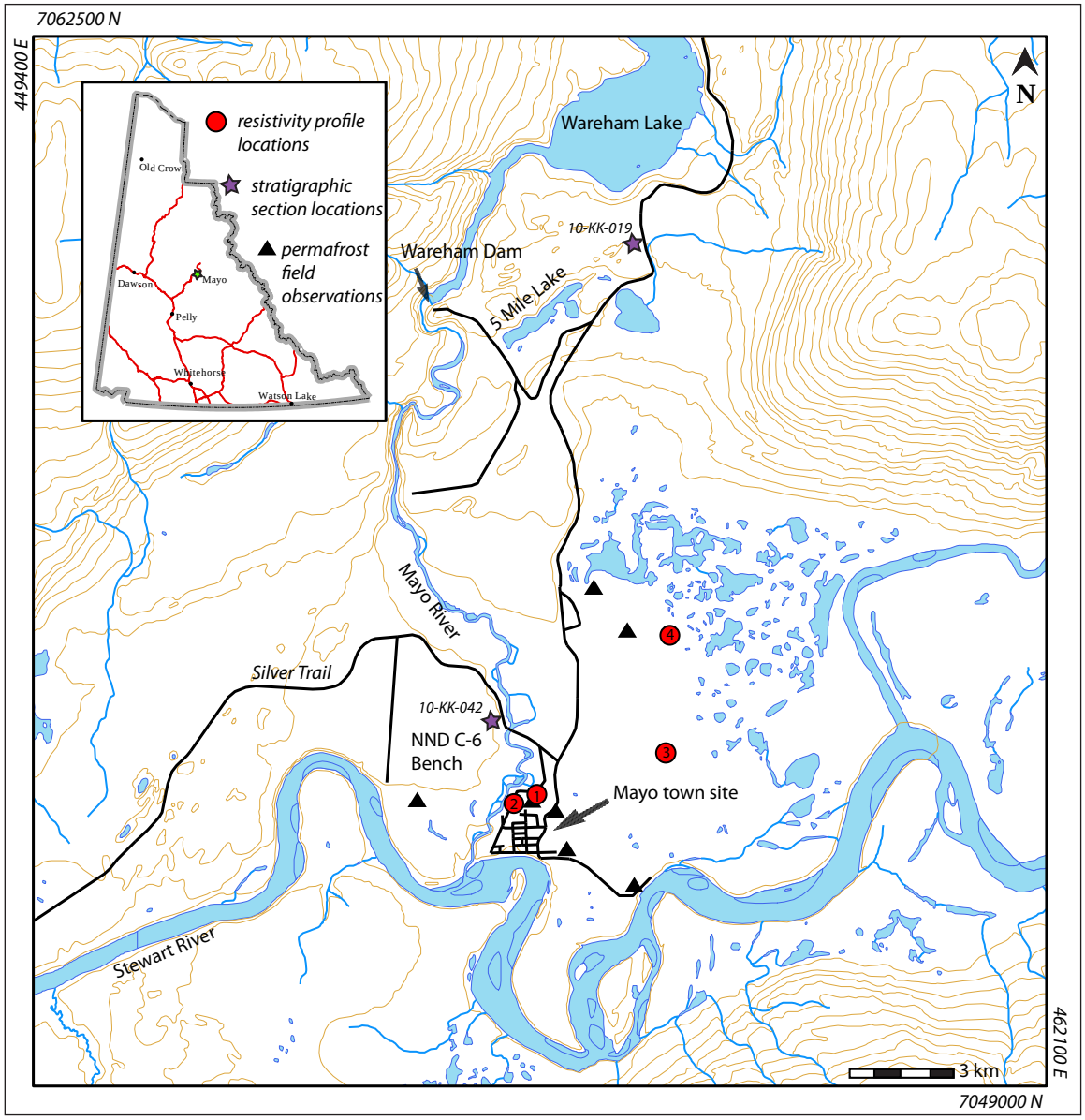

Figure 1. *Location of study area. Resistivity profile, permafrost field investigation and stratigraphic site locations are shown. Resistivity profile sites are numbered and represent Figure 26 (1); Figure 28 (2); Figure 30 (3); and Figure 34 (4).*

to determine the stability of surface sediments; detailed studies of hydrological processes, as well the characteristics of permafrost were also carried out. Mapping and describing existing landforms and sediments was completed through surficial geological mapping at a scale of 1:10 000 during the summer of 2010. Earlier mapping by Hughes (1983) and Giles (1993) and initial reviews of existing data (*i.e.,* borehole logs, geological maps and reports) demonstrated that the geological processes of greatest impact to community sustainability and safety are permafrost and hydrological processes.

To address the need for additional information related to these processes, detailed investigations were initiated to assess the current hydrological and permafrost conditions in the community of Mayo. Final hazard identification was completed by combining the results of the hydrological and

permafrost studies with surficial geological mapping to create a ranking of potential landscape hazards for distinct geological units within, and surrounding, the community of Mayo. Hazard rankings also include projected changes in climate variables such as temperature, precipitation and seasonality.

REGIONAL SETTING

The Village of Mayo (63°37' N, 135°52' W; see Figure 1) is located in central Yukon, within the Stewart River Plateau. It is at the confluence of the Mayo and Stewart rivers, in the broad Stewart River valley. The main development of the Village of Mayo occurs on the floodplain of the Stewart River. Mayo is within the Traditional Territory of the First Nation of Na-Cho Nyäk Dun. The town of Mayo was established in 1903, nearly 30 years after the first prospectors discovered gold in the area. The site of the village was chosen as a logical supply hub for the goldfields of Duncan Creek and was at the highest navigable point on the Stewart River for steamboats bringing in supplies from Whitehorse (Bleiler, 2006). First Nations people living in McQuesten Village at that time, soon moved to the new town site of Mayo before establishing their own village on the banks of the Stewart River just below Mayo, a place now called the Old Village (Peter *et al.*, 2006).

By the early 1920s, Mayo primarily serviced silver mines (Keno Mining District) rather than gold mines, and was experiencing a population boom of more than 800 people (Bleiler, 2006). Silver mining continued to be the primary economic driver in the Village of Mayo until a highway was built in 1950 and sternwheelers were no longer required to transport ore from Mayo. Placer gold and limited silver mining continue to feed the economy of Mayo, but on a smaller scale than the boom times of the early and mid-1900s.

A local improvement district was formed for the Mayo property owners in 1968, and the Village of Mayo was officially incorporated in 1984. The First Nation of Na-Cho Nyäk Dun signed a Land Claims and Self-Government Agreement with the Government of Canada in 1993 and had established the First Nation of Na-Cho Nyäk Dun Development Corporation by the mid-1990s. The Na-Cho Nyäk Dun Government and Development Corporation are now leading sustainable economic development initiatives within in the Village of Mayo.

SOCIAL SETTING

Population

The population of Mayo was 452 in June 2010. Population density per square mile was 286. On the whole, Yukon communities are becoming demographically stable (Yukon Bureau of Statistics (YBS, 2008a), and the same is true of Mayo; the population showed only a slight decline (-1.9%) between June 2009 and June 2010 (YBS, 2010). In general, young adults between the ages of 20-34 make up the cohort most likely to move into, or out of the community (YBS, 2008a). At the time the 2006 population census was conducted, there were 96 men for every 100 women in Mayo, the lowest male-to-female ratio in Yukon. Median age in the community at the time was 40.3 years (YBS, 2007). The proportion of the population declaring aboriginal identity in 2006 was 54% (YBS, 2008b).

Economy

At the time of the 2006 census, 23% of Mayo residents reported being employed in the private sector (*i.e.*, business, finance and administration). The service industry employed 20%, followed by the public sector (13%), trades (13%), primary industry (13%), management occupations

(10%), and the natural and applied sciences (7%; YBS, 2007). The current economic profile of Mayo is too small to justify a significant increase in the provision of regional services (*e.g.*, health care) and as a result, the current economic distribution is unlikely to change significantly over time (Village of Mayo (VOM), 2005).

Infrastructure

There are 115 occupied private dwellings in the Village of Mayo. The median value of a single-detached house in Mayo is $75,008, while the territorial average is $219,439 (YBS, 2009). The bulk of development in Mayo is concentrated in the village core, although the Na-Cho Nyäk Dun First Nation has been concentrating new development outside the municipal boundary on their C-6 site selection. In addition to the Na-Cho Nyäk Dun First Nation administration building (built in 2009), construction of 35-45 new housing units is anticipated on the C-6 site over the next 25 years. Future development in the downtown core is recommended in the Village of Mayo Official Community Plan, to increase density and improve infrastructure viability (VOM, 2005). Implementation of this Official Community Plan recommendation will ensure that the bulk of linear infrastructure in Mayo (*e.g.*, power, sewer and waterlines) will remain in the village core.

PHYSICAL SETTING

Physiography

The physiography of the Mayo region is characterized by rolling uplands with steep slopes leading into U-shaped valleys about 1000 m below the upland surface. The Stewart and Mayo rivers are incised into the Stewart Plateau to a depth of 490 m a.s.l.; most of the Village of Mayo is <500 m above sea level (a.s.l.), on the floodplain of the Stewart River.

Vegetation

Vegetation in the Mayo region is dominated by northern mixed deciduous and coniferous forest (boreal forest), consisting predominantly of white spruce (*Picea glauca*) with minor amounts of black spruce (*Picea mariana*) and paper birch (*Betula papyrifera*). Aspen (*Populus tremuloides*), balsam (*Populus balsamifera*) and poplar (*Populous*) are common. The northern limit of lodgepole pine (*Picea contorta*) is located near Mayo in the Stewart River valley. South-facing slopes commonly have artemesia grasslands or steppe vegetation (Cwynar *et al.*, 1987). The understory consists of feathermoss, willows, sagewort and ericaceous shrubs; sphagnum mosses are more common in wetter terrain.

Contemporary climate

The Mayo region is located in the Central Yukon Basin climate zone, and has a subarctic continental climate (Smith *et al.*, 2004) due to the topographic effects of the St Elias and Coast mountains (Wahl *et al.*, 1987). This climate zone is characterized by short, warm summers and long, cold winters. Mayo has major diurnal and seasonal temperature ranges and strong altitudinal temperature effects that vary with the seasons. Mean January temperature in Mayo is -26.9°C, while mean July temperature is 15.6°C, based on 30-year (1961-1990) climate normals measured at the Mayo A meteorological station (63°37’ N, 135°52’ W; Environment Canada, 2010). Temperature inversions are common in winter, resulting in very cold temperatures in the river valley at the townsite of Mayo, while in summer, the Stewart River valley can be one of the warmest valleys in the Yukon. This leads to extreme seasonal temperature ranges, whereby the minimum and maximum temperatures recorded in Mayo are separated by 98.3°C (Wellman and Gagné, 2010). The Pacific Ocean is the main source of moisture for the region (Smith *et al.*, 2004). The 30-year average precipitation at the Mayo A meteorological station is 318.4 mm, and

approximately 37% or ~1/3 of this precipitation falls as snow during the winter season; average January snow depth is 41 cm (Environment Canada, 2010). Month-by-month climate normal data are summarized in Figure 2.

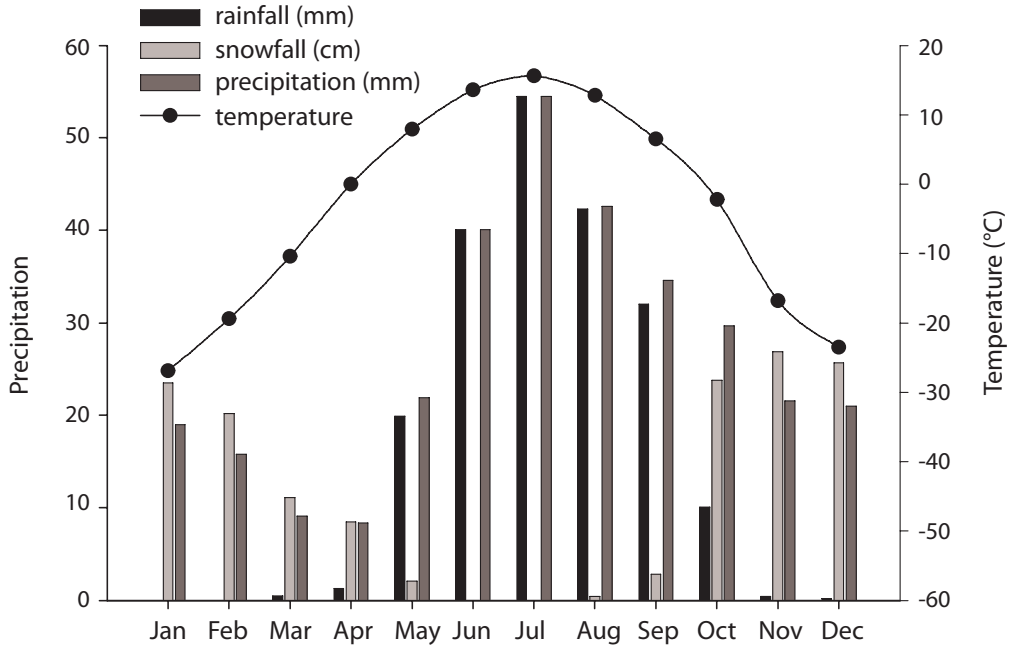

Figure 2. *Climate normal (1961-1990) temperature and precipitation for the Mayo A meteorological monitoring station (Environment Canada, 2010). To calculate total precipitation in millimetres, snowfall was converted to snow water equivalent (SWE) and summed with rainfall.*

Past climate trends

To examine past trends in climate in the Mayo region, Purves (2010) examined monthly, daily and hourly climate archives using the Climate Manager program. Data were acquired by Environment Canada and the Yukon Forest Service (Purves, 2010; Environment Canada, 2010). It should be noted that there was a slight change in the position of the Mayo A Environment Canada monitoring station on February 1, 1969, when the station moved to its current location. Trends in collected data were examined using linear regression analysis from data plots developed in Microsoft Excel. In some cases, climatic trends have been extended beyond the period of record to project potential future change. The subsections below describe trends in several climate parameters described by Purves (2010).

Mean Daily Winter Minimum Temperature

Data is available for every year between 1925 and 2009 inclusive, with the exception of 1926. There was a period of strong cooling in the middle of the last century, between 1943 and 1975, at a rate of ~1.6°C/10 yrs. Over the past thirty years, there has been a strong warming trend, at a rate of ~0.7°C/10 yrs. The mean daily minimum winter temperature for Mayo over the entire period of record increased by ~0.2°C/10 yrs. The mean minimum winter temperature between 1966 and 1977 was –29.3°C, while the mean minimum between 2000 and 2009 was -23.3°C.

Mean Daily Maximum Summer Temperature

Mayo experienced a period of declining mean daily maximum summer temperatures between 1941 and 1964, at a rate of ~5°C/10 yrs. Mean daily maximum summer temperatures increased over the last 30 years by ~0.4°C/10 yrs. Overall, for the full period of record, temperature increases are inferred to be ~0.1°C/10 yrs.

Mean Annual Temperature

Mean annual temperature data is available between 1929 and 2009 inclusive. There was a period of declining mean annual temperature, spanning 1947-1977. Mean annual temperature has increased over the last thirty years by ~0.3°C/10 yrs. Overall, for the full period of record, mean annual temperature is inferred to have increased by ~0.3°C/10 yrs.

Total Winter Precipitation

The period of record for this parameter encompasses the winters of 1925-2009, with the exception of 1926, 1946, 1994 and 1995. Mayo shows a very significant increase (~56%/10 yrs) in winter precipitation from 1933 to 1966, amounting to a nearly three-fold increase. There was a large decline in total winter precipitation between 1966 and 1968, and then an increase of ~7%/10 yrs for the thirty years between 1980 and 2009. However, when the period of analysis is limited to 1966-2005, the increase in winter precipitation is ~2%/10 yrs, demonstrating the effects of strong annual variability in this dataset. Over the entire period of record for Mayo, there is only a slight decline in total winter precipitation.

Total Summer Precipitation

Mayo has records of summer precipitation from 1926 to 2009, with the exception of 1995. There do appear to be some alternating periods of wetter and drier summers, but the overall trend shows an increase in summer precipitation of ~3%/10 yrs (*i.e.*, ~4 mm/10 yrs). Over the past thirty years, summer precipitation has increased ~6 mm/10 yrs, or 44%.

Total Annual Precipitation

The period of record for Mayo for total annual precipitation spans from 1927 to 2009. There is a trend towards increasing precipitation by ~2%/10 yrs (~6 mm/10 yrs) over the entire period of record. Over the past thirty years, annual precipitation has increased 67% (19 mm/10 yrs).

Snow on Ground for February 28

Data is available from 1955 to 2010, with the exception of 1995. This record shows a strong and steady decrease, amounting to ~11%/10 yrs (~7 cm/10 yrs). Over the past thirty years, there is a very slight increase in snow on ground as of February 28 by 7%.

Days Below –40°C

Data for Mayo indicates long-term cycles in the number of days below -40°C, but over the eighty years of available data, spanning 1929-2009, there is an indication of ~1 fewer day below -40°C per decade. Over the past thirty years, the rate has increased, and there are ~3 fewer days per decade below -40°C. If this trend were to continue, there would be no days below –40°C by 2047.

Frost-Free Days

Data for Mayo indicates long-term cycles in the number of frost-free days. However, when the entire period of record (1924-2009) is examined, there is a trend towards an increasing number of frost-free days at a rate of ~5 days/10 yrs (*i.e.*, an 84% increase). Over the past thirty

years, this value has declined slightly, to an increase of ~4 frost-free days per century, or a 32% increase.

ENVIRONMENTAL SETTING OF THE MAYO REGION

HYDROLOGY

Surface hydrology

The subwatershed of the Mayo region forms part of the Yukon River watershed, which covers 260 000 km^2 or 54% of Yukon Territory (Smith *et al.*, 2004). The area is situated in the Interior Hydrologic Region of the Territory, where drainage from the southern foothills of the Selwyn Mountains flows west to the Yukon River. The first and second-order streams descending from the foothills are generally steep and relatively short, producing rapid, flashy streamflow responses during the spring melt and some of the highest peak flows in Yukon. Mean annual runoff in the region is moderately high compared with other regions of the Territory, at 236-385 mm (Smith *et al.*, 2004). Peak river flows in the Interior Hydrologic Region generally occur in May and June in response to snowmelt inputs during the spring freshet, while secondary discharge peaks in response to late summer and autumn rainfall are also possible. Lowest flows are typically exhibited in this region in March and April, when groundwater contributions to streamflow, the only inputs to river discharge at this time, are minimal (Janowicz, 2008).

The Stewart River, which flows through the town of Mayo and is one of the principal tributaries of the Yukon River, drains a watershed of 51 000 km^2 (Water Survey of Canada, 2010). While overbank flooding is now uncommon in Mayo due to the dyke constructed along the riverbank that borders the town, Mayo has been severely flooded by the Stewart River in the past. The most significant flood was in 1936, when a heavy winter snowfall and an unseasonably warm, late spring caused water levels to rise 4.8 m above the usual high water mark. This event has been called one of the region's most severe climate events of the 20th century (Wellman and Gagné, 2010), and it caused considerable property and infrastructure damage. Overbank flooding also occurred in the spring of 1964, although this flood was not as severe as that of 1936. However, both flood events prompted the construction of, and additions to, the dyke that protects the community today, and have contributed to the development of a community flood response plan. In 1992, a flood alert was issued, because peak discharge on the Stewart River was alarmingly high, although the high water crest passed without causing any flooding at the townsite.

The Water Survey of Canada (WSC) has maintained gauging stations spanning the headwater tributaries of the Stewart River to its mouth, some of which provide real-time hydrometric data. (See Table 1 for a summary of station information and Figure 3 for a map of their locations.) The WSC reports daily average, monthly average, and peak yearly discharge for each station (Water Survey of Canada, 2010). A hydrograph of monthly average discharge for the Stewart River at its mouth (the longest available record in the region, spanning 1964-2009; Figure 3) demonstrates the typical seasonal pattern of a river in Yukon's Interior Hydrologic Region, with rapid increases in discharge in May and June, followed by a recession through summer and autumn. Average monthly discharge is low through the winter months, when groundwater is the only input to the river, and the lowest flows occur in March, prior to the spring freshet. Figure 3 also illustrates monthly average discharge for 1964, a year in which peak June discharge greatly exceeded the 1964-2009 average discharges, and for 2008, a year in which average June discharge was much below the 1964-2009 averages. The 2008 hydrograph also demonstrates the effects late-season

precipitation can have on Stewart River discharge, as is exhibited by the above-average flows between mid-July and November.

Table 1. Summary of Water Survey of Canada stations in the Mayo region (Water Survey of Canada, 2010). Stations are listed roughly in the order they appear from the headwaters of the Stewart River to its mouth at the Yukon River.

Station name	Station ID	Latitude	Longitude	Gross drainage area (km²)	Parameter	Period of record
Hess River above Emerald Creek	09DA001	63°20′8″ N	131°30′0″ W	4840	discharge	1977-1996
Beaver River below Matson Creek	09DB001	64°0′54″ N	134°8′21″ W	not available	discharge	1996-2009
Stewart River above Fraser Falls	09DC003	63°29′17″ N	135°8′6″ W	30600	discharge	1980-1995
Stewart River at Mayo	09DC002	63°35′26″ N	135°53′48″ W	31600	discharge	1949-1979
Stewart River at Mayo	09DC006	63°35′26″ N	135°53′48″ W	31600	level	1980-2009
Stewart River at Stewart Crossing	09DD002	63°22′56″ N	136°40′59″ W	35000	discharge	1961-1973
Stewart River at the mouth	09DD003	63°16′56″ N	139°15′16″ W	51000	discharge	1964-2009

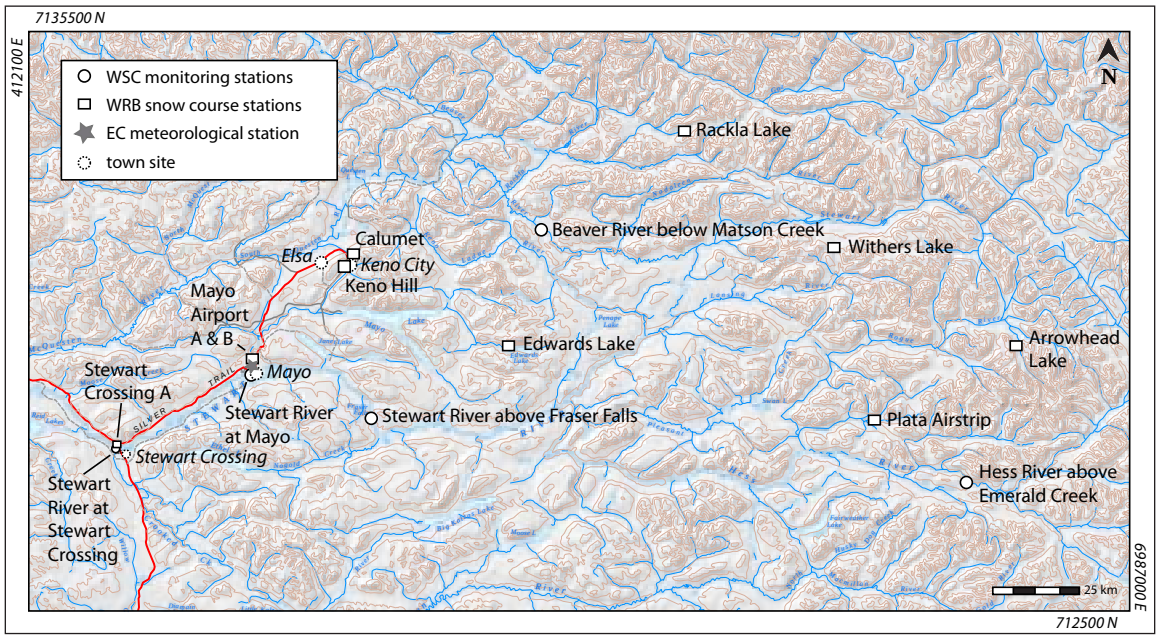

Figure 3. *Overview map of the Mayo region study area, showing meteorological, river discharge and snow course monitoring stations referenced in this report. Note that the scale of the map does not permit the display of the Water Survey of Canada's 'Stewart River at the mouth' monitoring station. It is located downstream (left) of Stewart Crossing at the junction of the Stewart and Yukon rivers. WRB - Water Resources Branch, Yukon government; WSC - Water Survey of Canada; EC - Environment Canada.*

Peak yearly discharge also provides a basis for assessing the dynamics of surface water hydrology of the Stewart River and its tributaries. Figure 4 presents peak yearly discharge for all WSC stations along the Stewart River and for its tributaries (see Table 1 for details of WSC station locations). As described, peak discharge usually takes place during the spring freshet, when snowmelt inputs are high. However, spring peak discharge (May and June) can sometimes be replaced by late summer peak discharge (August and September), as was the case for the

Stewart River at its mouth in 2008 (Figure 5). Figure 4 clearly demonstrates that peak discharge events measured at headwater stations are mirrored in the discharge records of downstream stations, highlighting the importance of headwater snowmelt inputs to the Stewart River system. It is also possible that in the years in which headwater snowpacks are deep (producing high

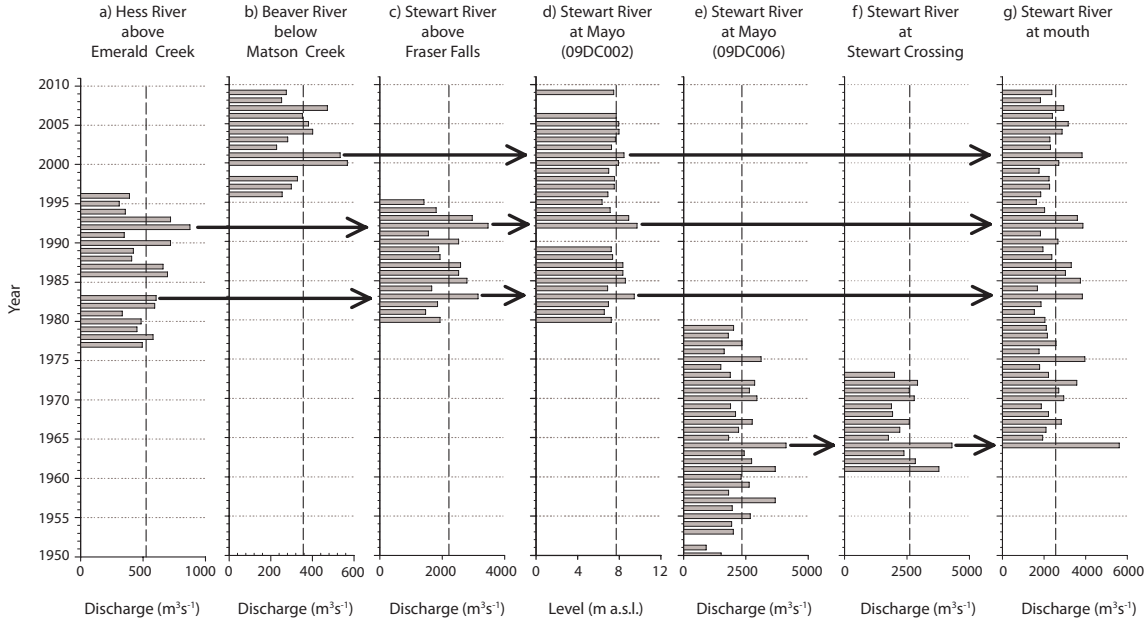

Figure 4. *Peak discharge (m^3s^{-1}) at WSC stations ranging from the headwaters of the Stewart River (plot a) to its mouth at the Yukon River (plot g; Water Survey of Canada, 2010). Note: plot d shows level in "metres a.s.l." rather than discharge. Vertical, long, dashed lines indicate average peak discharge for each station for its period of record. Arrows highlight events of above-average peak discharge (or level) that are evident in all existing records, demonstrating how peaks in headwater discharge propagate downstream.*

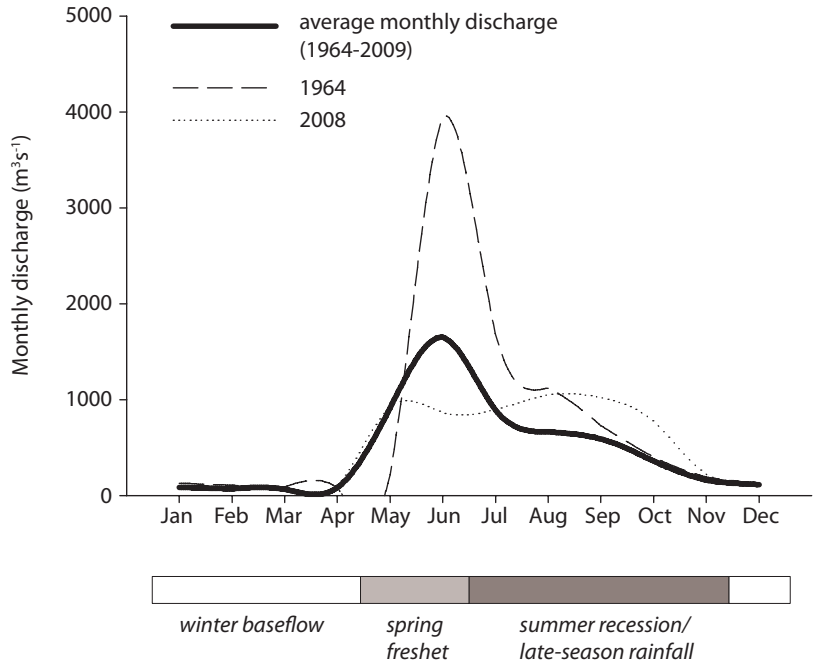

Figure 5. *Average monthly discharge hydrograph at the mouth of the Stewart River (heavy solid line). Also shown are hydrographs for the years 1964 (long-dashed line) and 2008 (dotted line), demonstrating high and low June discharge, respectively. The 2008 hydrograph also exhibits a secondary peak in late summer/autumn in response to late-season rainfall (Water Survey of Canada, 2010).*

volumes of snowmelt and high, peak spring discharge events), these are also years in which downstream snowpacks are deep. Thus, snowmelt contributions may continue to be significant along all reaches of the Stewart River and act as a key input to discharge along the river system.

Groundwater

As described, the Village of Mayo is built in the Stewart River valley, on the natural floodplain of the Stewart River. Residents of Mayo report frequent, often yearly, basement flooding in the spring (Wellman and Gagné, 2010). Because overbank flooding of the Stewart River does not accompany these events, it is highly likely that basement flooding is caused by groundwater. Many of the houses at which flooding has been reported, cluster along 4th Avenue (S. Stuart, pers. comm., Dec. 2010). It is possible that the groundwater table in this area is naturally higher than in other areas. Residents speculate that an underground stream or flowpath may be present. Hydrological field studies in the Mayo region would be necessary to evaluate this hypothesis, and, if conducted over the course of several consecutive thaw seasons, these studies could also be used to assess the responses of the groundwater table to hydrological change during the spring freshet.

Some test pits and boreholes have been excavated around Mayo over the past three decades (R. Trimble, EBA Engineering, pers. comm., 2010). These records indicate that the water table was encountered at a relatively shallow depth at several locations. Additionally, water levels in several private and commercial wells around Mayo are recorded in a database maintained by the Government of Yukon, Water Resources Branch (Water Resources Branch, 2010a). While it is inappropriate to use these data to interpret groundwater depths around the town of Mayo (because they lack georeference information and only represent conditions at a single point in time), it cannot be disputed that groundwater is not deep below the surface in the town of Mayo, and is in fact quite shallow in some areas.

Winter snowpacks

The Government of Yukon, Water Resources Branch maintains several snow courses in the Stewart River watershed during the latter part of the winter season. The locations and elevations of these snow courses, as well as their periods of record, are summarized in Table 2 (see Figure 3 for locations; Water Resources Branch, 2010b). Generally, snow depth was measured at each snow course on February 1st, March 1st, April 1st, May 1st and May 15th until the early 1980s, when the February 1st measurement was eliminated. The May 15th snow depth is not always measured at all stations in all sampling years. Snow water equivalent (SWE) is also reported for all sampling points.

To facilitate comparison between SWE at each snow course station, SWE values have been converted to z-scores, using the following formula for each value in a snow course dataset.

$$z\text{-}score = \frac{value - mean}{stdev}$$

Z-scores provide an indication of the variation of a particular data point around the mean, while preserving the patterns inherent in the dataset. Importantly, because they are a unitless parameter, z-scores are readily comparable between data from different sites.

Figure 6 presents compiled SWE z-score values for all snow courses. The dotted line, tracing a z-score of 0, provides a point of reference against which to evaluate potential changes in SWE over the periods of record. Based on a visual assessment, three potential periods of variability can be identified in this record, although the length of record for each snow course varies (see Table 2 for details on periods of record for each snow course). Period A, which spans 1968-1984,

Table 2. Mayo region snow course locations, elevations and periods of record (Water Resources Branch, 2010b). Stations are listed roughly in the order they appear from the headwaters of the Stewart River to its mouth at the Yukon River. Location information is given with as much precision as has been reported by Water Resources Branch, Yukon government. Stations marked with an asterisk have been excluded from the analysis presented in this report because of their short periods of record.

Station name	Station ID	Latitude	Longitude	Period of record	Elevation (m)
Arrowhead Lake	09DA-SC02	63°42′9″ N	131°10′13″ W	1986-2010	1120
Plata Airstrip	09DA-SC01	63°30′22″ N	132°2′43″ W	1978-2010	830
Withers Lake	09DB-SC01	63°58′49″N	132°17′53″ W	1986-2010	975
Rackla Lake	09DB-SC02	64°17′33″ N	133°14′38″ W	1987-2010	1040
Edwards Lake	09DC-SC02	63°41′44″ N	134°17′50″ W	1987-2010	830
Calumet	09DD-SC01	63°55′ N	135°24′ W	1975-2010	1310
Mayo Airport A	09DCSC01A	63°38′ N	135°53′ W	1968-2010	540
Mayo Airport B	09DC-SC01B	63°38′ N	135°53′ W	1987-2010	540
Keno Hill*	09DD-SC02	63°56′ N	135°15′ W	1975-1981	1355
Stewart Crossing A*	09DD-SC03	63°22′ N	136°41′ W	1983-1983	610

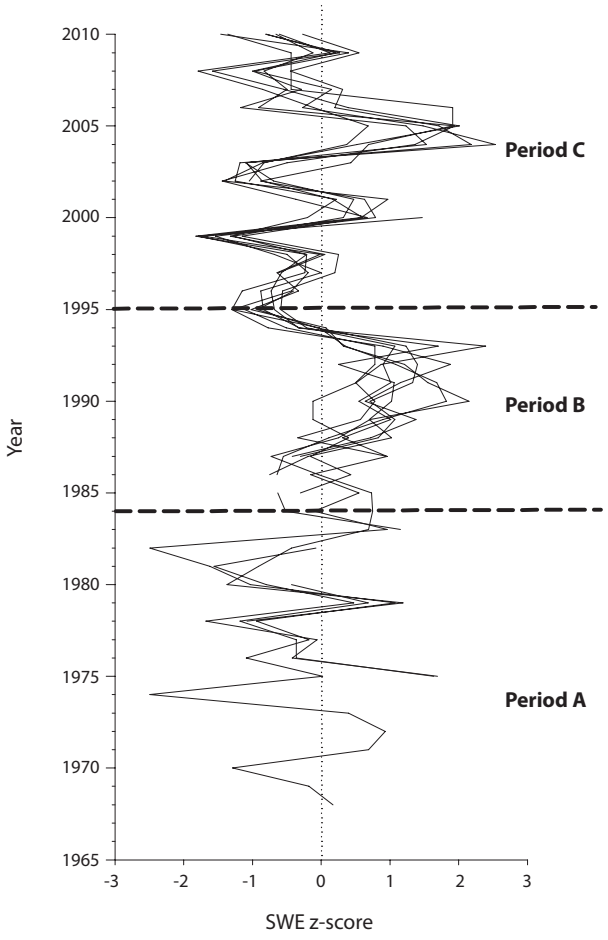

Figure 6. *Z-scores of snow water equivalent (SWE) for snow courses in the Mayo region (see Table 2 for details about each snow course; Water Resources Branch, 2010b). Data from each snow course have been superimposed on this figure. The vertical dotted line represents a z-score of 0 and acts as a reference point, while the horizontal heavy dashed lines indicate interpreted periods of decadal-scale shifts in SWE.*

represents a period in which SWE values appear to be generally lower than average; however, it is important to bear in mind that this portion of the record is the most data-sparse. Period B, which spans 1985-1995, appears to exhibit SWE values generally above average, while Period C (1996-2009) appears to exhibit SWE values that fluctuate around a z-score of 0.

To further examine the relationship between spring discharge on the Stewart River and winter snowpack, March 1st SWE is compared with peak spring discharge on the Stewart River at its mouth (Figure 7). This WSC station was chosen as the comparison site because it has the longest record of river discharge measured along the Stewart River and its tributaries (1964-2009), and because variations in peak discharge at this station reflect those of upstream stations (see Figure 4). Snow course data from March 1st were chosen for comparison because this measurement was consistently taken throughout the periods of record at all snow courses (*i.e.*, both before and after the early 1980s). Furthermore, April 1st snow depths sometimes exhibit declines from March 1st values, indicating that melting may have begun by April 1st in some years. Hence, March 1st values present a more reliable indication of the depth of the winter snowpack available to augment river discharge during the spring melt. SWE is presented in Figure 7, rather than snow depth, because SWE represents the amount of water contained in the snowpack and hence is a good indicator of available runoff during the snowmelt period. In fact, SWE is the most hydrologically important characteristic of snowcover (Walsh, 2005). Both SWE and Stewart River discharge are presented as z-scores, as this facilitates comparison between these two different parameters.

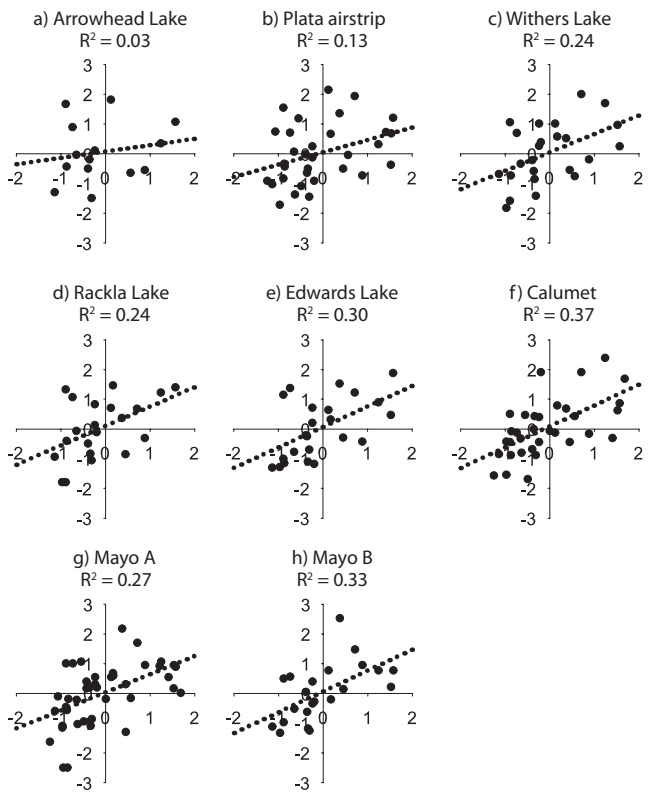

Figure 7. *Crossplots of z-scores illustrating peak spring discharge on the Stewart River at its mouth (plotted on the x-axis; Water Survey of Canada, 2010b) versus March 1st snow water equivalent at Stewart River watershed snow course stations (plotted on the y-axis; see Table 2 for station information; Water Resources Branch, 2010) over their corresponding periods of record. Stations are listed roughly in the order they appear from the headwaters of the Stewart River (plot a, Arrowhead Lake) to its mouth at the Yukon River (plot h, Mayo B). Linear regression lines have been calculated based on each dataset, and are shown as diagonal dotted lines. R^2 values, indicating the strength of the correlation between discharge and SWE (developed based on the linear regression for each plot), are given for each snow course station.*

First, to examine the correlation between March 1st SWE and spring peak discharge on the Stewart River, z-scores for each snow course are plotted against Stewart River discharge z-scores and the intersection of the two creates a point, as is shown on the crossplots in Figure 7.

Positive correlations exist between Stewart River peak spring discharge and March 1st SWE at all snow course stations, confirming that snowmelt is a key input to the Stewart River during the spring freshet. The strength of the correlation between peak spring discharge and March 1st SWE is defined by the R^2 value, which in this case is being used to describe the strength of the relationship between variables in a dataset. An R^2 of 0 indicates no correlation between the parameters being examined, while the highest possible correlation has an R^2 value of 1. In this dataset, the weakest correlation is with the Arrowhead Lake snow course station ($R^2 = 0.03$; note that the SWE record for Arrowhead Lake is sparse, which may contribute to the low correlation). The strongest correlation between discharge and SWE is with the Calumet snow course station ($R^2 = 0.37$). This is consistent with the findings of McCoy and Burn (2001), who observed that the highest correlation between spring flooding and snow depth was with Calumet.

Secondly, March 1st SWE values for Calumet (the record with the highest correlation; $R^2 = 0.37$) and Mayo A (the longest snow course record; $R^2 = 0.27$) are plotted alongside Stewart River spring peak discharge (Figure 8). Again, it is evident that years with high March 1st SWE values produce above-average peaks in downstream discharge. This figure also highlights the three periods of potential SWE variability identified in Figure 6. As described, Period A (1964-1984) appears to exhibit generally below-average March 1st SWE (see Figure 6). Peak spring discharge on the Stewart River during this 20-year period exceeds average peak spring discharge on 8 occasions, equivalent to once every 2.5 years. During Period B (1985-1995), when SWE appears to have been generally above-average, there were 6 above-average spring peak discharge events, equivalent to once every 1.4 years. Finally, during Period C (1996-2010), when SWE may have generally fluctuated around average, peak spring discharge exceeded average on 5 occasions, equivalent to once every 2.8 years.

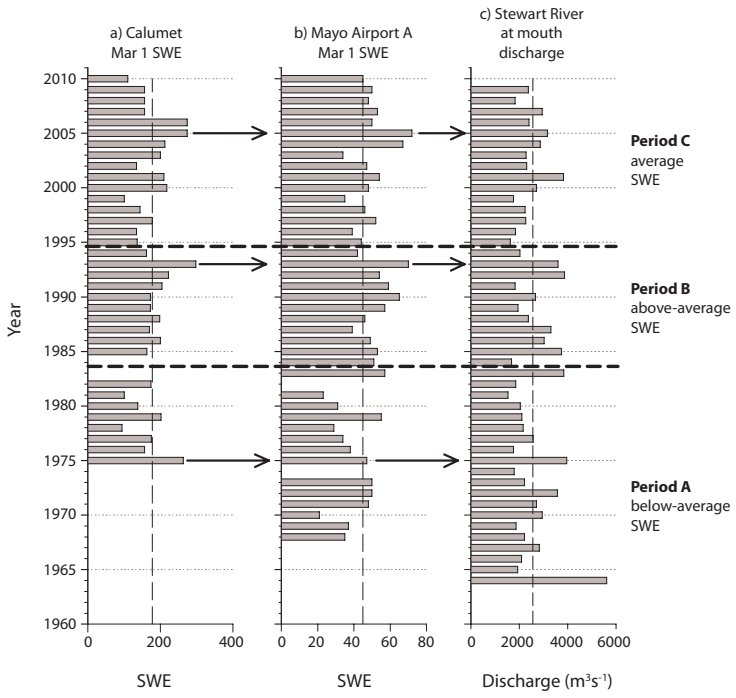

Figure 8. *March 1st snow water equivalents for snow courses at Calumet and Mayo A (plots a and b respectively; Water Resources Branch, 2010b), and peak spring discharge on the Stewart River at its mouth (plot c; Water Survey of Canada, 2010). Vertical dashed lines indicate average conditions for each parameter respectively. Heavy horizontal dashed lines border potential periods of SWE variability identified in Figure 6, which are labeled along the right margin of this figure. Arrows identify examples of high SWE values present in both snow course records and corresponding downstream spring discharge peaks.*

While the comparisons between SWE and discharge presented here and in the above paragraphs are rudimentary and likely reflect variability inherent in the system, they will serve as useful points for discussion of the effects of on-going climate change and variability on the hydrology of the Mayo region, as discussed further in the sections below.

SURFICIAL GEOLOGY

Surficial geology in Mayo reflects a glaciated landscape that has undergone significant modification from fluvial, eolian and permafrost processes. The Village of Mayo is located just inside the limit of the maximum extent of the last glaciation that occurred in Yukon, known as the McConnell Glaciation. This glacial advance occurred some 20 000 years before present, leaving behind morainal deposits on the slopes above the town site. Deglacial lakes, deltas and terraces filled the valley as the glacier retreated, leaving thick deposits of fine-grained lacustrine and coarse-grained glaciofluvial materials across the valley.

GLACIAL HISTORY

Glacial limits in the Mayo region were originally noted by Bostock (1966) and later the surficial geology was mapped by Hughes (1983). Bostock (1966) recognized four advances of the Cordilleran Ice Sheet: Nansen, Klaza, Reid and McConnell (from oldest to youngest). However, subsequent authors have rarely distinguished between events that are older than the Reid advance, and collectively refer to these older glacial episodes as the 'Pre-Reid' glacial event, which represents up to seven glacial advances (Figure 9). Only the most recent two glacial advances are easily distinguishable in the Mayo region. The Reid advance was more extensive than the McConnell advance, and reached its westward limit some 80 km west of Mayo at Reid Lakes. This advance likely took place ~130 000 years before present and inundated all but the highest peaks around Mayo (Ward *et al.*, 2008; Stroeven *et al.*, 2010). Late-Wisconsin

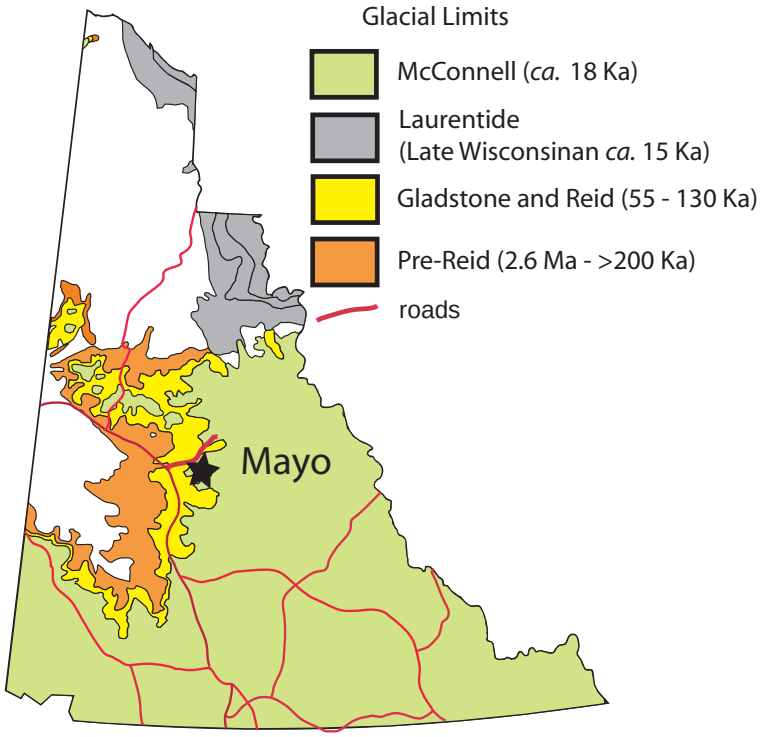

Figure 9. *Simplified glacial limits map of the Yukon (modified from Duk-Rodkin, 1999).*

McConnell-age glacial deposits are readily recognizable and well preserved in the Mayo region. The McConnell advance was the least extensive Cordilleran advance in Yukon and the western limit in central Yukon occurs some 20 km west of Mayo in the Stewart River valley. This less-extensive advance only reached elevations of ~700 m in the Mayo area and left most of the uplands ice-free.

The Quaternary history of the Mayo region was outlined by Giles (1993) based on his work at various exposures around the townsite of Mayo (Figure 10):

1. ***Mid-Wisconsinan interglacial (~30 000 years before present):*** A large wandering gravel-bed river flowed south through the Mayo River valley and into the Stewart River valley, similar in appearance to the modern Stewart River downstream of Mayo (Figure 10a). The Stewart River at this time was likely a small tributary to the Mayo River and would have formed a wide braidplain at its confluence with the larger Mayo River.
2. ***Proglacial:*** As ice advanced down the Stewart River valley, a pro-glacial lake formed in the Mayo River valley and discharged along the northwest margin of the ice in the Stewart River valley. The outlet of this lake incised deep meltwater channels in bedrock – one of which is currently being used by the Mayo River (the Wareham Dam is built in one of these channels). The discharge from this lake also contributed to thick gravel terrace deposits on the north side of the Stewart River valley (Figure 10b). When the southern outlet was blocked by advancing ice, water was diverted west through Minto Creek and formed a deeply incised meltwater channel in this valley.
3. ***Glacial maximum (~20-25 000 years before present):*** Ice in the Stewart River valley advanced past Mayo, forming a lateral or re-advance moraine across lower Mayo River valley (Figure 10c). Deposition of till was limited at this time, and ice-marginal drainage was likely maintained along the north margin of the ice sheet, forming high glaciofluvial terraces against the ice front.
4. ***Postglacial:*** As the ice sheet began to retreat, an ice mass blocked drainage below the Village of Mayo and impounded a lake that reached a depth of ~550 m in the Stewart River valley (Figure 10d). Meanwhile, retreat of the Stewart River valley ice allowed the lake in the Mayo River valley to begin draining south into the Stewart River valley. A minor re-advance likely formed a lateral moraine across the Mayo Valley and dammed water in the Wareham Lake basin to a depth of ~610 m.
5. ***Holocene (~10 000 years ago until present):*** After ice retreated and the remaining lakes drained, a large volume of fine-grained glaciolacustrine and glacially scoured material was available to be transported and reworked by eolian processes. The transport of fine-grained eolian material likely remained a dominant sedimentary process until moister conditions prevailed and vegetation became established ~9000 years ago (Wolfe *et al.*, 2011). Since this time, eolian deposition has been limited to cliff-top loess deposition above unvegetated sediment bluffs. The growth of permafrost in poorly drained, fine-grained materials is responsible for shifts in vegetation cover and the establishments of thermokarst lakes and ponds over much of eastern Mayo (Burn *et al.*, 1986). Ongoing incision of glacial sediments by the Stewart and Mayo rivers continues to transport large volumes of sediment within the map area.

Surficial materials

The surficial geology for Mayo (*see accompanying map "Surficial Geology of the Village of Mayo"*; Kennedy, 2011) has been mapped based on existing subsurface data, previous surficial geology mapping (Bostock, 1966; Hughes, 1983; Giles, 1993), air photo interpretation, and

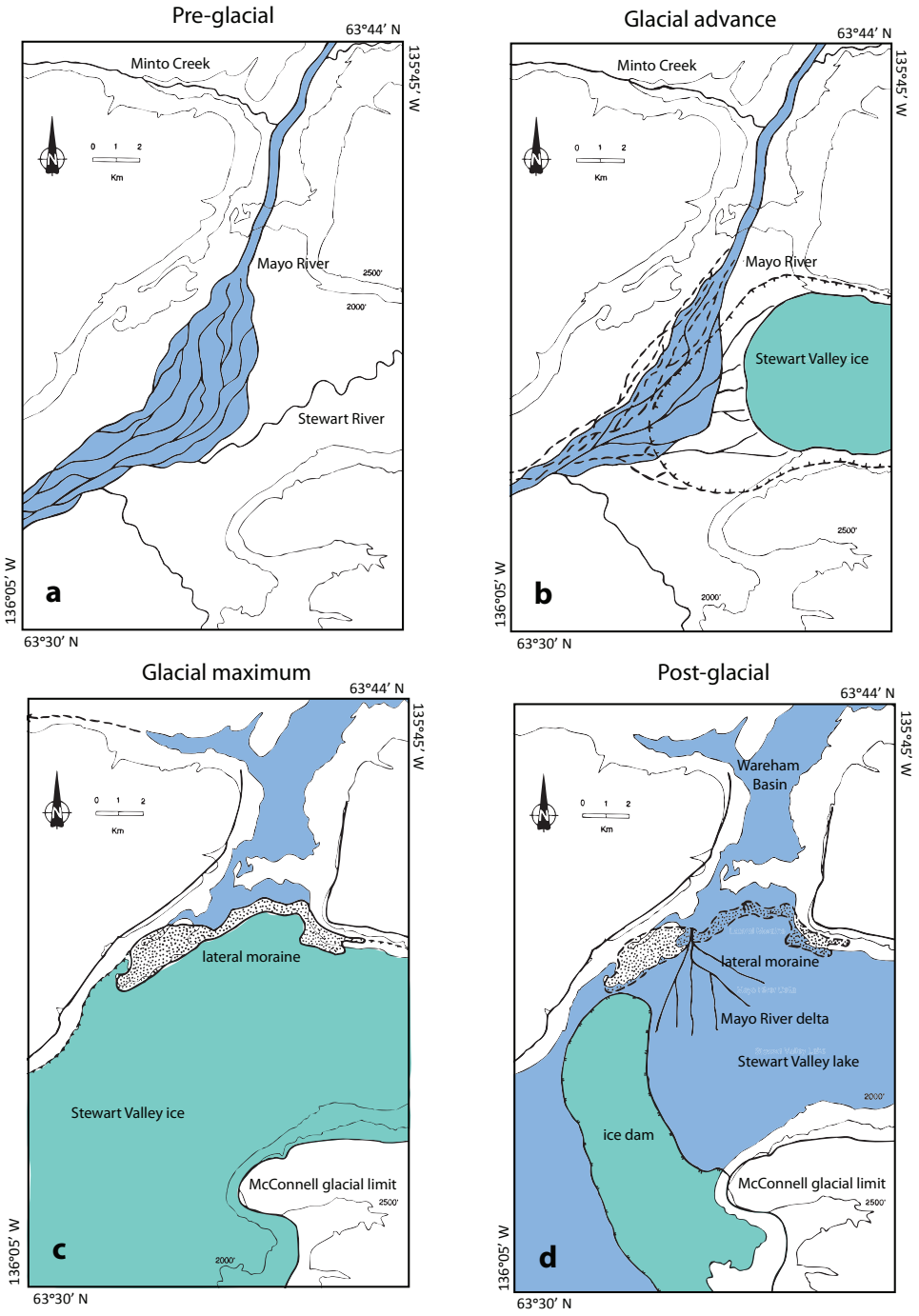

Figure 10. *Paleogeographic reconstruction of the Mayo region during pre-glacial* ***(a)****, glacial advance* ***(b)****, glacial maximum* ***(c)****, and immediately post-glacial* ***(d)*** *conditions. Figures from Giles (1993).*

ground truthing. New data includes textural information for more than 40 landforms (Appendix A), geophysical profiles of the subsurface (using Ground Penetrating Radar and Direct Current Electrical Resistivity), new shallow boreholes, and logging of riverbank exposures. Previously acquired subsurface geological data was made available from borehole, test pits, and water well

logs provided by EBA Engineering Consultants Ltd. (R. Trimble, EBA Engineering, pers. comm., 2010).

Surficial materials in the Mayo region are derived from glacial, fluvial, lacustrine, colluvial, eolian and organic processes. Each process, or combination of processes, forms distinct materials that can be characterized based on the grain size, sorting, structure, and general distribution of the material. Detailed descriptions of the surficial materials found in the Mayo map area are located in the map legend (*see accompanying map "Surficial Geology of the Village of Mayo";* Kennedy, 2011). Common materials in the Mayo region are those derived from glacial, glaciofluvial, glaciolacustrine and modern fluvial processes.

Moraine deposits include materials that have been deposited directly by a glacier or ice sheet without modification by any other agent of transportation. Moraine deposits in the Mayo region are characterized by poorly sorted, weakly compacted material lacking stratification and containing a heterogeneous mixture of particle sizes, usually in a matrix of sand, silt and clay (Figure 11). In general, moraine deposits in the map area are found in lateral and terminal moraines and moraine complex landforms. Moraines are located on surrounding hillsides at elevations of ~700 m a.s.l. and in broad east-trending bands in the Mayo River valley (Figure 12).

Figure 11. *This example of a typical moraine deposit lacks structure, grading and bedding, and is composed of a wide range of particle sizes.*

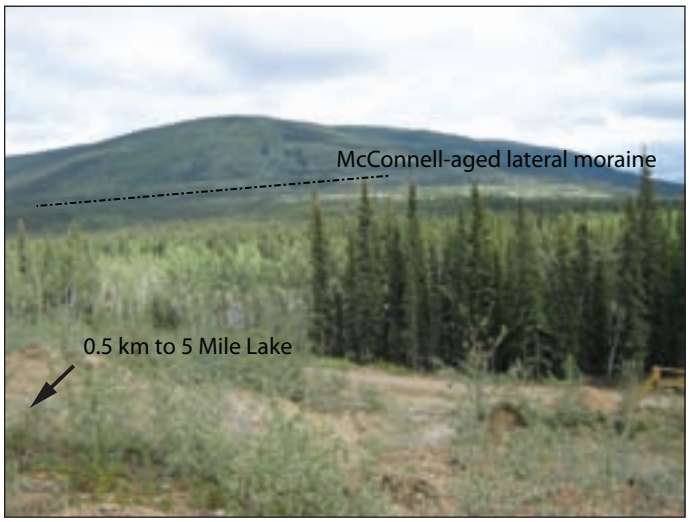

Figure 12. *A McConnell-aged lateral moraine (dashed line) is visible on a slope near Mayo. This moraine is continuous with moraine ridges that cross the Mayo River valley near 5 Mile Lake.*

Glaciofluvial deposits include materials that have been deposited by glacial meltwater either directly in front of, or in contact with, glacier ice. Glaciofluvial materials typically range from non-sorted and non-bedded gravel made up of a wide range of particle sizes, associated with very rapid aggradation at an ice front, to moderately to well-sorted, stratified gravel. Glaciofluvial materials are abundant in the Mayo region. They typically form kettled and hummocky plain surfaces, but are also present as ridged and undulating landforms when deposited along a glacier margin. There are generally two categories of glaciofluvial deposits in the Mayo region; those that formed in close proximity to the ice margin, and those that formed more distal to the ice in a dominantly fluvial environment. Proximal glaciofluvial deposits are characterized by a greater range in particle size and exhibit less well-defined stratification and sorting. Distal glaciofluvial deposits are characterized by well-stratified, well-sorted, more uniformly graded and bedded sediments (Figure 13).

Figure 13. *Well-sorted and graded beds of sand-pebble gravel are common deposits in distal glaciofluvial environments.*

Glaciolacustrine materials are deposited in, or along, the margins of glacial (ice-dammed) lakes and include sediments that were released by the melting of floating ice. Glaciolacustrine materials are common in the Mayo region and can include lake bed sediments consisting of stratified fine sand, silt and/or clay with rare lenses of till and/or glaciofluvial material (Figure 14). Coarse-grained sediments coming out of the Mayo River valley during and after deposition of the glacial lake sediments in the Stewart River valley, deposited fan and delta landforms at the north end of the glacial lake (Figure 15). Coarse-grained sediments in these landforms are often interbedded with fine-grained glaciolacustrine sediments, but in general, are significantly better drained, less ice-rich and more stable than landforms to the south and east that lack the coarse-grained component.

Fluvial deposits are materials that have been transported and deposited by streams and rivers. Fluvial sediments mapped in the Mayo area are predominantly those associated with floodplains, fluvial terraces and channels of the Mayo River (Figure 16). These deposits generally consist of stratified beds of gravel and/or sand with sand and/or silt and/or organic materials (and rarely clay). Fluvial deposits associated with the Stewart River are only mapped upstream of its confluence with the Mayo River, where sediments remain dominantly fine-grained. Point bar deposits of the Stewart River are composed primarily of sand and silt with minor organic materials.

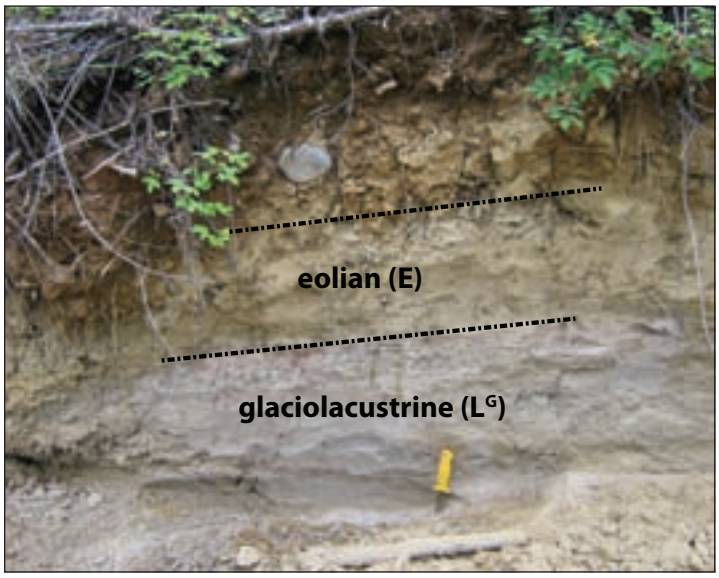

Figure 14. *Fine sand, silt and clay was deposited in glacial lakes (glaciolacustrine deposits, L^G) and subsequently reworked by wind into thick eolian deposits (eolian, E) in the Mayo region.*

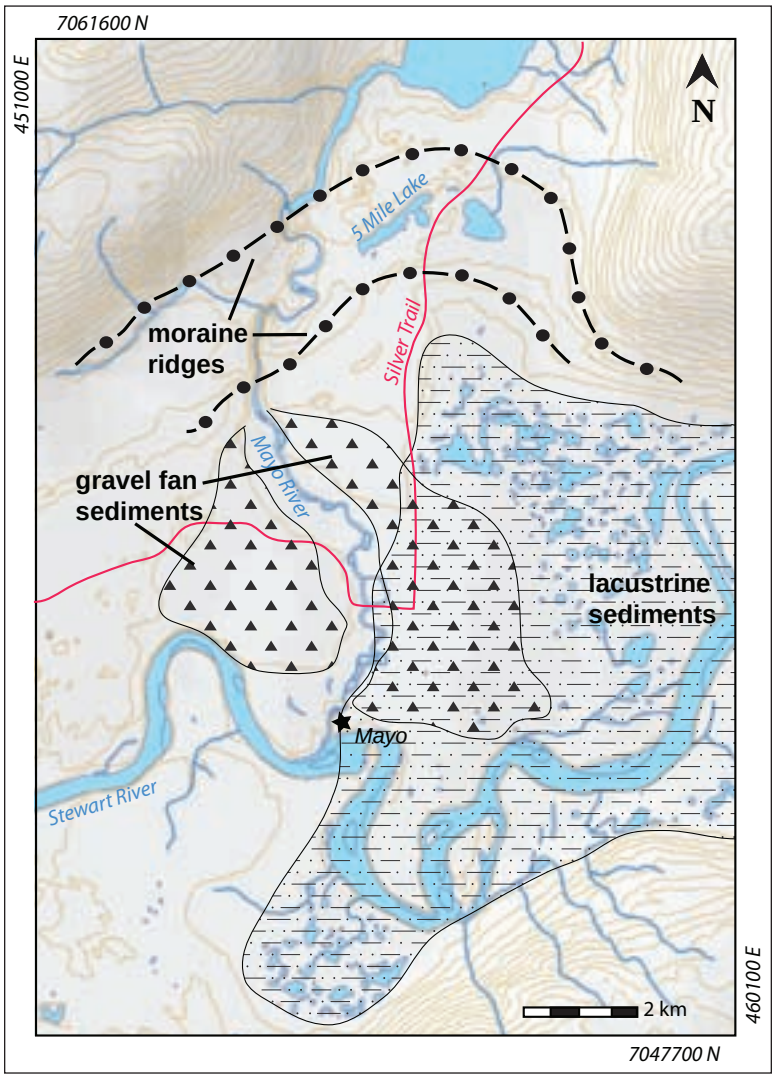

Figure 15. *Glaciolacustrine sediments (dashed pattern) are overlain and sometimes interbedded with gravel-rich glaciofluvial fan sediments (triangle pattern) around the Village of Mayo. Dashed lines outline moraine ridges.*

Figure 16. *Modern floodplain deposits of the Mayo River are typically coarse gravel and sand, and are associated with minor amounts of silt, clay and organic material that are deposited in overbank environments.*

STRATIGRAPHY

The vertical layering of sediments can be a strong control on landscape stability. Simplified stratigraphy of the Mayo region is presented in Figure 17. Bedrock is at surface near Wareham Dam, but descends steeply to the south to achieve depths of more than 300 m below the Village of Mayo (Stanley and Associates, 1990). This thick package of unconsolidated sediments that overlies bedrock is likely made up of deposits spanning many glacial periods. Moraine deposits are visible at surface only in the northern part of the map area, where bedrock is close to the surface. These deposits are likely found below glaciofluvial and glaciolacustrine sediments to the south; however, they are not well exposed. A typical layering of surficial materials near 5 Mile Lake is presented in Figure 18 (section 10-KK-019). Toward the southern part of the map area, glaciofluvial sediments dominate the landscape. These deposits frequently exhibit a wide vertical range in sediment types and textures, reflecting the high-energy environments they were deposited in. A typical layering of surficial materials near the First Nation of Na-Cho Nyäk Dun Main Administration Building is presented in Figure 19 (section 10-KK-042).

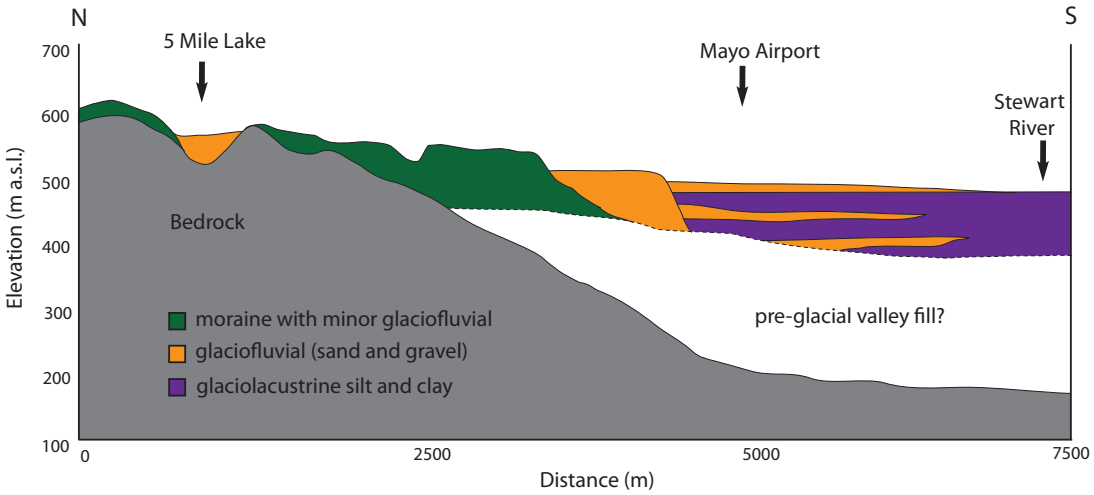

Figure 17. *A profile of the distribution of surficial sediments in the Mayo area illustrates the probable subsurface contacts between unconsolidated materials and underlying bedrock.*

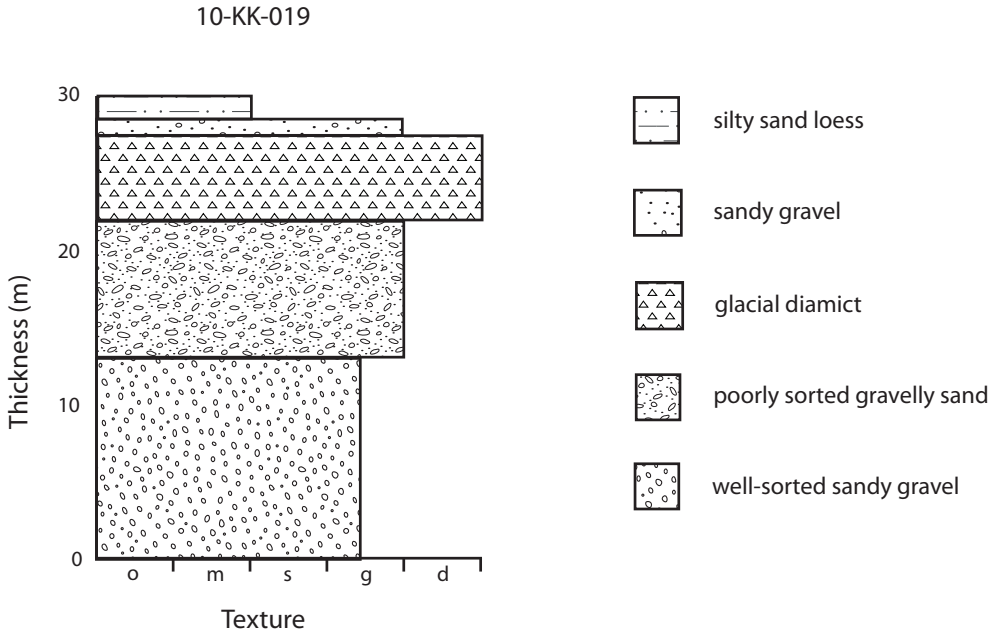

Figure 18. *Measured stratigraphic section 10-KK-019 near 5 Mile Lake; see Figure 1 for section location.*

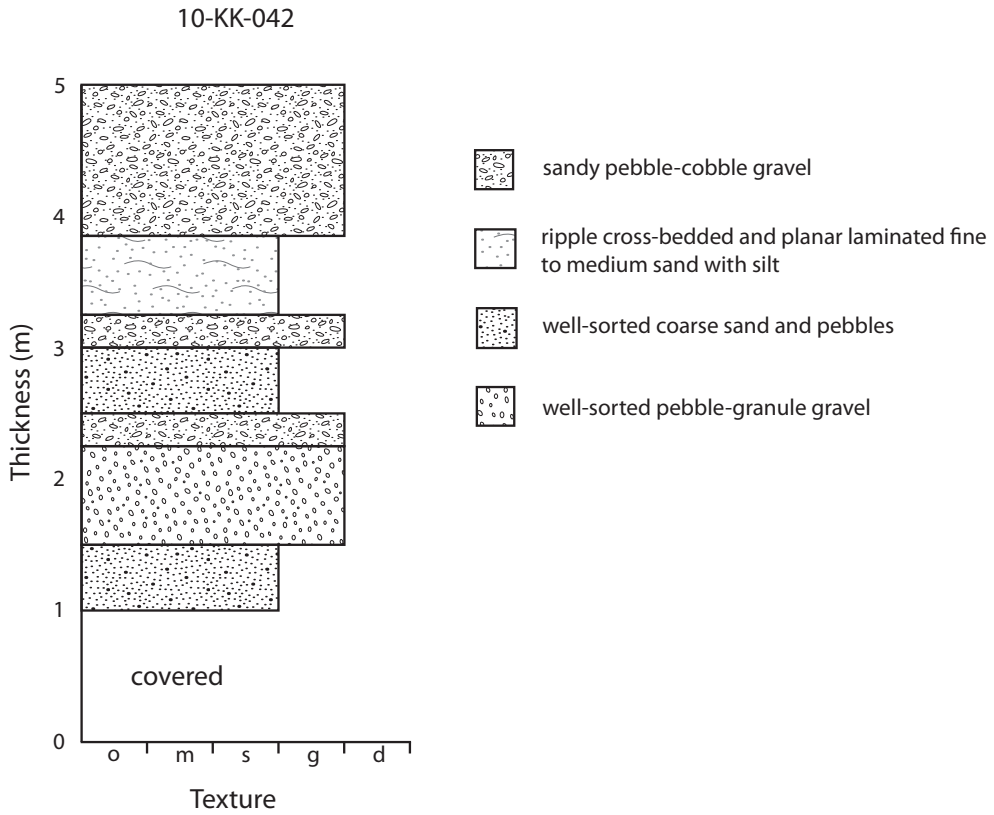

Figure 19. *Measured stratigraphic section 10-KK-042 near the First Nation of Na-Cho Nyäk Dun Main Administration Building; see Figure 1 for section location.*

Geologic hazards

The materials making up the surficial geology in and around Mayo are, for the most part, stable. However, geological, hydrological and climatological processes operating on these materials can pose a hazard to existing and future development. Mayo has abundant gravel and sand-rich landforms that are stable, well drained and ice free. Many of these landforms also occur above the floodplains of both the Mayo and Stewart rivers. These are ideal building sites for future infrastructure. Less stable landforms in the Mayo region include glaciolacustrine materials, moraine deposits, and some point bar deposits along the Stewart River.

Point bar landforms along the Stewart River are displaying tension cracking related to erosion of the landform along the river bank. These tension cracks are up to 500 m long, 2 m wide, and 1 m deep, and are oriented both perpendicular and parallel to the nearest river bank (Figure 20). These features likely form slowly and there is no evidence of catastrophic failure of the bank. Furthermore, all of the areas where these features were observed were outside of the dyke system on the Stewart River floodplain and are therefore already poor building sites.

Figure 20. *An example of the largest tension crack observed in point bar sediments deposited by the Stewart River. This crack is ~1.5 m deep and can be traced for more than 500 m.*

Moraine deposits in the Mayo area are mostly stable; however, the potential for buried glacier ice or permafrost to be present on these landforms is higher than other landforms because of the poor drainage capacity inherent in these materials. North-facing slopes are likely to contain permafrost. 'Policemans's Hill' or 'Glacier Hill' may have significant bodies of ice buried in the landform which are slowly melting and destabilizing the north-facing slope at the south end of Wareham Lake. Tension cracking is also present on this hillslope, and road maintenance is going to continue to be a problem until the ice melts completely and the landform reaches a stable position.

Glaciolacustrine sediments have, by far, caused the most damage to buildings and other infrastructure in the Mayo region. These sediments are almost always affected by permafrost, and the permafrost in these materials can be ice-rich. Thawing of permafrost can lead to significant settlement of the ground surface as is evidenced by the many hollows, depressions and thermokarst landforms on the eastern side of the Village.

The distribution of glaciolacustrine deposits is important for identifying potentially unstable landforms. Because they were deposited at a relatively low elevation, glaciolacustrine deposits are not exposed at surface in the Mayo area and require sub-surface investigations to describe their properties and identify their distributions. While the total thickness of glaciolacustrine materials is unknown, basement excavations, borehole and well drilling, as well as hand augering have all contributed to a basic understanding of thicknesses and distribution. Generally, glaciolacustrine sediments are present east of the Silver Trail and south of 5 Mile Lake; Figure 15). A fan of gravel overlies some of this area, and serves to insulate the permafrost and reduce thermokarst. The apex of the fan is located ~1 km northwest of the airport, and thins toward the south and east from >10 m thick, to less than 1 m thick at its southern extent (Figure 21).

The permafrost properties of surficial materials in the Mayo region are a significant source of potential landscape instability and will be discussed in detail in the following section.

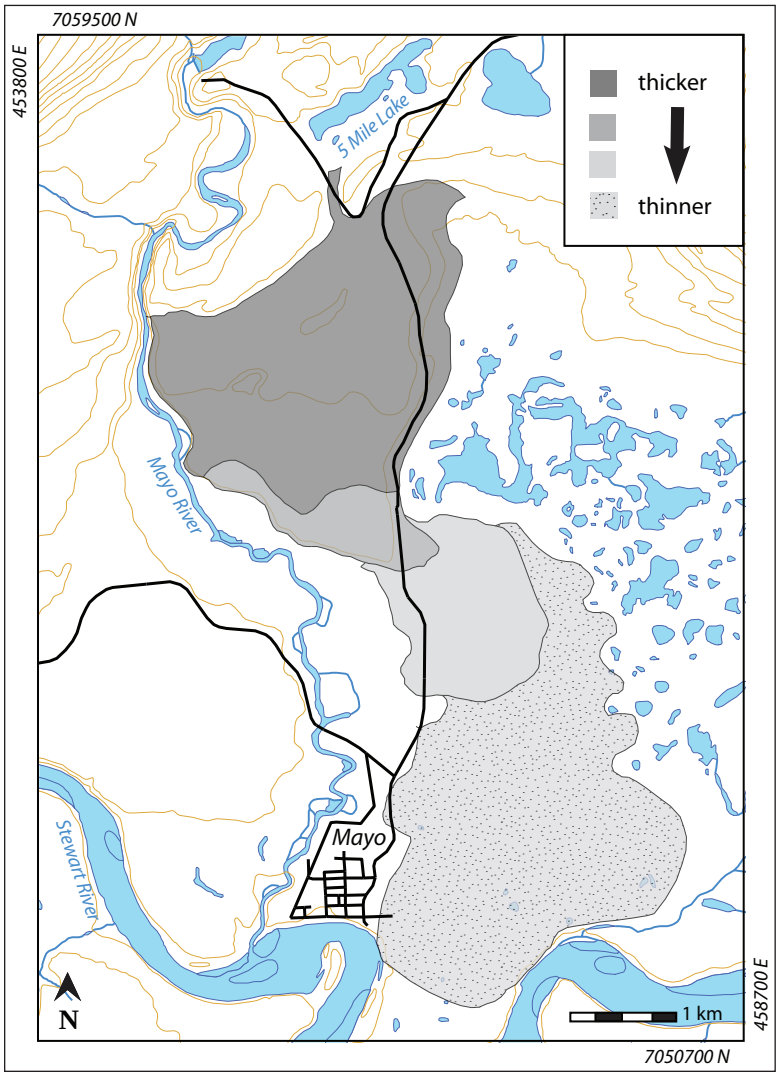

Figure 21. *A fan, which likely deposited into a glacial lake in the Stewart River valley, is thickest to the northwest of the airport and thins to the south and east.*

PERMAFROST

Earth materials (surficial materials, bedrock and ice in the ground) that remain at temperatures below 0°C for more than one year are called permafrost. The surface layer that lies on top of permafrost and freezes and thaws annually is called the active layer. The Village of Mayo is located in the extensive discontinuous permafrost zone according to the Permafrost Map of Canada (Heginbottom *et al.*, 1995), meaning that more than half, but less than 90%, of the natural landscape is expected to be underlain by permafrost (Figure 22). The distribution of permafrost shown on this map is considerably generalized and predictions were made using climatic information at the scale of the entire country.

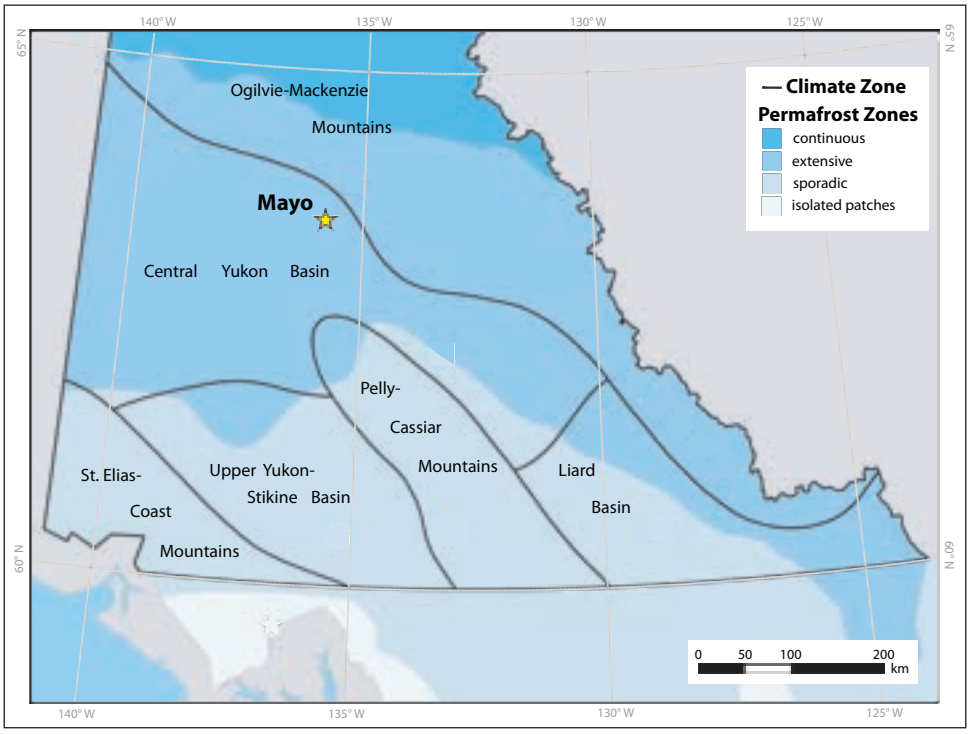

Figure 22. *Location of Mayo in relation to permafrost zones (after Heginbottom et al., 1995) and climatic regions in the Yukon (after Wahl et al., 1987).*

Permafrost in the discontinuous zone tends to be more likely associated with fine-grained sediments or peat deposits where there are typically thick organic mats (mosses and other similar ground covers), and coniferous vegetation. Permafrost is commonly found in colder micro-climates (such as on north-facing slopes and in valley bottoms). However, predicting which sites are affected by permafrost and which are not, over an area of discontinuous permafrost, is very challenging because of the number of factors that influence temperatures in the ground.

Figure 23 illustrates the results of recent permafrost probability modelling based on fieldwork carried out throughout the southern Yukon over the past five years (Lewkowicz and Bonnaventure, 2011; Bonnaventure *et al.*, *in press*). This map can be used to examine broad patterns of permafrost distribution across the landscape, but it is not a tool for site-level predictions because it does not take into account the effects of the local factors mentioned above (*i.e.*, surficial materials, vegetation and differential snow accumulation). The map shows probabilities ranging from 0.3 to 0.9, and values for the Village of Mayo range from 0.6 to 0.7. Probabilities are relatively high in the main valley floor and on north-facing slopes, as well

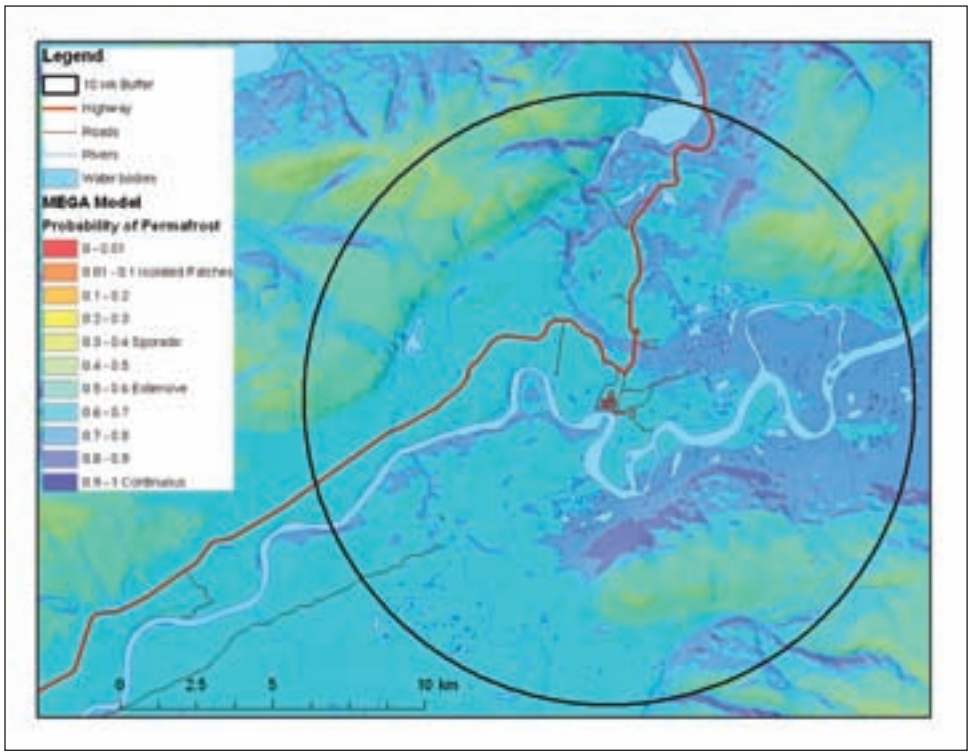

Figure 23. *Map of predicted permafrost probabilities under current climatic conditions, centred on Mayo, Yukon. The circle encloses terrain within 10 km of the Village of Mayo. Note: these predictions do not include local variations related to surficial deposits or any other types of micro-variability, and therefore, are not designed for use at the site level. Predictions are based on methods described in Lewkowicz and Bonnaventure (2011) and Bonnaventure et al., (in press).*

as lower on south-facing slopes and exposed ridges. This map supports the classification of Heginbottom *et al.* (1995) and indicates that in the absence of disturbance (which warms the ground and thereby thaws permafrost), it is highly likely that permafrost would be found at any given site in the vicinity of Mayo (2 out of 3 chances), but less likely on higher ground.

By definition, in the discontinuous permafrost zone, there must be some sites where ground temperatures average less than 0°C (permafrost sites) and others where temperatures are greater than 0°C (non-permafrost sites). The closer the temperatures of permafrost are to 0°C, the more likely it is that permafrost will thaw following disturbances such as vegetation clearance, construction, forest fire and climatic change. The impacts of this thaw will depend on how rapidly it occurs, and whether the permafrost contains a significant amount of ground ice, little ice, or no ice. It is critical to understand the characteristics and nature of permafrost prior to construction or infrastructure development, particularly in zones of discontinuous permafrost.

Little information is available regarding ground temperatures in the region around Mayo (R. Trimble, EBA Engineering, pers. comm., 2010). Burn (2000), however, gives a temperature of approximately -1.5°C at a depth of 12 m for an undisturbed forested site located on the opposite side of the Stewart River from the Village of Mayo (Figure 24). The base of permafrost at this site was at a depth of approximately 40 m. The active layer in the forest is usually between 0.6 m and 1.0 m thick (Leverington, 1995). Burn (2000) also showed that disturbance associated with

the thawing of ice-rich permafrost within a retrogressive thaw slump and subsequent changes in vegetation and snow warmed the ground at 1 m depth to temperatures above 0°C. Based on these observations, it is likely that permafrost temperatures in the Village of Mayo are between -1°C and 0°C, with slightly colder values in the surrounding area.

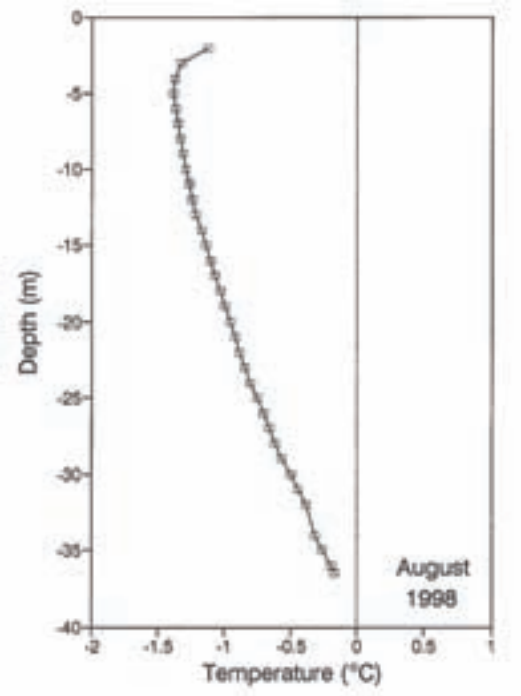

Figure 24. *Ground temperature profile in an undisturbed forested site located on the opposite side of the Stewart River from the Village of Mayo, August 13, 1998 (Burn, 2000).*

New field investigations for this report were undertaken in the summer and fall of 2010. Preliminary evaluations, including discussions with local area experts, led to the selection of representative sites that were assessed for permafrost conditions.

Direct current electrical resistivity profiling was carried out at nine sites. This geophysical technique uses a car battery to send electricity to a line of electrodes (stainless steel pins) inserted into the ground. The equipment (an ABEM Terrameter LS profiling system used with a Wenner array) measures the ability of the ground to conduct the electricity and builds up a profile whose depth depends on the spread of the array of electrodes (*i.e.*, 25 m for an array 160 m in length and 13 m for an 80 m array). Ice in frozen ground is a poor conductor of electricity while water in unfrozen soils is a good conductor, so the pattern that emerges can usually be interpreted in terms of frozen and thawed ground (Kneisel *et al.*, 2008). Like any geophysical technique, the more that is known in advance about the site, the more that can be interpreted, so if little information is available, the interpretations may not be definitive.

Permafrost characteristics and resistivity profiling

The investigated sites can be grouped into three classes of interest to the Mayo community. The first is the townsite itself, which mainly is located in the western part of the Village of Mayo town limits, and includes the oldest settled area. The second area is mostly undeveloped, and includes the eastern thermokarst/forested area, and an area located north of the airport property. A third group contains two sites with major infrastructure: the airport and the sewage lagoon (see Figure 1 for permafrost site locations).

Central village area

Four sites were investigated, three of them being surveyed by electrical resistivity profiling: The J.V. Clark School, the pump house, the corner of 6th and Laurier, and the First Nation of Na-Cho Nyäk Dun (NND) subdivision at the eastern edge of the village.

The J.V. Clark School area provides information about permafrost conditions in the inner areas of the village, as well as in the nearby surrounding uninhabited areas. The school was built on a site that had undergone several decades of permafrost disturbance, as a previous school building had existed there. An annex of Yukon College was subsequently added to the main building of the new school, and it experienced some thaw settlement several years later indicating that permafrost still existed on the site (Figure 25). Unlike the school, the annex was built on a formerly forested area, similar to the one surrounding the northern boundaries of the school property.

Figure 25. *Examples of infrastructure damage due to permafrost thawing and ground subsidence observed at the Yukon College annex, J.V. Clark School, Mayo.*

Field investigations were undertaken in the disturbed open land and in the wooded areas adjacent to the school. Field observations determined that permafrost is present in the forested areas, and it has a relatively thin active layer. Two resistivity surveys were undertaken at this site: one survey conducted at the extreme northern end of the property that extended from an open area close to the school sports field, into a disturbed wooded area; and a second survey, slightly further east, that extended from a disturbed open forest area, into a less disturbed and denser one. The results of the first survey suggest that permafrost is around 5 to 7 m thick, and given this minimal thickness, it must be relatively warm and hence susceptible to thaw. In the second survey, minor disturbance to the vegetation in the first half of the survey seems to have created a talik (a perennially thawed zone), while in that part of the survey where the vegetation is undisturbed, the permafrost is more than 25 m (Figure 26; see Figure 3 for location). Field observations and well logs (R. Trimble, EBA Engineering, pers. comm., 2010) support these interpretations; however, variability in active layer thickness and depth to permafrost is common (see Figure 27 for schematic subsurface profile under the J.V. Clark School).

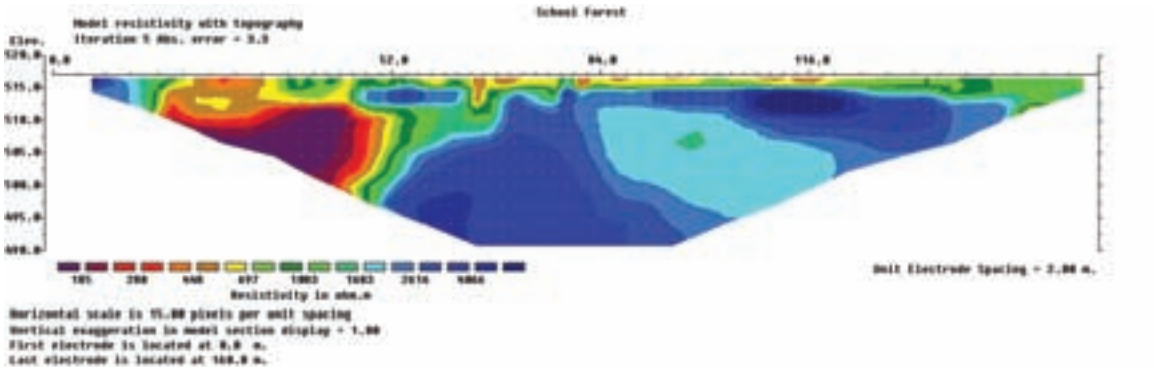

Figure 26. *Resistivity profile in the forest northeast of the school. Note: in this and the other resistivity profiles presented, blue colours represent high resistivities (generally meaning frozen conditions) and red colours represent low resistivities (generally meaning unfrozen conditions). The transition value between frozen and unfrozen is not fixed but is probably between 300 and 1000 ohm metres. Vertical axis represents elevation in metres a.s.l.*

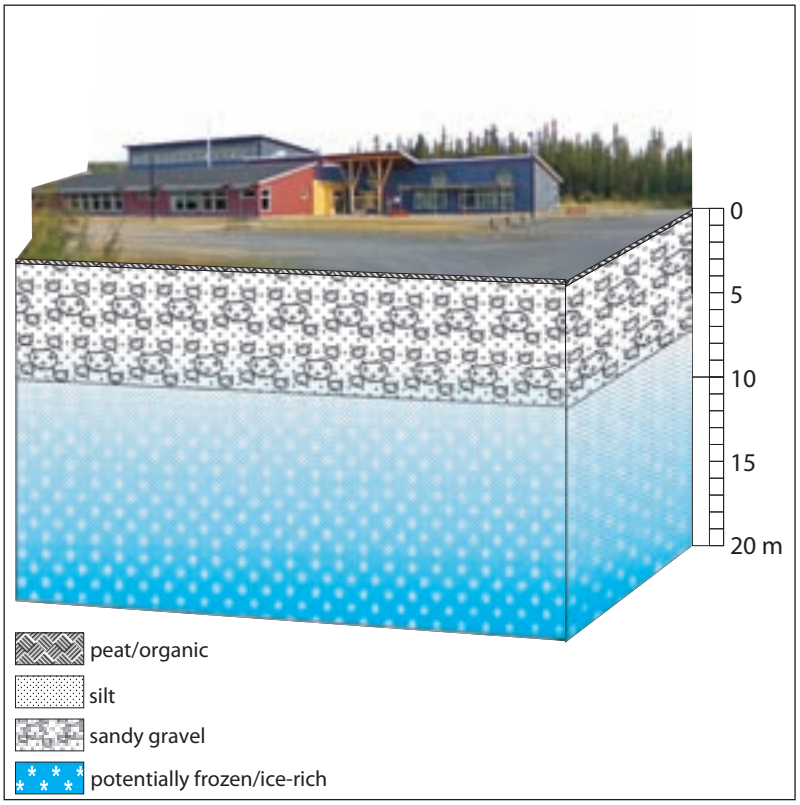

Figure 27. *Schematic diagram of the subsurface conditions below the J.V. Clark School, Mayo.*

A resistivity survey was conducted in the village close to the pump house (Figure 28; see Figure 3 for location). Physical probing encountered the frost table at 1.1 m, and the profiling illustrates a 7 to 8 m-thick permafrost layer overlying unfrozen sediments. The resistivity values within the permafrost suggested that it is at most moderately ice-rich, but this would require confirmation by coring as the values could also reflect high unfrozen moisture contents at temperatures very close to 0°C.

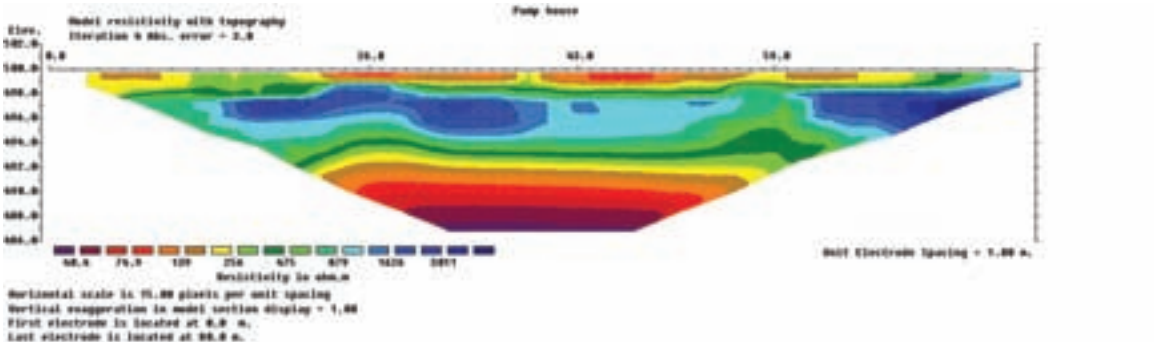

Figure 28. *Resistivity profile near the pump house, Mayo.*

The corner between 6th and Laurier was also investigated by resistivity survey. The profile was interpreted as representing a continuous layer of permafrost of moderate ice content extending to a depth of 4 m, overlain by an active layer, and at one end of the profile, possibly by a shallow supra-permafrost talik. Conditions below 4 m are uncertain and could be thawed or frozen.

A resistivity investigation was not conducted at the eastern NND subdivision; however, some field investigations were undertaken, and a survey previously done by EBA Engineering in this area was also examined (R. Trimble, EBA Engineering, pers. comm., 2010). This area is adjacent to the thermokarst field discussed below. Numerous problems were reported ranging from road settlement and subsidence, to moisture-related concerns in residential buildings. The borehole logs indicate that the underlying frozen silt may be ice-rich as it includes ice lenses up to 7 cm thick. A relatively shallow ice-rich silty-clayey sediment unit is probably responsible for most of the reported problems at this location (Figure 29).

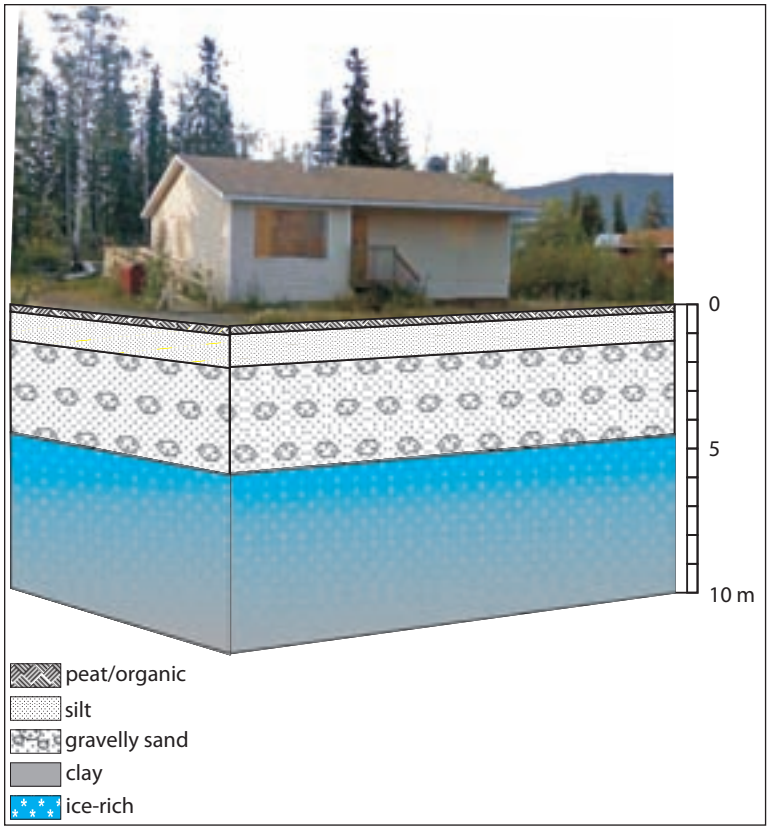

Figure 29. *Schematic diagram of the subsurface conditions below a house located in the eastern NND subdivision.*

In summary, the resistivity profiles indicate that permafrost may be present beneath sites within the developed area of the Village of Mayo, and it is probably warm (likely -0.5°C to 0°C), and has a low to medium ice content. The EBA borehole logs also suggest that most of the ground beneath the village is not ice-rich (R. Trimble, EBA Engineering, pers. comm., 2010). Nevertheless, residual permafrost still could be present at greater depths and even the ice-poor upper permafrost could potentially induce settlement if it thaws. The vegetation and the surficial organic layer should be maintained if possible during any future development, as they have a significant impact on preserving permafrost.

Eastern forested and thermokarst area

This area groups zones exhibiting similar geomorphological characteristics, including the presence of inactive and active thermokarst ponds/lakes. Numerous problems, such as road settlement, subsidence, and humidity-related concerns in dwellings, have been reported in developed sites located close or within this area (*i.e.*, the baseball field and the old NND subdivision located in the southeastern part of the village). As indicated above, the EBA borehole logs and published studies (*e.g.*, Burn *et al.*, 1986) demonstrate that the underlying frozen silt can be ice-rich.

Resistivity profiling was undertaken near the floatplane launch site, located between the Stewart River and the thermokarst terrain. The profile is interpreted as ice-rich permafrost in the top 10-15 m, but it is unclear whether permafrost or thawed soils are present beneath.

Another resistivity survey was conducted in a deciduous forest along the road leading to the NND Lands Department building, and crossing the thermokarst terrain area. The profile illustrates that 4-5 m-thick permafrost overlies unfrozen sediments, and a second permafrost layer possibly exists at depths below 15 m (Figure 30; see Figure 3 for location). If this interpretation is correct, it indicates that the site has been disturbed at least several decades in the past, probably by forest fire, resulting in deep thaw. As the site re-vegetated, permafrost began to form in the near-surface layers. These observations match those in EBA borehole logs (R. Trimble, EBA Engineering, pers, comm., 2010), and are also supported by observations made by Burn (2000), which show that permafrost can occur as deep as 40 m below surface in this area (Figure 31). Burn and Friele (1989) and Burn (2000) also show that the presence of an organic mat is a key element of permafrost preservation and that it can take 50 years or more for such conditions to redevelop after disturbance.

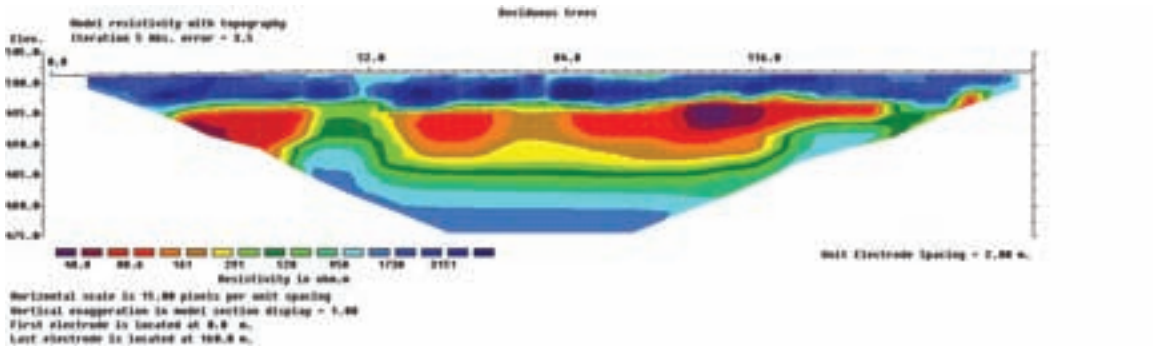

Figure 30. *Resistivity profile in deciduous forest near the road to the eastern NND subdivision, Mayo.*

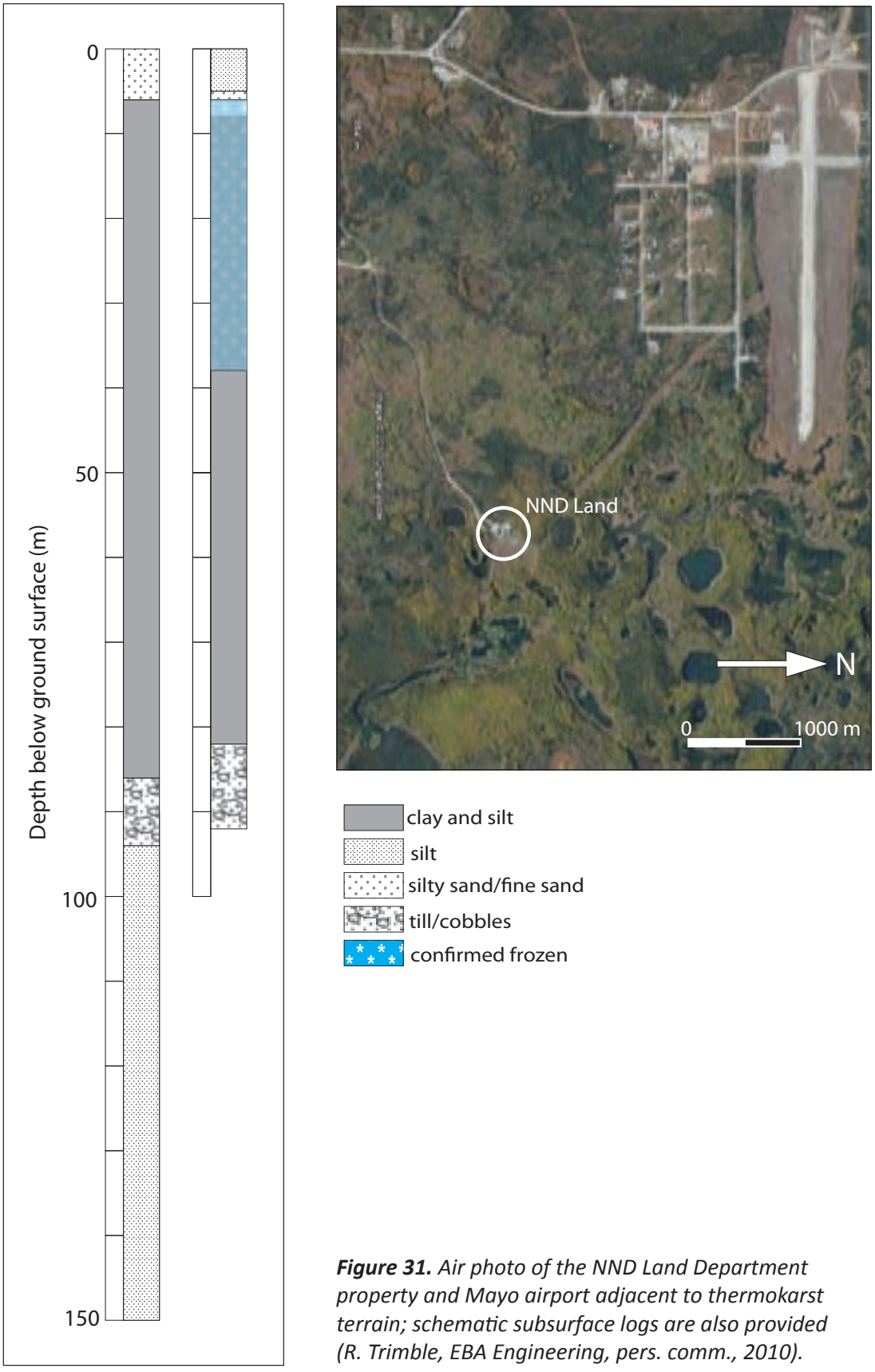

Figure 31. *Air photo of the NND Land Department property and Mayo airport adjacent to thermokarst terrain; schematic subsurface logs are also provided (R. Trimble, EBA Engineering, pers. comm., 2010).*

A third resistivity survey was undertaken about 1 km northwest of the Mayo airstrip, at the edge of the thermokarst zone. Interpretations from the first half of the profile demonstrate that there exists thin permafrost (3-4 m thick) that is relatively ice-rich overlying unfrozen sediments. These results contrast with the two previous surveys, and this may be due to the fact that this site is located at the boundary between two different surficial deposit areas.

Overall, this area has permafrost that can be problematic because it is potentially ice-rich in the upper part of the profile (*i.e.*, near surface) and it can extend as deep as 40 m below surface. In addition, because the ground can be saturated in some areas due to the thermokarst terrain, drainage problems unrelated or only partly related to permafrost could occur.

Major infrastructure

Two areas surrounding significant infrastructure for the community of Mayo were investigated: the airstrip and the sewage lagoon.

The northeast third of the Mayo airstrip shows evidence of ground thawing and settlement. Field observations suggest that overall ground subsidence has occurred over much of the area surrounding the Mayo airport as opposed to the thaw of very localized individual bodies of massive ground ice (Figures 32 and 33). A 320 m-long resistivity profile was run from the wetland/thermokarst area to the east of the Mayo airstrip, up a low ridge, and finally along the southern side of the affected airstrip section (Figure 34; see Figure 32 for airport configuration and Figure 3 for location). Permafrost extends to at least 25 m beneath the ridge and appears to be ice-rich to depths of 10-15 m. Much of the permafrost adjacent to the strip appears to have

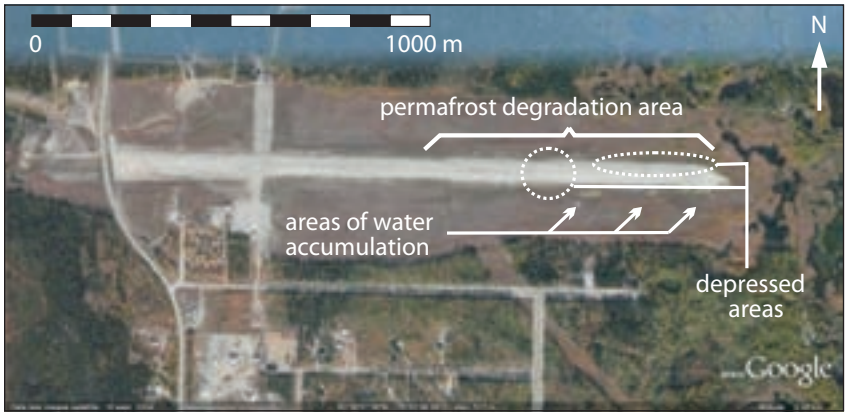

Figure 32. *Aerial photo image illustrating the configuration of the Mayo airport and the locations of reported degradation.*

Figure 33. *Examples of degradation observed on the Mayo airport landing strip.*

degraded at near-surface zones resulting in a talik, but frozen ground appears to still be present at depths below 10 m (Figure 35). The degradation of permafrost adjacent to the airstrip is linked to the clearance of the vegetation and the organic mat during construction, to landing strip management (*i.e.*, snow removal), and possibly to the flow of groundwater beneath the airstrip.

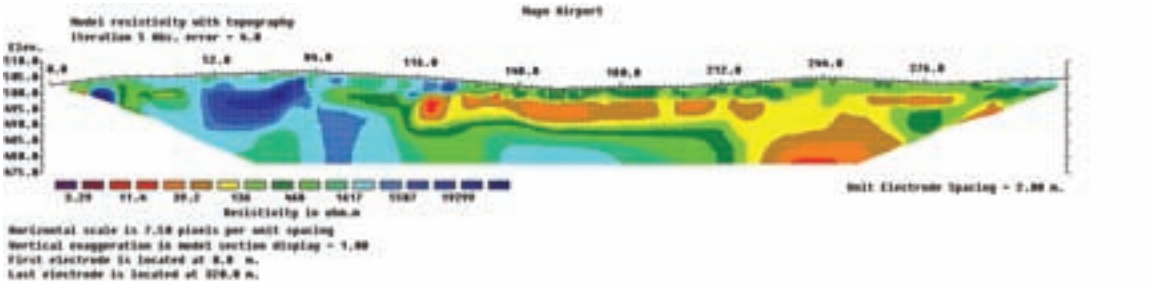

Figure 34. *Resistivity profile conducted from undisturbed terrain to an area along the southern side of the Mayo airstrip.*

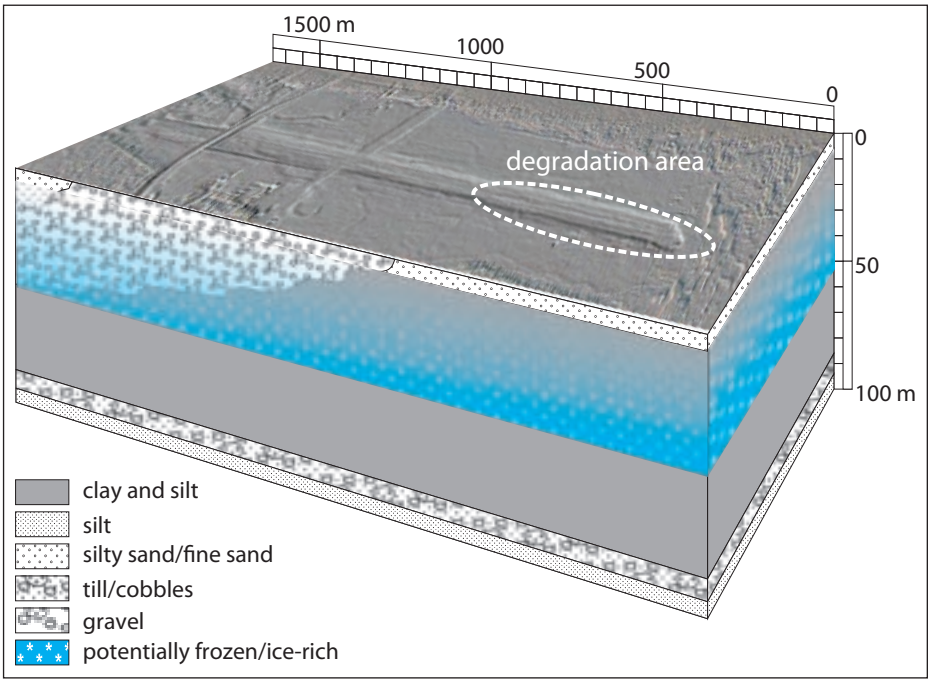

Figure 35. *Schematic diagram of the subsurface conditions below the Mayo airport.*

The second piece of community infrastructure examined was the sewage lagoon. No signs of ground surface settlement were noted. The resistivity survey started in the forest to the northwest of the lagoon and extended along a cleared area about 20 m from the lagoon fence. Probing determined the active layer to be ~70-90 cm thick in the forest, and the resistivity profile indicates that the permafrost extends to a depth of 25 m and contains pockets of more ice-rich or colder sediments in the top 8 m. In the cleared section, the permafrost table has descended to 3 m and a supra-permafrost talik is present. Results from the resistivity profile at this site confirm that permafrost in the area degrades following clearance of the forest and other vegetation, and that the degree of surface disturbance is directly related to how ice-rich the permafrost is.

Synthesis

Permafrost conditions in the Mayo area are variable and complex, as is typical of discontinuous permafrost zones. In terms of variability with depth, permafrost was found to be as thin as 5 m (indicating that it may have nearly disappeared), or as thick as 40 m. In addition to this vertical variability, permafrost has a lateral variability which is affected by numerous factors such as the history of ground surface disturbance, the type of sediments present, variability in slope aspect, groundwater flow, and the surface conditions which may affect surface runoff such as the type of vegetation (*i.e.*, presence of peat or other organic material).

Many of the sites examined exhibit thin permafrost. Although ground temperatures were not measured, it is inferred that this frozen ground is probably between -0.5°C and 0°C, and thus is sensitive to climate warming. Ground ice contents in the permafrost are inferred to vary from low to moderate at most of the sites examined; however, ice-rich sediments are documented in the Mayo area (R. Trimble, EBA Engineering, pers. comm., 2010). Even with low ice content, thaw of permafrost could induce uneven settlement and loss of support for infrastructure and therefore represent a concern during climate warming.

The presence of supra-permafrost taliks, mostly related to the removal of ground surface vegetation, emphasizes the protective role that vegetation and ground cover (especially mosses) plays on permafrost. The presence of an organic layer favours the preservation of permafrost because of its thermal properties (*i.e.*, the organic layer acts as an insulator to the permafrost). It is important to note however that a forest made up of predominantly deciduous trees with an understory lacking in mosses is not a firm indicator of the absence of permafrost in the Mayo area.

PROJECTED CLIMATE CHANGE AND POTENTIAL IMPACTS FOR THE MAYO REGION

This section is intended to summarize projected changes in climate for the Mayo region, and to identify potential impacts of these changes on the region's hydrology, surficial geology and permafrost.

CLIMATE

Projected changes in temperature and precipitation for the Mayo region have been developed for this report. Projections are derived from the regionally downscaled climate data provided by the Scenarios Network for Alaska Planning (SNAP) at the University of Alaska Fairbanks (SNAP, 2010). Projected precipitation and temperature data were based on raster values surrounding the geographic centre of Mayo, as determined by SNAP. The range encapsulated was 625 km^2. Changes in climate for the Mayo region were projected for two time periods (2030 and 2050) using two standard scenarios (B1 and A1B). The B1 and A1B scenarios are based on the Intergovernmental Panel on Climate Change (IPCC) Special Report on Emissions Scenarios (Nebojša *et al.*, 2000). The B1 scenario projects low to moderate degrees of climate change over the next century, while the A1B scenario anticipates medium to high degrees of climate change. These two scenarios were applied to this study because they provide a reasonable range in possible shifts in temperature and precipitation for Mayo by 2030 and 2050. Figures illustrating changes in mean annual, winter and summer temperatures and winter and summer precipitation, as well as additional parameters such as freeze and thaw dates, and growing season length are included in Appendix B.

Tables 3 to 5 outline projected annual and seasonal temperature changes, annual and seasonal precipitation changes, and annual and seasonal precipitation changes from baseline for the B1 and A1B scenarios for 2030 and 2050 respectively; these projections were developed by SNAP (2010). For the sake of comparison, baseline data from 1961-1990 climate normal conditions are also included (see *Contemporary Climate* section above, and Appendix B for more details about climate normal conditions in the Mayo region). Generally, temperature projections indicate that warming will occur over both time slices (2030 and 2050), and regardless of whether one applies the B1, or A1B projections. The following observations are ranges for temperature and precipitation for B1 and A1B projections respectively for the 2050 timeframe only. Increases in mean annual temperature for the Mayo region are projected to be between 2.1°C and 3.2°C (Table 3). Warming is expected to be more significant in winter (4.6°C to 6.4°C) than in summer (0.5°C to 0.8°C) (Table 3). Precipitation is also projected to increase in the Mayo region over both time slices and regardless of projection (Table 4). Annual precipitation may increase by between ~36% (B1 projection) and ~42% (A1B projection) by 2050 (Table 5). As with temperature, the projected increases in precipitation will vary seasonally, and the greatest proportional increases are predicted to occur in the winter and spring (Table 5).

Table 3. Projected yearly and seasonal temperature changes (expressed as °C) for the Mayo region based on the B1 and A1B IPCC scenarios for 2030 and 2050 respectively. Baseline climate normal values for 1961-1991 are also shown (Environment Canada, 2010). Values in brackets indicate direction and amount of projected change from baseline conditions.

Season	Baseline (1961-1990)	Modest climate change (B1)		Medium-high climate change (A1B)	
		2030	2050	2030	2050
Annual	-3.6	-1.9 (+1.7)	-1.5 (+2.1)	-2.1 (+1.5)	-0.4 (+3.2)
Spring	-0.8	-0.4 (+0.4)	-0.3 (+0.5)	-0.4 (+0.4)	1.5 (+2.3)
Summer	14.0	14.1 (+0.1)	14.5 (+0.5)	13.7 (-0.3)	14.8 (+0.8)
Autumn	-4.2	-2.9 (+1.3)	-2.1 (+2.1)	-2.9 (+1.3)	-1.2 (+3.0)
Winter	-23.3	-19.2 (+4.1)	-18.7 (+4.6)	-18.8 (+4.5)	-16.9 (+6.4)

Table 4. Projected yearly and seasonal precipitation changes (expressed as mm total precipitation) for the Mayo region based on the B1 and A1B IPCC scenarios for 2030 and 2050 respectively. Baseline climate normal values for 1961-1991 are also shown (Environment Canada, 2010). Note: snowfall has been converted to snow water equivalent and is also expressed in mm.

Season	Baseline (1961-1990)	Modest climate change (B1)		Medium-high climate change (A1B)	
		2030	2050	2030	2050
Annual	318	419.57	433.21	439.68	450.53
Spring	39	59.35	63.98	64.83	67.10
Summer	137	169.06	169.06	171.33	178.03
Autumn	86	115.45	117.61	120.84	125.55
Winter	56	75.71	76.58	80.41	82.12

Table 5. Projected yearly and seasonal precipitation changes from baseline (1961-1990 climate normal) conditions (Environment Canada, 2010) for the B1 and A1B IPCC scenarios for 2030 and 2050 respectively. See Table 4 for a summary of values for each time period and projection.

Season	Increase from 1961-1990 baseline							
	Modest climate change (B1)				Medium-high climate change (A1B)			
	2030		2050		2030		2050	
	mm	%	mm	%	mm	%	mm	%
Annual	101.57	31.90	115.21	36.20	121.68	38.30	132.53	41.70
Spring	20.35	52.20	24.98	64.10	25.83	66.20	28.10	72.10
Summer	32.06	23.40	32.06	23.40	34.33	25.10	41.03	29.90
Autumn	29.45	34.20	31.61	36.80	34.84	40.50	39.55	46.00
Winter	19.71	35.20	20.58	36.80	24.41	43.60	26.12	46.60

HYDROLOGY

Because hydrological data for the Mayo region is limited, examples and case studies from scientific literature are used to identify potential impacts of climate change on aspects of the Arctic hydrological system in general, and in the Mayo region specifically.

Temperature

Regionally downscaled climate data provided by the Scenarios Network for Alaska Planning (SNAP) at the University of Alaska Fairbanks suggests that by 2030, under a modest climate change scenario (*i.e.*, the IPCC B1 scenario; see Nebojša *et al*., 2000 for details), annual temperature in Mayo will increase by 1.7°C, while winter temperatures could increase by 4.1°C (Table 3). Many of the impacts of increasing temperature have the potential to affect the hydrology of the Mayo region. These include the effects described above, such as a shorter winter season, reduced snow accumulation, an increased potential for winter rain and mid-winter melts, earlier and more severe spring river break-ups, lower summer and fall river discharge, increased evaporation, and increased groundwater infiltration. As with many potential impacts of climate change, the interplay between these impacts can be difficult to assess. However, data suggesting that many of these changes are already taking place, including earlier spring break-ups and shorter winter seasons, provides a useful indication of what may be expected in the future.

The most significant impact of increasing temperatures will manifest in the winter and spring, and will affect the duration of the snowcover season and the accumulation of winter snowpacks, hence affecting spring river discharge. The timing of freeze-up and break-up will also be affected. Warmer temperatures will reduce the length of the snowcover season (Lemmen *et al*., 2007; Wrona *et al*., 2005) and hence the amount of time available for snow accumulation. An increase in the proportion of rain to snow during the fall and winter also has the potential to reduce snowpack accumulation, while warmer temperatures may cause rain-on-snow events, promoting mid-winter melting (McBean, 2005; Wrona *et al*., 2005). The timing of break-up and freeze-up is also intimately linked with temperature, that is, ice freeze-up and break-up dates correlate most strongly with air temperatures in the preceding one or two months. In northern areas, freeze dates reflect the climate prevailing in October and November, while break-up dates reflect April and May temperatures (Magnuson *et al*., 2000). Higher temperatures could result in an earlier spring break-up, which is often associated with increased break-up severity. (However, warmer winter temperatures could counteract this effect, because reduced snowpack depths may mean

thinner ice develops on rivers, hindering severe break-up conditions (Wrona *et al*., 2005)). Evidence of earlier spring break-ups is already being recorded in Yukon, whereby ice break-up on the Yukon River at Dawson and on Alaskan rivers have occurred earlier in the year, likely in response to higher spring temperatures (Brabets and Walvoord, 2009). An earlier spring break-up and a shorter snowcover season may subsequently affect the timing and magnitude of the spring meltwater pulse. Higher spring temperatures can cause a more rapid spring melt (Wrona *et al*., 2005), while an increased number of days with mid-winter or early spring thaws can result in a more protracted snowmelt, causing declines in runoff intensity and lower runoff peaks (McBean, 2005). Furthermore, an earlier spring runoff generally correlates with lower summer and fall flows (Barnett *et al.*, 2005).

Evaporation rates can also be affected by temperature increases. While temperature increases in summer are projected to be smaller than those in winter, summer temperature increases of 1-3°C will still have a significant effect on evaporative losses (Wrona *et al*., 2005). Rising temperatures generally cause increased evaporation and evapotranspiration (Walsh, 2005), which, coupled with a longer snow-free season, can result in increased water loss from surface waters and potentially cause negative water balances. Increased evaporation can also reduce soil moisture (Barnett *et al*., 2005), which could in turn affect the vitality of the terrestrial ecosystem.

Increased temperatures also contribute to permafrost thawing, both directly (*e.g.*, through warming of the ground surface and subsequent deepening of the active layer) and indirectly (*e.g.*, through reductions in the ground-insulating capacity of the winter snowpack by declines in snow accumulation). Thaw of the permafrost table can have numerous effects on hydrology, including increased groundwater infiltration, lags between snowmelt and peak spring discharge, lower summer flows, and increased winter flows. In low-permafrost catchments, river flow varies most strongly with summer temperature, while in high-permafrost catchments, flow varies most strongly in response to changes in precipitation (Jones and Rinehart, 2010). This suggests a positive feedback cycle, in which warmer temperatures enhance permafrost thawing, which in turn affects the sensitivity of stream hydrology to temperature increases. The effects of melting permafrost on hydrology are discussed in more detail below (see *Permafrost and groundwater dynamics* section below).

Precipitation and snowcover

For most cold regions, winter snowcover accumulation is the main contributor to spring runoff (Romolo *et al*., 2006). The seasonal storage of snow comprises a major portion of the freshwater budget, and its melt accounts for major runoff in downstream areas (Prowse, 2009). Hence, changes in the amount of snowfall or the proportion of precipitation comprised of snow will affect surface and groundwater hydrology. The International Panel on Climate Change has consistently reported increases in precipitation over the 20th century at northern high latitudes (Walsh, 2005) of ~0.5-1% per decade (McBean, 2005). Purves (2010) identified a trend towards increasing precipitation in Mayo by 2%/10 yrs (5.9 mm/10 yrs) between 1927 and 2009. In general, observations suggest that the greatest changes in precipitation have occurred during the fall and winter, in particular in the shoulder seasons (*e.g.*, November and April). This is consistent with other studies showing increases in precipitation over the Arctic between 1948 and 2005 (Lemmen *et al*., 2007), as well as increases in summer precipitation in the Yukon Territory, where the greatest increases have occurred in the southeast and central regions (Janowicz, 2010).

However, despite increases in precipitation, snowcover has largely declined across the Arctic. In the Northern Hemisphere, there has been a documented decline in snowcover of ~10% between 1972 and 2003 (Walsh, 2005, Lemmen, 2007). This change is important, because a large

winter snowpack is critical for the development of ice-jam flood events (Romolo *et al*., 2006) and for producing high downstream discharge. In the Mayo region, Purves (2010) identified a decline in Februray 28th snow-on-ground of 11%/10 yrs between 1955 and 2010. It is evident that despite documented increases in precipitation, snowcover has declined; this apparent contradiction is likely related to increasing temperatures during the same time period, causing shorter snowcover seasons. It is important to be aware that such interplays between different climate parameters complicate projections of climate warming impacts on complex ecosystems. Implications of a shorter snowcover season are discussed further below, in the section *Freeze-up, break-up and river discharge*.

Climate models generally predict modest increases in global precipitation by the end of the 21st century, although there is considerable variability among model outputs. However, terrestrial North America is an area with one of the highest projected increases in precipitation, and the largest increases are projected for fall and winter (Wrona *et al*., 2005). Most models suggest annual precipitation will increase 15-30% by 2080 (Lemmen *et al*., 2007). SNAP climate projections for Mayo by the year 2030 and 2050 suggest increases in annual precipitation of ~32% and 36%, respectively; winter and summer precipitation is expected to increase by ~35% and 37%, and ~23% and 23%, respectively, under a moderate climate change scenario (*i.e.*, the IPCC B1 scenario; see Table 5 and Nebojša *et al*., 2000 for details). By 2050, under a medium-high climate change scenario (*i.e.*, the IPCC A1B scenario; see Table 5 and Nebojša *et al*., 2000 for details), annual precipitation is expected to increase by ~42%, whereby the increase in winter precipitation is predicted to be ~47%. It is interesting to note that SNAP's highest projected precipitation increases occur in spring, regardless of time slice or scenario applied. Increases in precipitation during the spring break-up have the potential to increase river discharge and the severity of the spring break-up, particularly if increased spring precipitation falls as rain.

Projected changes in the ratio of precipitation to evaporation are generally positive, indicating that it is likely there will be more frequent and longer wet periods (Walsh, 2005). Climate change is also expected to cause major repartitioning of snow and rainfall (Prowse, 2009). In other words, if increases in precipitation coincide with increases in temperature, which is highly likely, the proportion of rainfall relative to snowfall could increase (Brabets and Walvoord, 2009), as could the number of rain-on-snow events, which are often conducive to the development of flash floods (McBean, 2005). This will have a significant effect in catchments with high amounts of permafrost, where stream flow exhibits a rapid response to rainfall due to increased surface runoff on frozen ground (Jones and Rinehart, 2010). In conjunction with these changes, projected declines in mean snowcover range between -9% and -18% by the 2071-2090 time period (Walsh, 2005).

It is apparent that while precipitation is projected to increase in the future, the decline in snowcover extent and duration will have negative effects on river discharge (discussed in more detail below). In the Stewart River watershed, this could mean earlier, potentially lower spring discharge peaks, with higher summer discharge in response to increases in rainfall. However, lower spring discharge peaks could be offset somewhat by projected increases in spring precipitation in the Mayo region. Regardless of their nature, these changes will affect the timing and shape of the seasonal hydrograph, and will have significant implications for both surface and groundwater dynamics.

Freeze-up, break-up and river discharge

Climate change has the potential to alter river discharge and the timing of events in the annual hydrograph (see Figure 5 for an example of a Stewart River hydrograph). Changes in the timing of river freeze-up and break-up, as well as the amount of winter precipitation and duration of the

snowcover season, are the primary mechanisms that will be discussed in this section.

There is increasing evidence that river ice break-up is occurring earlier in spring, and freeze-up is occurring later in fall (Janowicz, 2010; Lemmen *et al*., 2007; Magnuson *et al*., 2000). Many factors affect the timing of break-up and freeze-up, but trends in both scenarios generally reflect changes in fall and spring air temperatures (Brabets and Walvoord, 2009; Lemmen *et al*., 2007). Projections indicate a 1-day advance per 0.2°C increase in air temperature for break-up, and vice versa for freeze-up (Walsh, 2005). SNAP's projections for the Mayo region indicate earlier thaw dates and later freeze-up dates, regardless of the time slice or scenario examined. For example, under a moderate climate change scenario (*i.e.*, IPCC B1 scenario), by the year 2030, thaw dates may occur up to 14 days earlier in Mayo, and one month earlier in the headwaters of the Stewart River. Likewise, freeze-up dates may occur up to 5 days later in Mayo, and 20 days later in the headwaters of the Stewart River. In a study of historical trends in lake and river ice in the northern hemisphere, Magnuson *et al*. (2000) found that between 1846 and 1995, there have been shifts towards later freeze-up and earlier break-up dates. In their study, freeze-up dates occur later by 5.8 days per century, while break-up dates occur earlier by 6.5 days per century. Furthermore, they found that interannual variability in freeze-up and break-up dates has increased since the 1950s. Canadian data of break-up and freeze-up dates have documented that western Canadian sites have a predominant trend towards earlier break-ups (Lemmen *et al*., 2007). These long-term trends in river ice phenologies provide evidence that freshwater ecosystems are already responding to warming trends (Magnuson *et al*., 2000). In addition to altering freeze-up and break-up dates, increases in temperature have the potential to produce more frequent and sustained mid-winter thaws (Beltaos *et al*., 2006). In fact, the first mid-winter break-up in Yukon was observed on the Klondike River at Dawson in the winter of 2002-03 as a result of rain and warm weather in December 2002 (Janowicz, 2010).

While temperature increases may affect the timing of freeze-up and break-up, the duration of the snow accumulation season and the amount of snowfall have an influence on the magnitude and timing of the spring discharge peak. Firstly, later fall freeze-up and earlier spring break-up reduce the length of the snowcover season, resulting in a shorter period in which snow can accumulate and hence potentially affecting the volume of the spring snowmelt pulse (Hay and McCabe, 2010; Walsh, 2005). Secondly, earlier snowmelt has the potential to reduce the seasonal regulatory effect of alpine snow storage (Prowse, 2009), especially if there are significant temperature increases at higher latitudes (for example, in the Stewart River headwaters). An earlier snowmelt season could also mean that the initiation of melt takes place during cooler spring temperatures, resulting in a more protracted melt and lower peak spring river discharge (Walsh, 2005). If the amount of winter snowfall declines, there is potential for two contrasting effects: 1) shallower snow depths could reduce the spring albedo, allowing more incoming solar radiation to be absorbed and the spring melt and river-ice break-up to occur earlier; and 2) shallower snow depths could mean a decline in the insulating effects of snowcover on river ice in winter and result in the development of thicker ice (Walsh, 2005). Both scenarios could alter the timing and severity of the spring break-up.

In terms of overall river discharge, future projections based on model scenarios show discharge increases of 20-30% on the Yukon River by 2050 compared with a 1961-1991 baseline (Lemmen *et al*., 2007; Arnell, 1999). Arora and Boer (2001) project a 10% increase in Yukon River discharge under a double-CO_2 scenario. Annual mean flows in permafrost regions of northwestern Canada show slight positive trends over the last three decades in both continuous and discontinuous permafrost zones, while annual peak flows have largely decreased in the sporadic permafrost region (although the decrease is not statistically significant) (Janowicz, 2008). Déry *et al*. (2009) suggest there is an intensifying hydrological cycle in northern Canada, manifested in a 15.5%

increase in annual river flows due in part to many above-average flows recorded over the last decade. As SNAP's climate projections suggest, it is highly likely that the Stewart River and its tributaries will become ice-free earlier in the spring, shortening the on-ice travel season. The primary pulse of river discharge will also likely occur earlier in the spring (manifesting as an earlier discharge peak on the annual hydrograph). However, if the snow accumulation season is shorter, as SNAP's projections suggest, or the rate of melt protracted, there may be a decline in the magnitude of the spring pulse. The rate and timing of the spring melt are important factors in determining the occurrence of floods (Romolo *et al*., 2006) and river discharge later in the season.

Permafrost and groundwater dynamics

As permafrost thaws, surface water-dominated systems will transition towards groundwater-dominated systems (Prowse, 2009). Where permafrost is thick and the active layer thin (*i.e.*, before climate-induced permafrost degradation), pathways between melt-induced runoff and the stream channel are short, and there is little or no infiltration or interaction between surface and subsurface hydrological processes. As permafrost thaws and the active layer becomes thicker, infiltration and groundwater recharge may be enhanced during the spring, and hence augment groundwater contributions to streamflow (Janowicz, 2008). Consequently, many studies predict increases in stream baseflow (Brabets and Walvoord, 2009; Hodgkins, 2009; Lemmen *et al*., 2007; Wrona *et al*., 2005), particularly during the winter months when groundwater contributions are the only inputs to ice-covered streams (Janowicz, 2008). An increase in the infiltration of spring snowmelt runoff and summer rainfall may reduce both the spring discharge peak and summer precipitation-induced discharge peaks (Wrona *et al*., 2005), and there is potential for a decrease in annual peak flows with increased capacity for subsurface storage (Janowicz, 2008). Changes in surficial topography as a result of permafrost thawing, such as ground slumping, may promote ponding in some areas (Lemmen *et al*., 2007), or the drainage of surface water bodies in others (Hofmann *et al*., 1998), altering local drainage patterns.

It is highly possible that spring and summer river discharge of the Stewart River will decline, and there will be a longer lag between the initiation of snowmelt and peak spring discharge in the headwaters and downstream. However, winter discharge is likely to increase, because more water will be stored as groundwater and will be capable of boosting winter flows. Surficial hydrology around the Mayo region may also change, as thawing permafrost may cause drainage of some ponds and the formation of others. The consequences of thawing permafrost on hydrology can be significant.

Relevance for Mayo region hydrology

Based on the scientific literature discussed above, it is possible to speculate about potential impacts of climate change on the hydrology of the Mayo region. The following changes are based on projected increases in both temperature and precipitation:

- Shorter snowcover season, with reduced snowpack depth (especially during spring) and lower insulating capacity of the snowpack.
- Increased frequency of rain-on-snow events and increase in overall proportion of rain to snow.
- More frequent mid-winter and early spring thaws.
- Earlier break-up and later freeze-up of river ice.

- Thinner river ice cover (as a result of a shorter cold-weather season) or thicker river ice cover (as a result of lower snowpack insulation capacity).
- More rapid spring melt (if spring temperatures are significantly increased) or more protracted spring melt (if spring temperatures warm earlier in the season, but to a lesser degree).
- Increased or decreased break-up severity (depending on timing of melt, ambient air temperatures, amount of winter baseflow, thickness of river ice, *etc.*).
- Earlier and smaller spring snowmelt pulse and river discharge peaks.
- Lower summer and fall river discharge, as a result of lower spring discharge.
- Higher summer and fall river discharge, as a result of increased rainfall during the same period.
- Increased winter baseflow.
- Increased evaporation.
- Increased permafrost thawing.
- Increased infiltration of the spring snowmelt pulse, reducing spring overland flow and delaying the spring discharge peak.
- Higher rates of groundwater recharge and increased groundwater storage, causing a hydrological transition towards an increasingly groundwater-dominated system.
- Increased surface ponding (where permafrost thawing causes ground subsidence), or drainage of some surface ponds (where permafrost thawing removes a barrier to drainage).

In the Mayo region, the most significant areas of impact may be related to river discharge and changes in the depth to the groundwater table. Discharge in the headwaters of the Stewart River catchment is an important contributor to downstream river discharge, and there is a positive correlation between the snow water equivalent (SWE) of the winter snowpack (the most hydrologically important characteristic of snowcover (Walsh, 2005)) and spring streamflow downstream. This relationship is further supported by records of past SWE and river discharge, which demonstrate that during periods of below-average SWE, flooding was less frequent, while the opposite was true during periods of high SWE. The strong relationship between SWE and river discharge highlights the importance of the winter snowpack on streamflow generation and regional hydrology. Hence, changes in snowpack depth, the duration of the snowcover season, or the timing of the spring melt, will all affect discharge in the Stewart River watershed and the Mayo region. In fact, because the spring discharge peak is the most hydrologically significant event of the year, it is highly susceptible to change, and the typical riverine hydrograph of the area may be altered (see Figure 5).

The potential impacts of thawing permafrost are also relevant to the hydrology of the Mayo region, where permafrost has a strong influence on surface and groundwater hydrology (Burn, 1994). At the forefront of these potential impacts is the potential for increased groundwater recharge and storage as a result of permafrost thawing. There is evidence suggesting that the groundwater table is close to the surface in some parts of the townsite of Mayo. If groundwater storage does increase, it is possible that the height of the water table will also increase, exacerbating existing spring flooding problems in the town. However, without detailed field

studies of the height and variability of the groundwater table in the area, it is difficult to be certain whether such a change would be significant or not.

SURFICIAL GEOLOGY

Projected changes in climate should not affect the stable landforms in the Mayo region in any significant manner. Changes in temperature and precipitation may, however, negatively influence landforms that are already exhibiting some forms of instability. Increased bank erosion caused by higher than normal discharge of the Stewart River could potentially accelerate tension cracking of point bar sediments on the floodplain of the river. Areas subjected to tension cracking will likely continue to be regions that are also subjected to flooding risk.

Increasing temperatures will have the greatest impact on surficial materials and landforms that are currently frozen. As these materials thaw, we can expect significant changes to the landscape. Hazards associated with permafrost affected materials will be discussed in more detail below.

PERMAFROST

In predicting the impacts of future climate warming on permafrost in the Mayo area, a number of key points need to be considered:

- Current scientific research indicates that permafrost temperatures are already inferred to be close to 0°C in undisturbed areas and therefore permafrost is highly susceptible to degradation. Additionally, permafrost is thin in disturbed areas.
- Permafrost degradation is accelerated by surface disturbance due to geomorphic processes, forest fire or removal of vegetation.
- Permafrost is ice-rich when associated with glacio-lacustrine deposits, but generally appears to have medium or low ice contents in other types of surficial materials (*e.g.*, glaciofluvial deposits).
- Thaw of permafrost from above takes decades to occur because heat has to be added to melt the ice in the ground; however, it can occur more rapidly if thermokarst ponds start to develop in depressions since water warms the ground much faster.
- Progressive thaw of permafrost containing more ice than pore space will result in settling of the ground surface, therefore causing damage to infrastructure.

Predicted mean annual air temperatures for the Mayo region were extracted from a new model created for the southern half of the Yukon and based on measurements of air temperatures at about 100 stations in the mountains and valleys (Lewkowicz and Bonnaventure, 2011). The results are useful for understanding the influence of terrain on the range of temperatures. In essence, temperatures get warmer with altitude in winter and colder with altitude in summer, almost balancing each other out over the entire year. Consequently, despite a considerable elevation range (480 to 1150 m a.s.l.), predicted temperatures do not vary greatly across the Village of Mayo and the surrounding area, ranging from -2.8 to -3.4°C (Figure 36). If typical lapse rates (rate of decrease of temperature with height) of -6.5°C/km pertained in the area, the highest mountain summits would be expected to have mean annual temperature values of -7.3°C, about 4°C colder than is predicted. The significance of this analysis is that all parts of the study area are relatively close to 0°C, so that a rise in mean annual air temperatures of 1°C or 2°C would likely have significant impacts across the entire landscape.

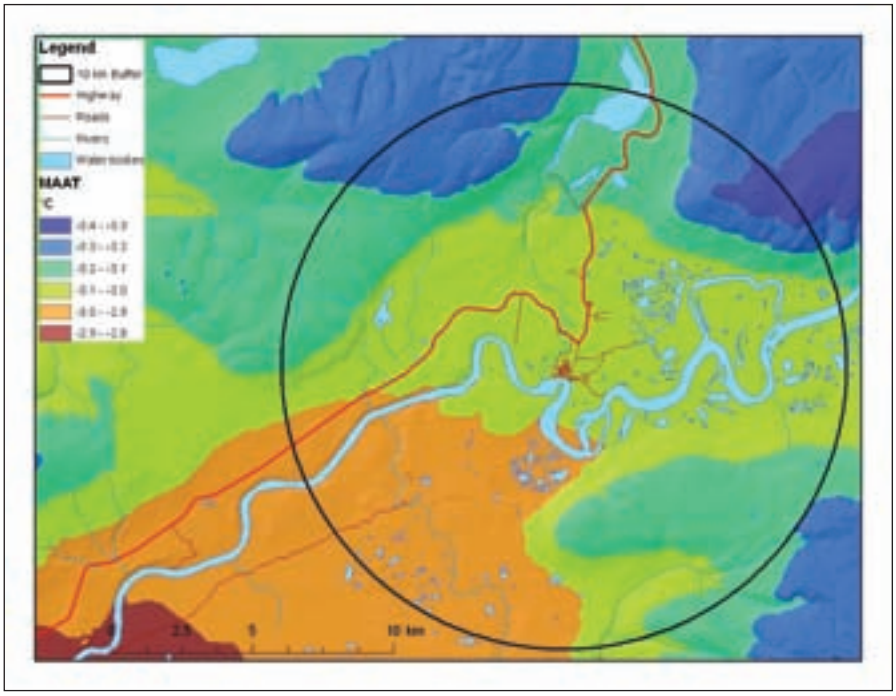

Figure 36. *Map of the spatial pattern of mean annual air temperatures (MAAT) predicted under current climate conditions, and centred on Mayo. The circle denotes a 10 km buffer that encircles the village of Mayo. Note the narrow temperature ranges (as shown in the legend) reflecting the relative homogeneity of mean annual air temperatures across the area caused by gentle lapse rates within the forest.*

The timing of permafrost thaw has not been investigated in detail for this report, but the long-term changes can be examined using the permafrost probability model described earlier which employs a scenario-based approach (see Bonnaventure and Lewkowicz, 2010). These predictions permit a first-order estimation of climate change impacts. The predictions are made by adjusting elevation in the model in accordance with the local lapse rate (*i.e.*, rate of decrease in temperature with height) to generate a 1°C or 2°C change in mean annual air temperature. As indicated above, it is important to note that such changes would happen over decades rather than years providing surface water bodies are not created as the latter would warm subsurface temperatures more rapidly.

A rise in mean annual air temperature (MAAT) of 1°C has a dramatic effect on the amount of permafrost in the area around Mayo and in the village itself. Probabilities in the valleys fall to about 0.3 (*i.e.*, they are halved relative to the present day) and are still lower on ridge crests (Figure 37). Only north-facing slopes retain probabilities >0.5 (*i.e.*, similar to current probabilities).

Still greater change would occur if the MAAT rises by 2°C (Figure 38). The probability of permafrost in the Mayo area falls to about 0.1. Since these predictions do not take into account disturbance to the terrain which leads to warming of the subsurface and which the DC resistivity profiles prove to be significant, it is reasonable to infer that a 2°C warming would essentially eliminate permafrost in any disturbed site in the Mayo area.

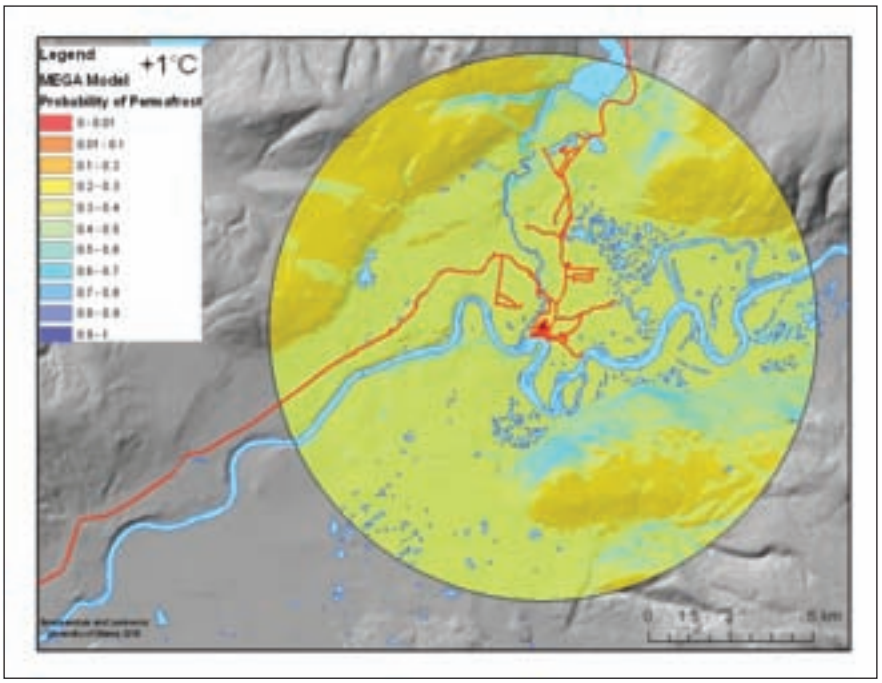

Figure 37. *Map of equilibrium predicted permafrost probabilities following an increase in mean annual air temperature (MAAT) of 1°C. Note: these predictions do not include local variations related to surficial deposits or other types of micro-variability. Based on methods described in Bonnaventure and Lewkowicz (2010), Lewkowicz and Bonnaventure (2011) and Bonnaventure et al. (in press).*

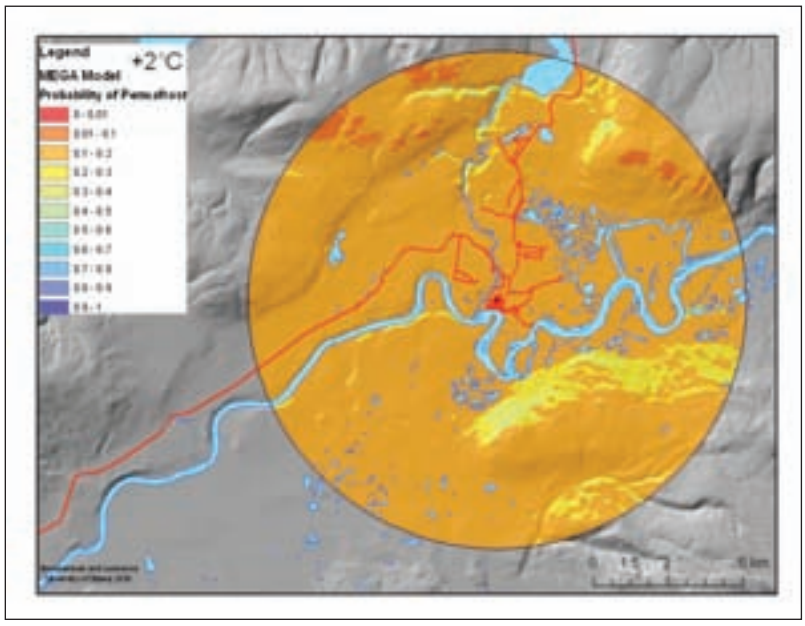

Figure 38. *Map of equilibrium predicted permafrost probabilities following an increase in mean annual air temperature (MAAT) of 2°C. Note: these predictions do not include local variations related to surficial deposits or other types of micro-variability. Based on methods described in Bonnaventure and Lewkowicz (2010), Lewkowicz and Bonnaventure (2011) and Bonnaventure et al. (in press).*

The limited climate change modeling cannot definitively predict how much time it would take for permafrost to react to climate warming. Even thin permafrost may take decades to thaw if it is ice-rich because the latent heat of fusion must be satisfied. However, what the modelling

suggests is the inevitability of change to permafrost if warming occurs in the Mayo area, and the higher sensitivity of the response in this region compared to areas where lapse rates are stronger (Bonnaventure and Lewkowicz, 2010).

SYNTHESIS OF MAYO REGION ENVIRONMENTAL CHANGE

The potential environmental changes identified in the preceding sections of this report can be used to identify current and future landscape hazards in the Mayo region. The combined properties of surficial material type, landform shape and slope, hydrological regime, climate regime, and permafrost conditions have been used to arrive at a set of hazard 'rankings' that can be used to assess the potential stability of landscape units around the Village of Mayo (*see accompanying map "Geological Hazard Rankings, Village of Mayo, Yukon"*).

Based on processes acting on distinct geological units, a hazard ranking of low, medium, or high has been assigned to each geological unit in the hazard map area. Rankings are qualitatively assigned to reflect the following conditions:

1. **Low:** Stable landform. Unlikely to be affected by mass movement, thermokarst, subsidence, bank erosion, flooding or instability. These landforms typically consist of gravel or sand, are well drained and have shallow to moderate slopes. Low hazard landforms may contain little to no permafrost and are above the floodplain of the Stewart or Mayo rivers.
2. **Medium:** Unlikely to be affected by mass movement, thermokarst, subsidence, bank erosion, flooding or instability. These landforms typically consist of gravel, sand, glacial diamict or colluvial materials. They are well to moderately drained and have shallow to steep slopes. Medium hazard landforms may have moderate amounts of permafrost and may occur within an area of shallow groundwater.
3. **High:** Unstable landform. Likely to be affected by mass movement, thermokarst, subsidence, bank erosion, flooding or instability. These landforms typically consist of glacial diamicts, colluvial materials, glaciolacustrine, lacustrine and fluvial deposits. They are generally moderately to poorly drained and have shallow to steep slopes. High hazard landforms may have a significant thickness of permafrost containing high ice contents, be prone to gravity-induced erosion, and occur within the floodplain of the Stewart or Mayo rivers.

It is important to note that hazard rankings are based on general observations of surface materials, drainage, slope angle, vegetation and the presence of permafrost in landforms; limited subsurface information provided by Direct Current resistivity profiling, shallow drilling and probing of permafrost, and textural analyses were also applied. This has resulted in a *projected* risk ranking that will require geotechnical and/or engineering analyses to quantify.

In classifying polygons, we have taken a precautionary approach and applied a category of higher risk where we are not confident in assigning a lower-risk category. However, every polygon will contain zones of lower and higher risk than the overall polygon classification. It is for this reason that this map should serve only as an initial guide for planning purposes. Any development will still require detailed site investigations.

Results of hazard classifications in the developed area of the Village of Mayo conclude that this region is at a medium to high risk of landscape instability (Figure 39; *see also accompanying map "Geological Hazard Rankings, Village of Mayo, Yukon"*). Hazards in this area are largely related to flooding risk and the potential for permafrost thaw. Specifically, polygon numbers 3, 5, 14,

Figure 39. *Detailed view of hazard rankings in the developed area surrounding the Village of Mayo. Polygon numbers are discussed in the text and summarized in Appendix C. High, medium and low hazard rankings are represented by red, yellow and green polygons, respectively.*

15, 23, 43, 61, 94, 101, 102, 103, 105 and 106 are ranked at high (red) risk due to the presence of thick organic mats, standing water likely related to thermokarst processes, and undisturbed forest. Many of these areas also have thin active layers, and reported evidence of permafrost. Polygon numbers 5, 6, 7, 8, 10, 12, 13, 39 and 40 are ranked at high (red) risk due to flooding potential on the Mayo River. Flooding on the Mayo River may also affect polygon numbers 7, 15, 61 and 101. A breakdown of the risk related to each polygon is presented in Appendix C.

FUTURE RESEARCH NEEDS AND NEXT STEPS

HYDROLOGY

This report identifies the significant lack of data with regards to groundwater characteristics in the Mayo region. In fact, groundwater data for the Mayo region are very sparse. While many boreholes, test pits and water wells have been excavated in the Village of Mayo and all groundwater occurrences were recorded, no long-term monitoring records of any wells or test pits are available. Rather, data represent single site investigations and provide no context for investigating temporal variability. There is a lack of geo-referenced, spatially comparable groundwater data (*e.g.*, available data lacks reference to an elevation datum, thus making comparison between sites inappropriate). Additionally, records of wells and test pits excavated in the Mayo region span three decades, and were developed at different times of the year, further complicating comparison between sites and preventing robust evaluation of seasonal and long-term trends in groundwater levels. Importantly, this data gap prevents a detailed investigation of the causes of the frequent spring flooding reported in the Village of Mayo, which is a major concern of the town's residents. Without a detailed understanding of the nature of Mayo's groundwater reserves, it is difficult to speculate about the impacts of projected climate change in this respect, and whether spring flooding may persist or increase under the climate change scenarios investigated in this report. To address these concerns, a groundwater monitoring program should be developed for the Village of Mayo, focusing especially on flood-prone areas. Initial data could be used to develop a map of the water table in the area, including water table height, primary recharge areas, and direction and velocity of subsurface flows. Data collected over several seasons and consecutive years could be used to assess year-to-year changes in groundwater hydrology and, when compared with climate data for the region, may offer some indications of the variability in groundwater dynamics in response to climate variability. This type of investigation is especially warranted, given that the Village of Mayo's Official Community Plan calls for additional development in the downtown core (VOM, 2005).

PERMAFROST

The results of this study suggest a number of potential avenues for research on permafrost in the Mayo area.

First, temperature measurements in boreholes are needed inside and around the community. These could be used to track long-term change in ground temperatures as a result of climate warming and land clearing. The most sensitive sites in which to monitor climate are those where permafrost contains little ice, while the most vulnerable are those where permafrost is ice-rich. It would be useful to install monitoring sites in both types of terrain. The data from these sites should also be used to support environmental programs at the Mayo school.

Second, additional measurements using DC resistivity would be useful beneath the airstrip. Permafrost under the airstrip is very vulnerable to thaw, particularly at its eastern end, therefore subjecting a very important piece of local infrastructure to further damage. Conditions beneath the airstrip may be complex based on the DC resistivity profile run alongside it. Further work to establish these variations through long and cross-profiles would be desirable, especially if ground temperature cables are also installed.

Third, investigations using DC resistivity in combination with borehole drilling should be undertaken in areas where the community plans future development. The effectiveness of the technique was shown to be high when combined with information about ground temperatures

at a given site. The ability to generate a two-dimensional profile and even three-dimensional images indicates that this method should be used in the future as a standard technique for site investigations in the discontinuous permafrost zone.

MAYO HAZARDS MAPS AND RESEARCH: GENERATING ACTION FROM SCIENCE

The knowledge and data generated by the Mayo Hazards project can be used in a number of ways to inform planning and policy developers and establish a baseline from which future science can be generated. This study has identified numerous actions for the community of Mayo and includes the monitoring of permafrost degradation, the investigation of hydrological change in the landscape, and adaptation planning.

Adaptation planning is currently underway in the Mayo region, and the hazards project has contributed significantly to the assessment of vulnerability for the community of Mayo. In particular, the hazards mapping project has increased the understanding of how landscape characteristics may evolve in Mayo as regional climate conditions change. This information will be utilized in the adaptation plan to provide the basis for evaluating how community infrastructure, security and well-being may be influenced, and how the community might take action to respond.

The results of this report will also be utilized in the adaptation planning process and will be applied to future environmental scenarios of change, or provide baseline information of how landscape change may occur, as a component of the Mayo Adaptation Project. These scenarios will then provide the framework for assessing the influence of variability and uncertainty on risk. For example, the variable rate and distribution of potential permafrost decline will inform how and when the community must act. By integrating this variability into decision-making through multiple scenarios, planners can build better adaptation strategies. In this way, the science of hazard assessment is an important foundation from which to build action.

REFERENCES

Arnell, N.W., 1999. Climate change and global water resources. Global Environmental Change, vol. 9, p. 31-49.

Arora, V.K. and Boer, G.J., 2001. Effects of simulated climate change on the hydrology of major river basins. Journal of Geophysical Research, vol. 106, p. 3335-3348.

Barnett, T.P., Adam, J.C. and Lettenmaier, D.P., 2005. Potential impacts of a warming climate on water availability in snow-dominated regions. Nature, vol. 438, p. 303-309, DOI:10.1038/nature04141.

Beltaos, S., Prowse, T.D., Bonsal, B.R., MacKay, R., Romolo, L.A., Pietroniro, A. and Toth, B., 2006. Climatic effects on ice-jam flooding of the Peace-Athabasca Delta. Hydrological Processes, vol. 20, p. 4031-4050.

Bleiler, L., 2006. Mayo: the last half of the Twentieth Century. *In:* Heart of the Yukon: a natural and cultural history of the Mayo area, L. Bleiler, C. Burn and M. O'Donoghue (eds.), Village of Mayo, Mayo, Yukon Territory, p. 99-104.

Bonnaventure, P.P. and Lewkowicz, A.G., 2010. Modelling climate change effects on the spatial distribution of mountain permafrost at three sites in northwest Canada. Climatic Change, vol. 105, numbers 1-2, p. 293-312, DOI 10.1007/s10584-010-9818-5.

Bonnaventure, P.P., Lewkowicz, A.G., Kremer, M. and Sawada, M., (*in press*). A regional permafrost probability model for the Southern Yukon and Northern British Columbia, Canada. Permafrost and Periglacial Processes, 2011.

Bostock, H.S., 1966. Notes on glaciation in central Yukon Territory. Geological Survey of Canada, Paper 65-36, 18 p.

Brabets, T.P. and Walvoord, M.A., 2009. Trends in streamflow in the Yukon River Basin from 1944 to 2005 and the influence of the Pacific Decadal Oscillation. Journal of Hydrology, vol. 371, p. 108-119.

Burn, C.R., 1991. Permafrost and Ground Ice Conditions Reported during Recent Geotechnical Investigations in the Mayo District, Yukon Territory. Permafrost and Periglacial Processes, vol. 2, issue 3, p. 259-268.

Burn, C.R., 1994. Permafrost, tectonics, and past and future regional climate change, Yukon and adjacent Northwest Territories. Canadian Journal of Earth Sciences, vol. 31, p. 182-191.

Burn, C.R., 2000. The thermal regime of a retrogressive thaw slump near Mayo, Yukon Territory. Canadian Journal of Earth Sciences, vol. 37, p. 967–981.

Burn, C.R. and Friele, P.A., 1989. Geomorphology, vegetation succession, soil characteristics and permafrost in retrogressive thaw slumps near Mayo, Yukon Territory. Arctic, vol. 42, p. 31-40.

Burn, C.R., Michel, F.A. and Smith, M.W., 1986. Stratigraphic, isotopic, and mineralogical evidence for an early Holocene thaw unconformity at Mayo, Yukon Territory. Canadian Journal of Earth Sciences, vol. 23, p. 794-803.

Cywnar, L.C., Schweger, C.E. and Matthews, J.V.Jr., 1987. Quaternary Flora and Fauna of Yukon. *In:* Guidebook to Quaternary Research in Yukon, S.R. Morrison and C.A.S. Smith (eds.), XII INQUA Congress, Ottawa, Canada. National Research Council of Canada, Ottawa, p. 29-30.

Déry, S.J., Hernández-Henríquez, M.A., Burford, J.E. and Wood, E.F., 2009. Observational evidence of an intensifying hydrological cycle in northern Canada. Geophysical Research Letters, vol. 36, no. 13, L13402, DOI:10.1029/2009GL038852.

Duk-Rodkin, A., 1999. Glacial limits map of Yukon. Geological Survey of Canada, Open File 3694; Exploration and Geological Services Division, Yukon Region, Indian and Northern Affairs Canada, Geoscience Map 1999-2, 1:1 000 000 scale.

Environment Canada, 2010. Canadian Climate Normals 1961-1990. http://climate.weatheroffice.gc.ca/climate_normals/index_1961_1990_e.html, [accessed January 2011].

Giles, T.R., 1993. Quaternary sedimentology and stratigraphy of the Mayo region, Yukon Territory. Unpublished MSc Thesis, University of Alberta, Edmonton, AB, 206 p.

Hay, L.E. and McCabe, G.J., 2010. Hydrologic effects of climate change in the Yukon River Basin. Climate Change, vol. 100, numbers 3-4, p. 509-523.

Heginbottom, J.A., Dubreuil, M.A. and Harker, P.T., 1995. Permafrost Map of Canada. *In*: The National Atlas of Canada, 5th Edition, (1978-1995), published by Natural Resources Canada, sheet MCR 4177, 1: 7 500 000 scale.

Hodgkins, G.A., 2009. Streamflow changes in Alaska between the cool phase (1946-1976) and the warm phase (1977-2006) of the PDO: The influence of glaciers. Water Resources Research, vol. 45, W06502, DOI: 10.1029/2008WR007575.

Hofmann, N., Mortsch, L., Donner, S., Duncan, K., Kreutzwiser, R., Kulshreshtha, S., Piggott, A., Schellenberg, S., Schertzer, B. and Slivitzky, M., 1998. Climate change and variability: Impacts on Canadian water. *In:* The Canada Country Study: Climate Impacts and Adaptation, G. Koshida and W. Avis (eds.), Environment Canada, p. 1-53.

Howes, D.E. and Kenk, E., 1997. Terrain Classification System for British Columbia (Version 2). Recreational Fisheries Branch, Ministry of Environment and Surveys and Resource Mapping Branch, Ministry of Crown Lands, Province of British Columbia, Victoria, BC, 102 p.

Hughes, O.L., 1983. Surficial Geology and Geomorphology, Janet Lake, Yukon Territory. Geological Survey of Canada, Preliminary Map 4-1982, 1:100 000 scale.

Huntington, H. and Weller, G., 2005. Chapter 1: An Introduction to the Arctic Climate Impact Assessment. *In:* Arctic Climate Impact Assessment Scientific Report, C. Symo, L. Arris and B. Heal (eds.), Cambridge University Press, p. 1-20.

Janowicz, R., 2008. Apparent recent trends in hydrologic response in permafrost regions of northwest Canada. Hydrology Research, vol. 39, no. 4, p. 267-275.

Janowicz, R., 2010. Observed trends in the river ice regimes of northwest Canada. Hydrology Research, vol. 41, p. 462-470.

Jones, J.B. and Rinehart, A.J., 2010. The long-term response of stream flow to climatic warming in headwater streams of interior Alaska. Canadian Journal of Forest Research, vol. 40, p. 1210-1218.

Kennedy, K.E., 2011. Surficial Geology of the Village of Mayo (part of NTS 105M/12) Yukon. Yukon Geological Survey Open File 2011-3, 1:20 000 scale.

Kneisel, C., Hauck, C., Fortier, R. and Moorman, B., 2008. Advances in geophysical methods for permafrost investigations. Permafrost and Periglacial Processes, vol. 19, p. 157-178.

Lemmen, D.S., Warren, F.J., Lacroix, J. and Bush, E., (editors), 2008. From Impacts to Adaptation: Canada in a Changing Climate 2007. Government of Canada, Ottawa, ON, 448 p.

Leverington, D., 1995. A field survey of late-summer depths to frozen ground at two study areas near Mayo, Yukon Territory, Canada. Permafrost and Periglacial Processes, vol. 6, p. 373-379.

Lewkowicz, A.G. and Bonnaventure, P.P., 2011. Equivalent elevation: a method to incorporate variable lapse rates into mountain permafrost modeling. Permafrost and Periglacial Processes, vol. 22, *in press*, DOI:10.1002/ppp.720.

Magnuson, J.J., Robertson, D.M., Benson, B.J., Wynne, R.H., Livingstone, D.M., Arai, T., Assel, R.A., Barry, R.G., Card, V., Kuusisto, E., Granin, N., Prowse, T.D., Stewart, K.M. and Vuglinski, V.S., 2000. Historical Trends in Lake and River Ice Cover in the Northern Hemisphere. Science, vol. 289, p. 1743-1746, DOI:10.1126/science.289.5485.1743.

McBean, G., 2005. Arctic Climate: Past and Present. *In:* Arctic Climate Impact Assessment Scientific Report, C. Symon, L. Arris and B. Heal (eds.), Cambridge University Press, Cambridge, UK, p. 21-60.

McCoy, V.M., Burn, C.R., 2001. Climate Change in Central Yukon. Unpublished report produced for the Village of Mayo, Carleton University, Ottawa, ON.

Nebojša, N., Davidson, O., Davis, G., Grübler, A., Kram, T., La Rovere, E.L., Metz, B., Morita, T., Pepper, W., Pitcher, H., Sankovski, A., Shukla, P., Swart, R., Watson, R. and Dadi, Z., 2000. Emissions Scenarios: A Special Report of Working Group III of Intergovernmental Panel on Climate Change. Intergovernmental Panel on Climate Change, Geneva, Switzerland, 27 p.

Peter, D.L., Hogan, J. and the First Nation of Na-Cho Nyäk Dun Lands and Resources Department, 2006. History of the First Nation of Na-Cho Nyäk Dun. *In:* Heart of the Yukon: a natural and cultural history of the Mayo area, L. Bleiler, C. Burn and M. O'Donoghue (eds.), Village of Mayo, Mayo, Yukon Territory, p. 86-92.

Prowse, T.D., 2009. Introduction: hydrological effects of a shrinking cryosphere. Hydrological Processes, vol. 23, p. 1-6.

Purves, M., 2010. Climate Change in the Yukon, Updated Observations. Yukon Weather Center Internal Report YWC-10-110, 81p*. Private correspondence from the author January 24, 2011.*

Romolo, L.A., Prowse, T.D., Blair, D., Bonsal, B.R. and Martz, W.L., 2006. The synoptic climate controls on hydrology in the upper reaches of the Peace River Basin. Part I: snow accumulation. Hydrological Processes, vol. 20, p. 4097-4111

Scenarios Network for Alaska Planning (SNAP), 2010. Climate Projections for the Region of Mayo. Unpublished Data produced for the Northern Climate ExChange, Yukon College, Whitehorse, YT.

Smith, C.A.S., Miekle, J.C. and Roots, C.F. (eds.), 2004. Ecoregions of the Yukon Territory – Biophysical Properties of Yukon Landscapes. Agriculture and Agri-Food Canada, PARC Technical Bulletin 04-01, Summerland, BC, 313 p.

Stanley and Associates Engineering Ltd., 1990. Construction and testing of warm water well PW 2, Mayo, Yukon. Unpublished report produced for the Village of Mayo, Mayo, YT, 21 p.

Stroeven, A., Fabel, D., Codilean, A.T., Kleman, J., Clague, J.J., Miguens-Rodriguez, M. and Sheng, X., 2010. Investigating the glacial history of the northern sector of the Cordilleran Ice Sheet with cosmogenic ^{10}Be concentrations in quartz. Quaternary Science Reviews, vol. 29, p. 3630-3643.

Village of Mayo (VOM), 2005. Village of Mayo Official Community Plan. Village of Mayo and Inukshuk Planning and Development Ltd., Mayo, YT, p. 1-29.

Wahl, H.E., Fraser, D.B., Harvey, R.C. and Maxwell, J.B., 1987. Climate of Yukon. Atmospheric Environment Service, Environment Canada, Climatological Studies, no. 40, 323 p.

Walsh, J.E., 2005. Chapter 6: Crysophere and Hydrology. *In*: Arctic Climate Impact Assessment Scientific Report, C. Symon, L. Arris and B. Heal (eds.), Cambridge University Press, p. 183-242.

Ward, B.C., Bond, J.D., Froese, D. and Jensen, B., 2008. Old Crow tephra (140 ± 10 ka) constrains penultimate Reid glaciation in central Yukon Territory. Quaternary Science Reviews, vol. 27, p. 1909-1915.

Water Resources Branch, 2010a. Yukon Water Well Registry. Yukon Department of Environment, Government of Yukon, Water Resources Branch, http://www.environmentyukon.gov.yk.ca/pdf/YukonWaterWellsSummary.pdf, [accessed 24 November 2010].

Water Resources Branch, 2010b. Yukon Snow Survey Network. Yukon Department of Environment, Government of Yukon, Water Resources Branch, http://www.environmentyukon.gov.yk.ca/monitoringenvironment/snow_survey.php, [accessed November 2010].

Water Survey of Canada, 2010. National Water Quantity Survey Program. Environment Canada, http://www.wsc.ec.gc.ca/applications/H2O/index-eng.cfm, [accessed November 2010].

Wellman, S. and Gagné, A., 2010. Environmental stresses along the Silver Trail: A history. Draft report prepared for the Northern Climate Exchange, Yukon College, Whitehorse, YT, 39 p.

Wolfe, S., Bond, J. and Lamothe, M., 2011. Dune stabilization in central and southern Yukon in relation to early Holocene environmental change, northwestern North America. Quaternary Science Reviews, vol. 30, issues 3-4, p. 324-334.

Wrona, F., Prowse, T.D. and Reist, J.D., 2005. Chapter 8: Freshwater Ecosystems and Fisheries. *In:* Arctic Climate Impact Assessment Scientific Report, C. Symon, L. Arris and B. Heal (eds.), Cambridge University Press, Cambridge, UK, p. 353-452.

Yukon Bureau of Statistics (YBS), 2007. Information Sheet #C06-02 – July 2007: Age and Sex. The Yukon Government Executive Council Office Bureau of Statistics, Whitehorse, Yukon, 4 p.

Yukon Bureau of Statistics (YBS), 2008a. Information Sheet #C06-06 – March 2008: Mobility and Migration. The Yukon Government Executive Council Office Bureau of Statistics, Whitehorse, Yukon, 4 p.

Yukon Bureau of Statistics (YBS), 2008b. Information Sheet #C06-08 – April 2008: Aboriginal Data. The Yukon Government Executive Council Office Bureau of Statistics, Whitehorse, Yukon, 4 p.

Yukon Bureau of Statistics (YBS), 2009. Information Sheet #C06-12 – July 2009: Housing Shelter and Costs. The Yukon Government Executive Council Office Bureau of Statistics, Whitehorse, Yukon, 4 p.

Yukon Bureau of Statistics (YBS), 2010. Information Sheet No. 58.35 – July 2010: Population Report. The Yukon Government Executive Council Office Bureau of Statistics, Whitehorse, Yukon, 4 p.

APPENDIX A - SURFICIAL GEOLOGY TEXTURES

Sample ID	Gravel content (%)	Sieve - #10 (>2.00 mm) % pebbles	Sieve - #35 (>0.50 mm) % coarse sand	Sieve - #230 (>0.063 mm) % fine sand	Sieve # 635 (>0.020 mm) % silt	Sieve - pan % mud	Texture	% Sand by hydrometer	% Silt by hydrometer	Clay content (%)
1	10	0.5	2.5	23	36	38	loam	40	47	13
2	67	44	37	14	2.3	2.8	sand	95	4	0
3	27	18	34	31	6.7	9.8	sand	87	10	3
4	65	23	47	28	1	1.2	sand	98	0	0
5	14	6.9	6.7	30	32	25	loam	51	40	9
6	12	2.5	3.8	19	32	42	loam	38	49	13
7	32	9.7	7.2	28	23	32	loam	44	44	12
8	58	35	20	21	12	12	sandy loam	70	22	8
9	81	28	29	27	7.1	9.4	loamy sand	82	12	6
10	0	0	0.8	21	43	35	silt loam	34	52	14
11	4	1.8	4.1	16	30	49	loam	38	46	16
12	49	13	14	30	20	22	sandy loam	65	27	9
13	35	16	17	28	18	21	sandy loam	68	24	8
14	42	9.7	15	33	22	21	sandy loam	66	32	2
15	51	16	35	44	1.7	3.7	sand	94	4	2
16	0	0	8.6	65	24	2.5	loamy sand	83	17	0
17	50	17	27	32	12	12	loamy sand	79	18	3
18	67	20	36	34	5.3	5.4	sand	90	8	2
19	60	27	49	22	1.5	1	sand	95	3	2
20	62	15	48	35	0.8	0.9	sand	97	0	0
22	0	1.5	5.4	19	27	47	loam	35	50	15
23	69	31	34	23	3.7	7.8	loamy sand	83	14	3
24	49	48	36	10	2.8	2.8	sand	90	8	2
25	0	0	0.6	39	33	27	sandy loam	56	33	11
26	62	33	52	13	0.7	1.1	sand	98	0	0
28	97	58	22	10	2.4	8.2	sandy loam	70	20	10
29	28	19	42	32	2	5.2	sand	93	3	4
30	60	27	44	23	3.6	2.4	sand	92	5	3
31	81	30	45	24	0.9	0.9	sand	97	0	0
32	62	16	30	45	3.9	4.9	sand	89	8	3
33	66	20	30	36	5.8	8.7	loamy sand	86	11	4
34	0	0	0.3	14	29	57	silt loam	28	53	20
35	62	24	26	27	8.8	15	sandy loam	71	21	9
36	17	16	42	40	1.1	1.6	sand	96	3	0
37	0	0	0.8	69	13	17	sandy loam	78	15	8

APPENDIX A - SURFICIAL TEXTURES, *continued*.

Sample ID	Gravel content (%)	Sieve - #10 (>2.00 mm) % pebbles	Sieve - #35 (>0.50 mm) % coarse sand	Sieve - #230 (>0.063 mm) % fine sand	Sieve # 635 (>0.020 mm) % silt	Sieve - pan % mud	Texture	% Sand by hydrometer	% Silt by hydrometer	Clay content (%)
38	61	27	26	34	4.2	9.3	loamy sand	86	6	8
39	6	2.7	11	67	10	9.3	sand	87	11	2
40	11	1.8	9.1	22	32	36	loam	45	46	9
41	59	20	36	36	4.9	3.5	sand	94	6	0
42	0	0	0	22	43	34	sandy loam	51	46	3
43	88	7.1	13	45	9	26	sandy loam	71	15	14
44	31	0	0.3	53	20	26	sandy loam	59	35	6
45	0	0	0.2	13	47	40	silt loam	36	55	9
46	14	11	35	47	4	3.1	sand	97	0	2
47	0	0	1.5	36	31	32	sandy loam	57	38	5
48	4	2.7	3.6	5.4	15	73	clay loam	22	48	30
49	65	42	37	17	3	1.8	sand	93	4	3
50	0	0.3	2.9	78	11	8	sand	88	8	4
51	57	45	25	26	1.9	2.4	sand	96	2	0
52	0	0.3	7.3	42	22	28	sandy loam	66	28	6

APPENDIX B - SNAP PROJECTIONS

This section provides figures, focusing on the Mayo region, that illustrate projected changes in several climate parameters. Projections are derived from the regionally downscaled climate data provided by the Scenarios Network for Alaska Planning (SNAP, 2010) at the University of Alaska Fairbanks. Projected precipitation and temperature data were based on raster values surrounding the geographic centre of Mayo, as determined by SNAP. The range encapsulated was 625 km^2. Changes in climate for the Mayo region were projected for two time periods (2030 and 2050) using two standard scenarios (B1 and A1B) developed by the Intergovernmental Panel on Climate Change (IPCC). The B1 and A1B scenarios are based on the IPCC Special Report on Emissions Scenarios (Nebojša *et al.*, 2000). The B1 scenario projects low to moderate degrees of climate change over the next century, while the A1B scenario anticipates medium to high degrees of climate change. These two scenarios were applied in this study because they provide a reasonable range in possible shifts in temperature and precipitation for Mayo by 2030 and 2050.

Appendix B1 - Projected changes in mean annual temperature for 2030 and 2050, based on the B1 and A1B scenarios, respectively. Baseline (1961-1990 climate normal) conditions are provided.

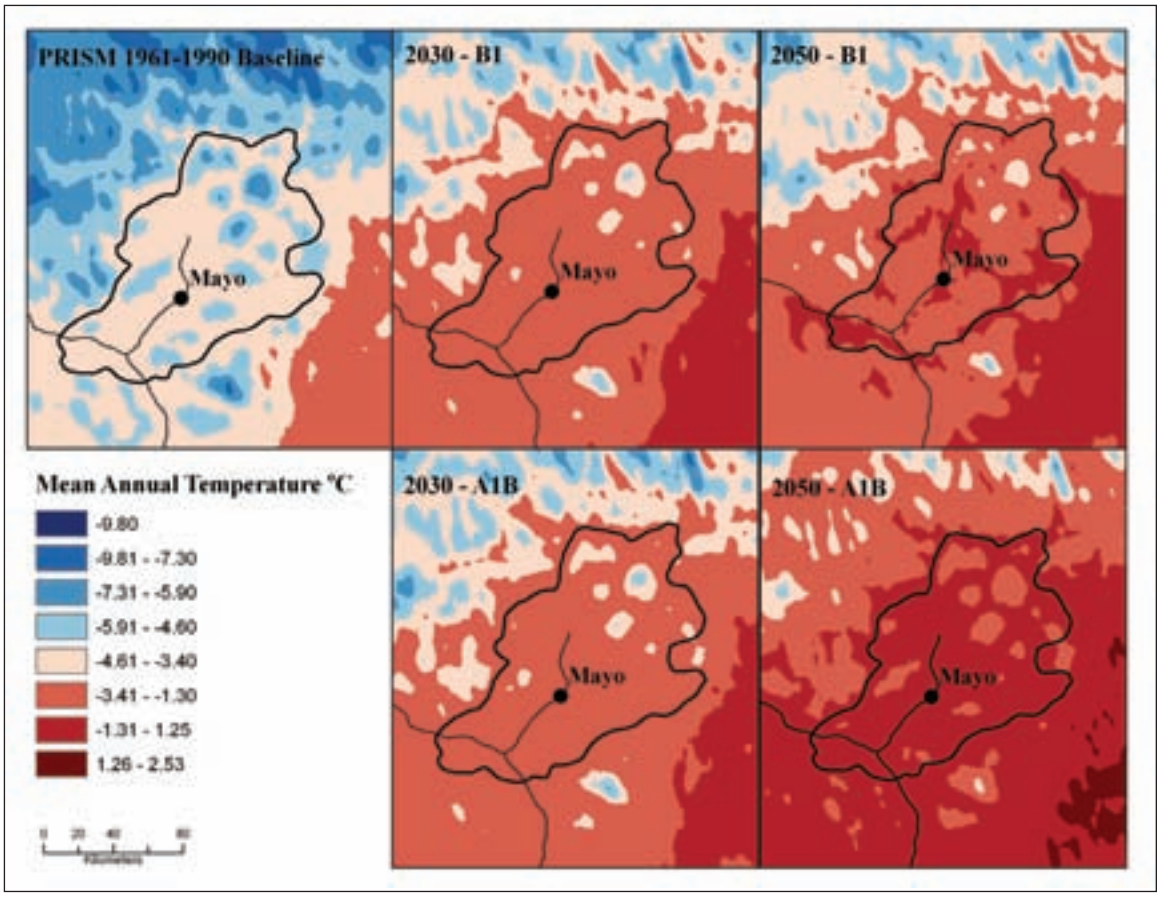

APPENDIX B - SNAP PROJECTIONS, *continued*.

Appendix B2 - Projected changes in mean spring temperature for 2030 and 2050, based on the B1 and A1B scenarios, respectively. Baseline (1961-1990 climate normal) conditions are provided.

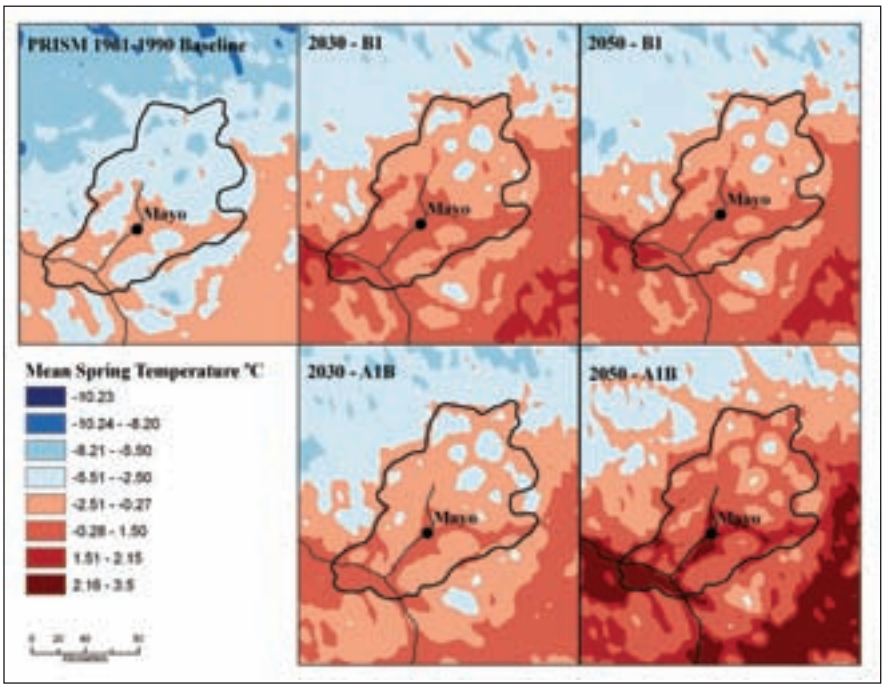

Appendix B3 - Projected changes in mean summer temperature for 2030 and 2050, based on the B1 and A1B scenarios, respectively. Baseline (1961-1990 climate normal) conditions are provided.

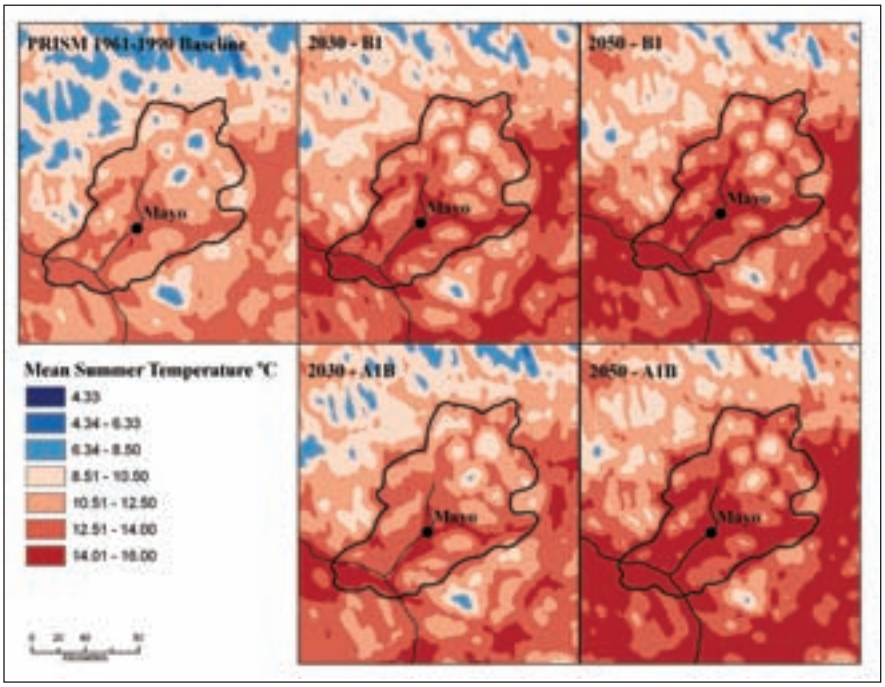

APPENDIX B - SNAP PROJECTIONS, *continued*.

Appendix B4 - Projected changes in mean autumn temperature for 2030 and 2050, based on the B1 and A1B scenarios, respectively. Baseline (1961-1990 climate normal) conditions are provided.

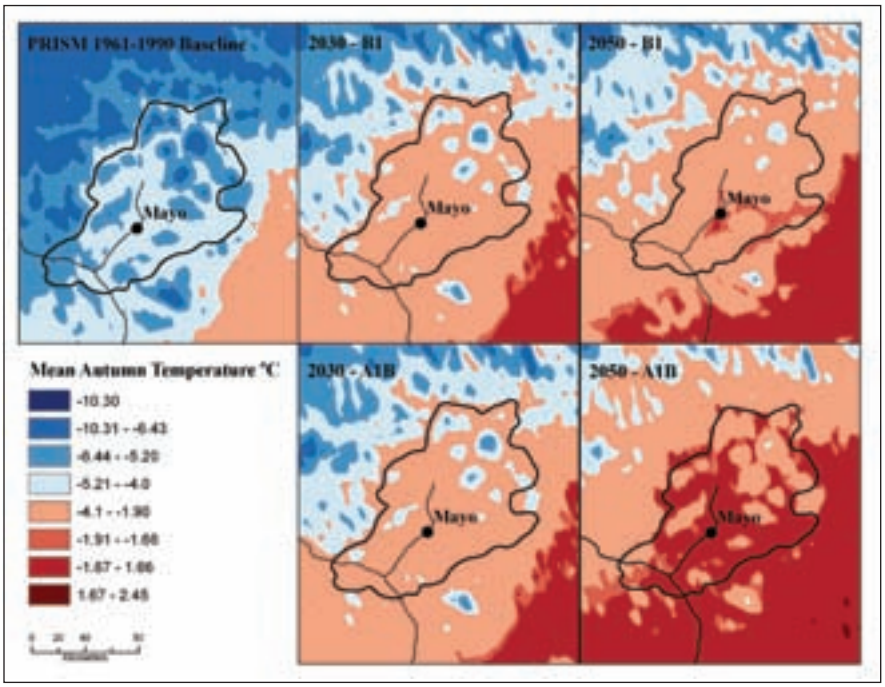

Appendix B5 - Projected changes in mean winter temperature for 2030 and 2050, based on the B1 and A1B scenarios, respectively. Baseline (1961-1990 climate normal) conditions are provided.

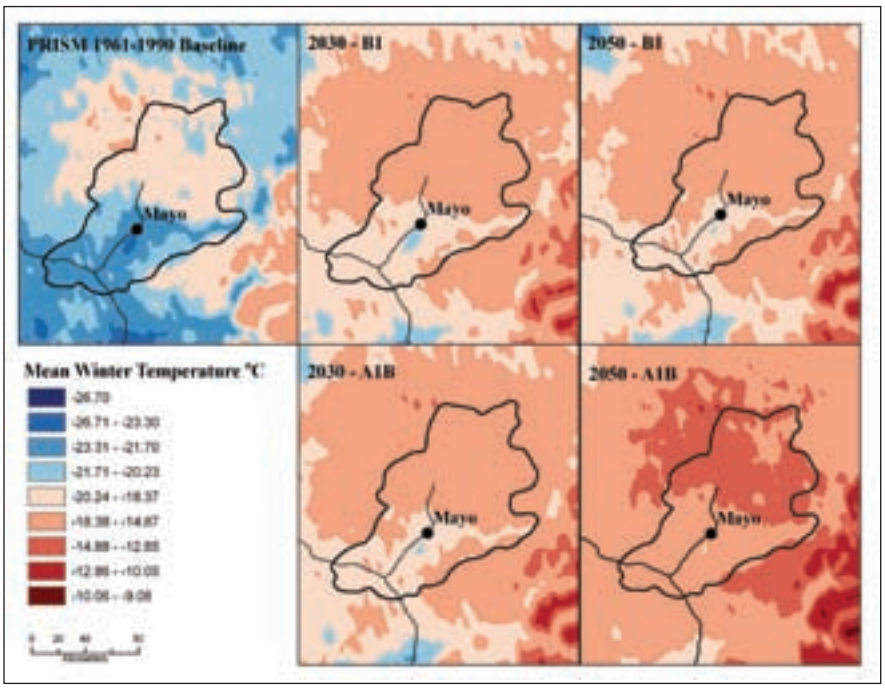

APPENDIX B - SNAP PROJECTIONS, *continued*.

Appendix B6 - Projected changes in total annual precipitation for 2030 and 2050, based on the B1 and A1B scenarios, respectively. Baseline (1961-1990 climate normal) conditions are provided.

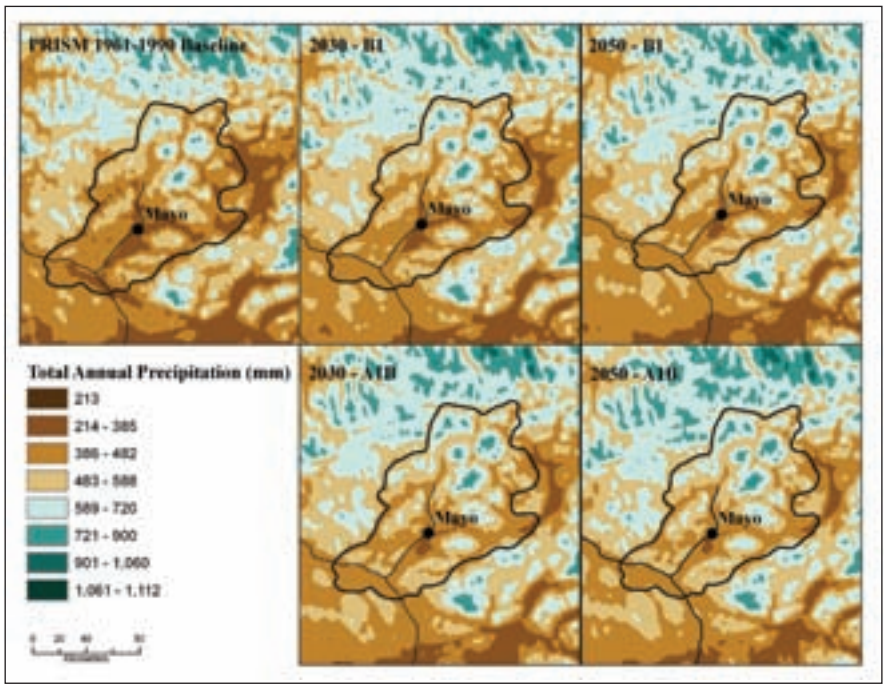

Appendix B7 - Projected changes in total spring precipitation for 2030 and 2050, based on the B1 and A1B scenarios, respectively. Baseline (1961-1990 climate normal) conditions are provided.

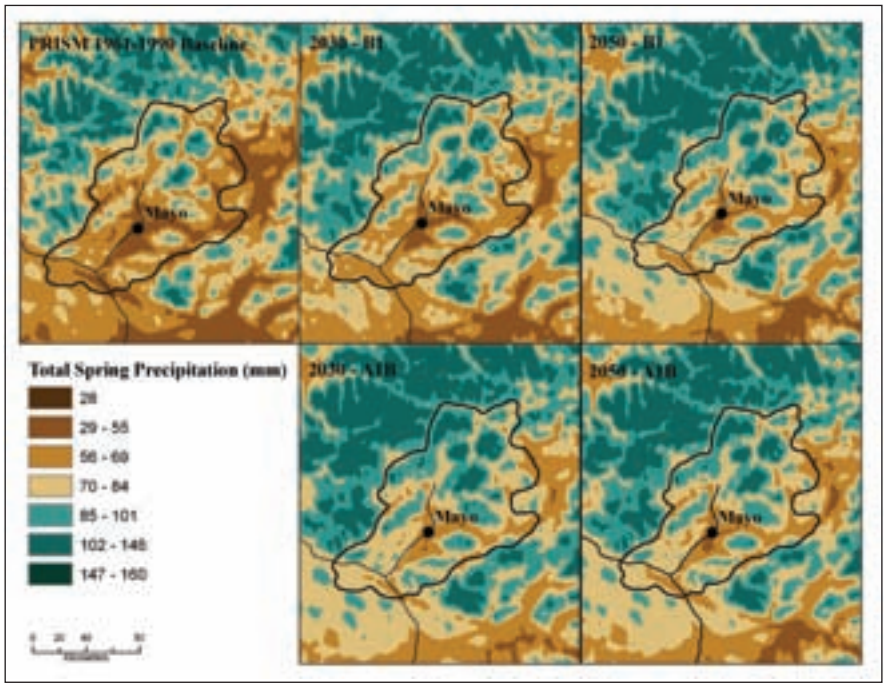

APPENDIX B - SNAP PROJECTIONS, *continued*.

Appendix B8 - Projected changes in total summer precipitation for 2030 and 2050, based on the B1 and A1B scenarios, respectively. Baseline (1961-1990 climate normal) conditions are provided.

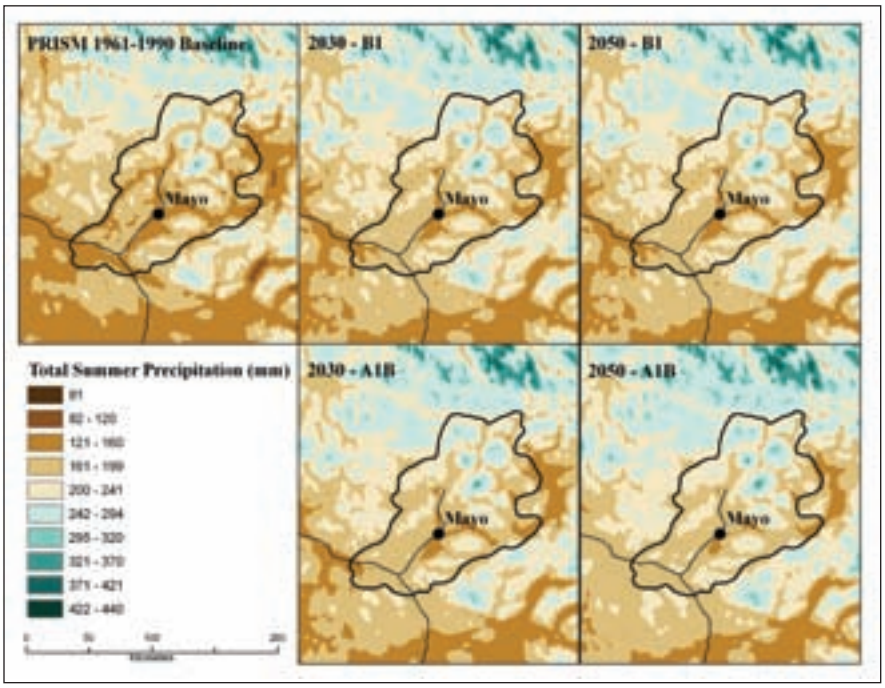

Appendix B9 - Projected changes in total autumn precipitation for 2030 and 2050, based on the B1 and A1B scenarios, respectively. Baseline (1961-1990 climate normal) conditions are provided.

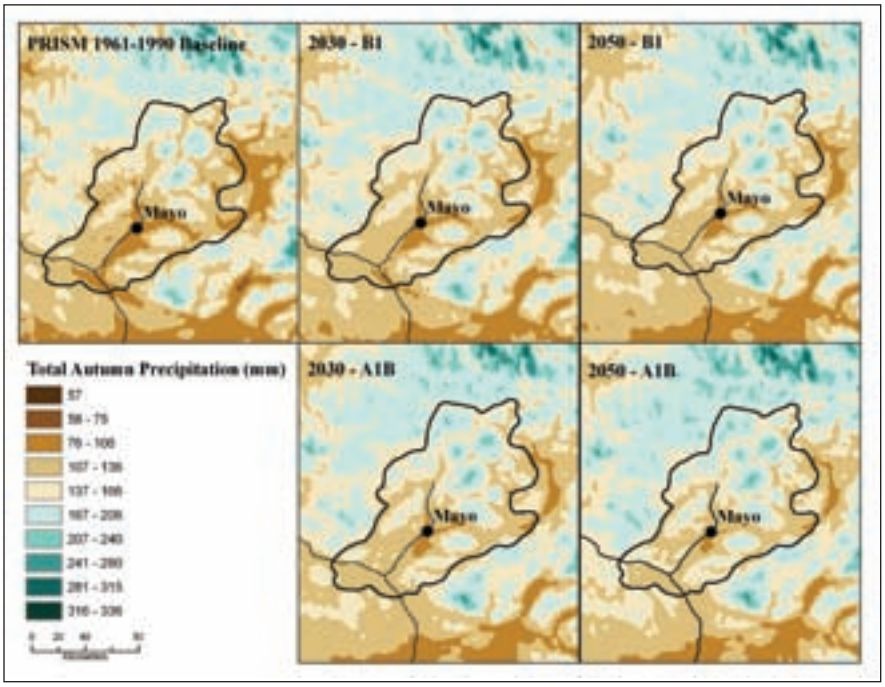

APPENDIX B - SNAP PROJECTIONS, *continued*.

Appendix B10 - Projected changes in total winter precipitation for 2030 and 2050, based on the B1 and A1B scenarios, respectively. Baseline (1961-1990 climate normal) conditions are provided.

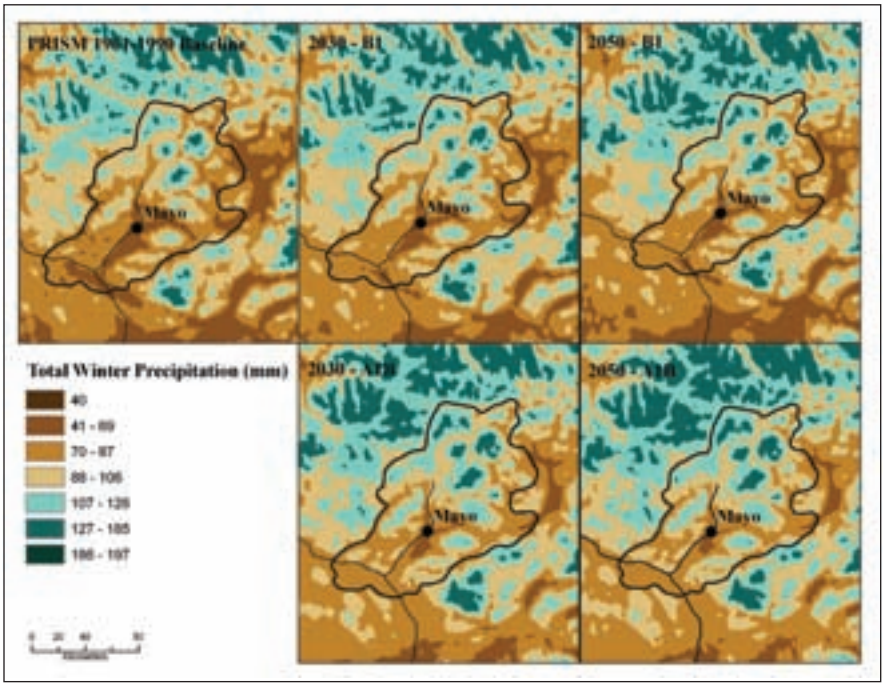

Appendix B11 - Projected changes in date of thaw for 2030 and 2050, based on the B1 and A1B scenarios, respectively. Baseline (1961-1990 climate normal) conditions are provided.

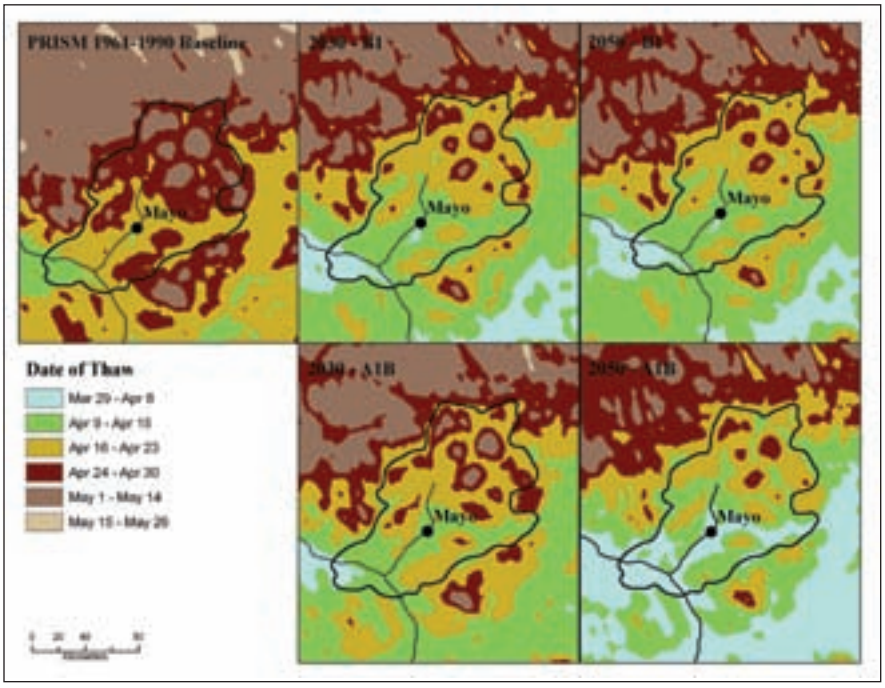

APPENDIX B - SNAP PROJECTIONS, *continued*.

Appendix B12 - Projected changes in date of freeze-up for 2030 and 2050, based on the B1 and A1B scenarios, respectively. Baseline (1961-1990 climate normal) conditions are provided.

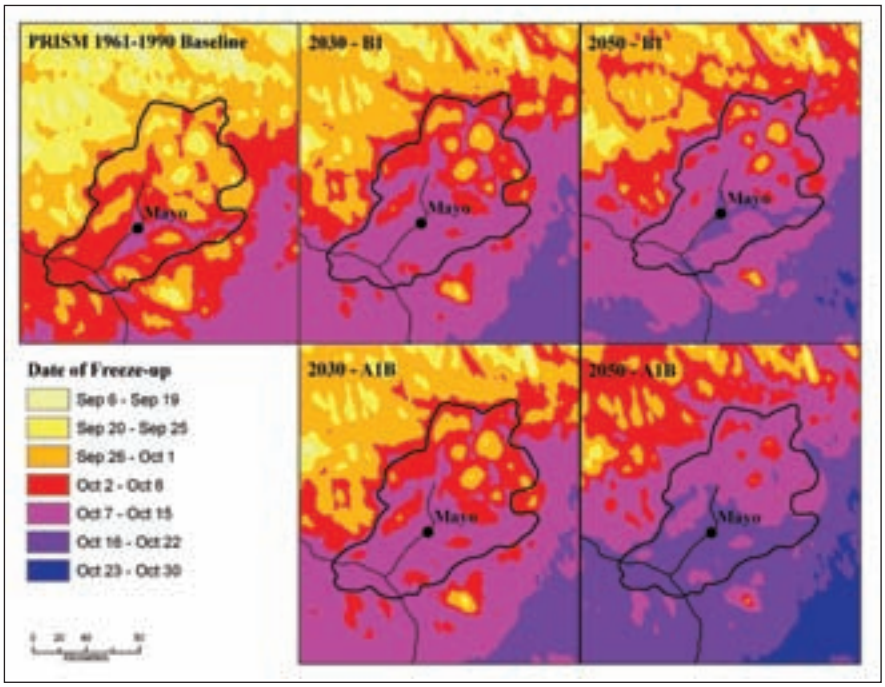

Appendix B13 - Projected changes in length of growing season for 2030 and 2050, based on the B1 and A1B scenarios, respectively. Baseline (1961-1990 climate normal) conditions are provided.

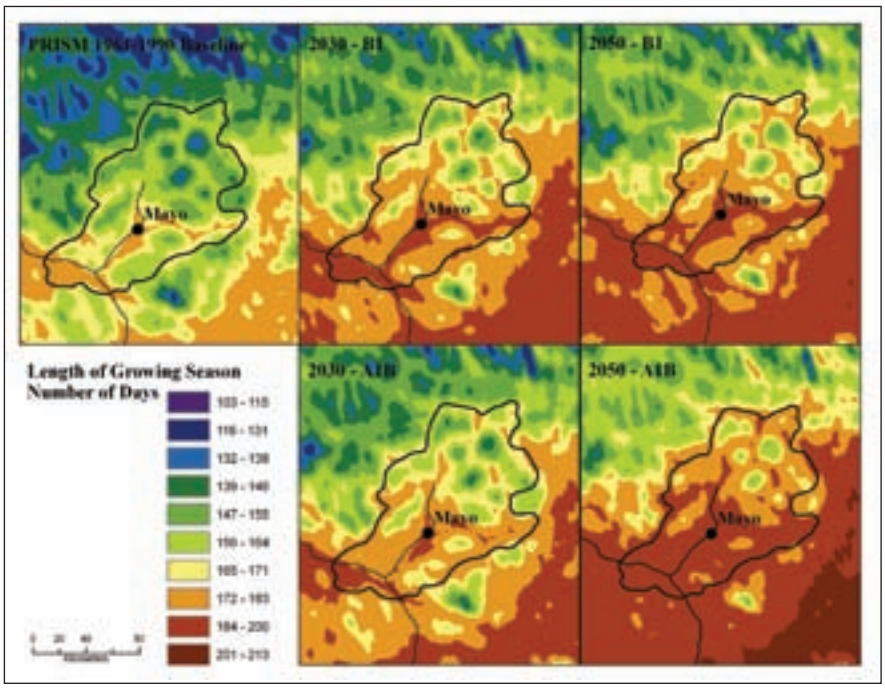

APPENDIX C - POLYGON HAZARD DESCRIPTION

Polygon number	Hazard rank	Map colour	Geologic label	Landscape hazards	Area (km²)
1	3	Red	eOw\gszFp	flooding (Stewart River), permafrost	651
2	3	Red	uOb\zscFp-X	permafrost	149
3	2	Yellow	gszFp	flooding (Stewart River, Mayo River), permafrost	62
4	3	Red	eOw\gszFp-Bb	flooding (Mayo River), permafrost	201
5	3	Red	uOw\gszFp-Bb	flooding (Mayo River), permafrost	302
6	3	Red	gszFAp	flooding (Stewart River, Mayo River), permafrost	56
7	2	Yellow	gszFp	flooding (Mayo River), permafrost	46
8	3	Red	eOw\gszFp-Bb	flooding (Mayo River), permafrost	84
9	3	Red	gszCba	mass movement (steep slope)	457
10	3	Red	eOw\gszFp-Bb	flooding (Mayo River), permafrost	116
11	3	Red	eOw\gszFp-Bb	flooding (Mayo River), permafrost	157
12	3	Red	uOp\szFp	flooding (Mayo River), permafrost	76
13	3	Red	uOp\zscFp-X	flooding (Mayo River), permafrost, shallow groundwater table	338
14	1	Green	zsEw\gsFGp/Mh	permafrost	1174
15	1	Green	szEv\pksFGtd	permafrost	2538
16	1	Green	zsEv\pskFGpd	permafrost	898
17	1	Green	zsEAb\pksFGt	permafrost	826
18	1	Green	zsEw\pzsMh-X	permafrost	5608
19	2	Yellow	gsFGb\kpdMb\R	permafrost, mass movement (steep slope)	126
20	3	Red	uOw\gszFGf	permafrost (thermokarst), shallow groundwater table	184
21	3	Red	szgFt-Xt	flooding (Stewart River), permafrost (thermokarst), shallow groundwater table	3489
22	2	Yellow	uOw\zpkMr/gsFGp-X	permafrost, shallow groundwater table	317
23	2	Yellow	gszFGp/zpkMb-X	permafrost	349
24	3	Red	uOb/zscLb/gsFGp-X	permafrost, shallow groundwater table	692
25	1	Green	gszFGp-T//kpzMr	permafrost	2153
26	2	Yellow	sgFGp\R	mass movement (steep slope)	51
27	3	Red	gsFt	flooding (Mayo River), permafrost	85
28	2	Yellow	gsFt	flooding (Mayo River), permafrost	52
29	3	Red	zdCb/sgFGt	permafrost, mass movement	100
30	2	Yellow	zdCb/sgFGt	permafrost, mass movement	80
31	3	Red	zdCv/sgFGt	mass movement (steep slope)	256
32	1	Green	zsEw\gsFGp-E	permafrost	948
33	2	Yellow	zpkMr//zsEw-X	permafrost	3126
34	2	Yellow	eOv\sdCb/zpkMb-X	permafrost	2083
35	3	Red	eOw\gszFp-Bb	flooding (Mayo River), permafrost	112
36	3	Red	eOw\gszFp-Bb	flooding (Mayo River), permafrost	78
37	2	Yellow	gsFt-X	permafrost	219
38	2	Yellow	gszFt-X	permafrost	340

APPENDIX C - POLYGON HAZARD DESCRIPTION, *continued*.

Polygon number	Hazard rank	Map colour	Geologic label	Landscape hazards	Area (km²)
39	3	Red	uOw/zgsFt-X	flooding (Mayo River), permafrost	176
40	2	Yellow	uOw/zgsFt-X	flooding (Mayo River), permafrost	93
41	1	Green	gsFt	permafrost	44
42	3	Red	psdCf	mass movement (steep slope)	47
43	3	Red	psdFf	mass movement (steep slope)	50
44	2	Yellow	szdCa/pskFGt	mass movement (steep slope)	240
45	1	Green	zsEw\zgkMr/spFGp	permafrost	3557
46	2	Yellow	zsEv\zgkMr/spFGp	permafrost	211
47	2	Yellow	zsEw\zgkMr/spFGp\R	permafrost	206
48	1	Green	zsEb\sgFGp	permafrost	853
49	2	Yellow	zsCv/zsEb/gsFGp	permafrost, shallow groundwater table	1024
50	2	Yellow	zsEv\zgkMr/spFGp	permafrost	157
51	1	Green	zsEv\gsFGp	permafrost	662
52	3	Red	szgFt-Xt	flooding (Stewart River), permafrost	531
53	3	Red	szgFt	flooding (Stewart River), permafrost	857
54	3	Red	szgFt-Lk	flooding (Stewart River), mass movement, permafrost	110
55	3	Red	szgFt	flooding (Stewart River), permafrost	514
56	3	Red	uOw\sgzFGp/zscLGb-Xt	permafrost (thermokarst), shallow groundwater table	412
57	1	Green	gszFGf\zscLGp	permafrost	1615
58	1	Green	sgzFGt	permafrost	339
59	2	Yellow	sgzFGp\zscLGp-Xt	permafrost	4349
60	2	Yellow	szLv\gszFGb	permafrost	93
61	3	Red	zdgCb-X	permafrost, mass movement (steep slope)	666
62	2	Yellow	zsEb/gsFGp-X	permafrost	601
63	3	Red	zpsCb-X	permafrost, mass movement (steep slope)	262
64	1	Green	gsFGt	permafrost	665
65	1	Green	/zsEv\gszFGt	permafrost	560
66	2	Yellow	zsEv\szpCa/szcLGb-X	permafrost, mass movement	1014
67	2	Yellow	szEv\zscLGb/spkFGt	permafrost, mass movement	1040
68	1	Green	/zsEv\gsFGt	permafrost	415
69	2	Yellow	zdsCvb/zpkMb-X	permafrost	1149
70	2	Yellow	zsCb/gszFGp-X	permafrost	1290
71	3	Red	zsCb/szcLGb-X	permafrost	186
72	3	Red	uOb/szFf-X	permafrost, shallow groundwater table	260
73	3	Red	uOw/szgFf-X	permafrost, shallow groundwater table	345
74	2	Yellow	zsCv/szcLGb-X	mass movement	50
75	2	Yellow	zsCv/szcLGb-X	mass movement	71
76	2	Yellow	/zsEv/gsFGp	permafrost, mass movement	759

APPENDIX C - POLYGON HAZARD DESCRIPTION, *continued*.

Polygon number	Hazard rank	Map colour	Geologic label	Landscape hazards	Area (km²)
77	2	Yellow	gszFGp/zpkMb-X	permafrost, shallow groundwater table	727
78	3	Red	zscLGb/gsFGp-X-Lk	permafrost, mass movement	105
79	2	Yellow	zpkMb//gszFGp-X	permafrost	648
80	2	Yellow	uOw\spzCb/gsFGp-X	permafrost	111
81	2	Yellow	uOb\szdCa//gsFGp-X	permafrost	298
82	1	Green	zsEv\gsFGp	permafrost	1014
83	1	Green	zsEb\gsFGp	permafrost	1282
84	2	Yellow	szgFp-X	permafrost	87
85	2	Yellow	szFp\zscLGp-X	permafrost	533
86	2	Yellow	zsdCv/zpkMb-X	permafrost, mass movement	212
87	3	Red	szgFt-Xt	flooding (Stewart River), permafrost	88
88	3	Red	eOw\gszFp-X	flooding (Stewart River), permafrost	345
89	3	Red	zscLGp/szFp-Xt	permafrost (thermokarst), shallow groundwater table	8156
90	3	Red	zsEv\zscLGv/spkFGt-V	permafrost, mass movement	364
91	2	Yellow	zsCv/zsEb/gsFGp	permafrost, mass movement	34
92	3	Red	/zscLv/sgzFGp-X	permafrost, mass movement	558
93	2	Yellow	A	permafrost, shallow groundwater table	182
94	2	Yellow	gsA	permafrost, shallow groundwater table	384
95	2	Yellow	gszFp	permafrost, shallow groundwater table	74
96	3	Red	sgzFGp//gsA	permafrost, shallow groundwater table, flooding (Mayo River)	425
97	3	Red	uOw/sgzFGp\zscLGp-Xt	permafrost (thermokarst), shallow groundwater table	78
98	3	Red	uOw/sgzFGp\zscLGp-Xt	permafrost (thermokarst), shallow groundwater table	104
99	3	Red	uOw/sgzFGp\zscLGp-Xt	permafrost (thermokarst), shallow groundwater table	47
100	3	Red	uOw/sgzFGp\zscLGp-Xt	permafrost (thermokarst), shallow groundwater table	126
101	3	Red	uOw/sgzFGp\zscLGp-Xt	permafrost (thermokarst), shallow groundwater table	321
102	3	Red	sgzCb	mass movement (steep slope)	290
103	3	Red	gszFAp	flooding (Mayo River), permafrost	208
104	2	Yellow	zdCb/sgFGt	mass movement, permafrost	213
105	1	Green	gszFGtf//zsEw	permafrost	3475
106	2	Yellow	zpkMr\R-X	permafrost	1055
107	2	Yellow	zsEv\gszFGp-E	mass movement (steep slope)	1192
108	1	Green	zsEv\gsFGt	permafrost	752
109	3	Red	gsFp-B	flooding (Mayo River)	1071
110	3	Red	sgzCb	mass movement (steep slope)	261